



THE UNITED NATIONS UNIVERSITY



ORKUSTOFNUN
NATIONAL ENERGY AUTHORITY

**GEOPHYSICAL LOGS AND POROSITY
ANALYSIS IN THE ELLIDAÁR FIELD
REYKJAVÍK, ICELAND**

Somma Techawann

**Geothermal Training Programme
Reykjavík, Iceland
Report 14, 1987**

ABSTRACT

The geothermal wells RV-25, RV-28 and RV-32 are located in the Elliðaár field, Reykjavík. Geophysical logs of temperature, caliper, resistivity, natural gamma ray and neutron-neutron have been run to the maximum depths of 1,632 meters, 1,345 meters and 1,352 meters for wells RV-25, RV-28 and RV-32 respectively. Lithology logs of these wells show rock units of basalt, hyaloclastite tuff, dolerite, sediments and basaltic breccia. The rock alteration causes the low resistivity zones in these wells. Analysis of the geophysical log data has been done by the combination of empirical and statistical log interpretation approach to obtain the meaningful information on the rock formations. Histograms and crossplots of the corrected log data have been generated on the computer. The crossplot technique has been applied to obtain the coefficients in Archie's formula by the plots of resistivity (R_0/R_W) against porosity (ϕ) for determination of the porosity type (matrix and fractured porosity). The average porosity of approximately 20-25% are determined from the neutron-neutron log for these wells, and the results from the crossplots indicate fractured porosity in most cases. Silica distribution from the natural gamma ray log in these wells shows the main rock types of basaltic composition (silica content of 45-52%). The resistivity log indicates rock alteration in several intervals. The log results have been found reliable and can be correlated to the lithology log in general. Some difficulties in the well log analysis have been found, in most cases, due to the effects rock alteration and bed thickness. The recommendations for possible logging work in the future are included.

TABLE OF CONTENTS

ABSTRACT	iii
TABLE OF CONTENTS	v
LIST OF TABLES	viii
LIST OF FIGURES	ix
1. INTRODUCTION	1
2. THEORY AND APPLICATION	3
2.1. Temperature Log	3
2.2. Caliper Log	3
2.3. Resistivity Log	4
2.4. Natural Gamma Ray Log	6
2.5. Neutron-Neutron Log	8
3. MAIN ENVIRONMENTAL EFFECTS AND SOME LOGGING PARAMETERS	11
3.1. Hole Diameter	11
3.2. Mud Type and Mud Density	11
3.3. Bed Thickness	11
3.4. Logging Speed	12
3.5. Hydrothermal Alteration Effect	13
4. LOGGING EQUIPMENT AND FIELD PROCEDURE	14
5. STANDARD CALIBRATION	18
5.1. Calibration of Natural Gamma Ray Log	18
5.2. Calibration of Neutron-Neutron Log	18
6. WELL SIZE CORRECTION	20
6.1. Correction of Resistivity Log	20
6.2. Correction of Natural Gamma Ray Log	20
6.3. Correction of Neutron-Neutron Log	21

7. DATA PROCESSING	23
7.1. Depth Correction	23
7.2. Data Processing for Resistivity Log	23
7.3. Data Processing for Natural Gamma Ray Log	24
7.4. Data Processing for Neutron-Neutron Log	24
7.5. Crossplots and Histograms	25
7.6. Plotting Programs	25
8. RESULTS AND ANALYSIS	26
8.1. Resistivity	26
8.1.1. Distribution of Resistivity in Well RV-25	27
8.1.2. Distribution of Resistivity in Well RV-28	27
8.1.3. Distribution of Resistivity in Well RV-32	27
8.2. Porosity	28
8.2.1. Distribution of Porosity in Well RV-25	28
8.2.2. Distribution of Porosity in Well RV-28	28
8.2.3. Distribution of Porosity in Well RV-32	28
8.3. Resistivity-Porosity Relation	29
8.3.1. Resistivity-Porosity Crossplots in Well RV-25	30
8.3.2. Resistivity-Porosity Crossplots in Well RV-28	31
8.3.3. Resistivity-Porosity Crossplots in Well RV-32	32
8.3.4. Correlation of Archie's Coefficients among Wells RV-25, RV-28 and RV-32	32
8.4. Silica	33
8.4.1. Distribution of Silica Content in Well RV-25	33
8.4.2. Distribution of Silica Content in Well RV-28	33
8.4.3. Distribution of Silica Content in Well RV-32	34

9. DISCUSSION	35
10. CONCLUSIONS AND RECOMMENDATIONS	37
ACKNOWLEDGEMENTS	38
NOMENCLATURE	39
REFERENCES	42
APPENDIX 1 - Lithology and geophysical logs in well RV-25	44
APPENDIX 2 - Lithology and geophysical logs in well RV-28	54
APPENDIX 3 - Lithology and geophysical logs in well RV-32	62
APPENDIX 4 - Resistivity-porosity crossplots in well RV-25	70
APPENDIX 5 - Resistivity-porosity crossplots in well RV- 28	75
APPENDIX 6 - Resistivity-porosity crossplots in well RV- 32	82

LIST OF TABLES

Table 1 - Schematic classification for phases of neutron life	86
Table 2 - Thermal neutron cross-section for some principal elements	87
Table 3 - Slowing down power of elements	88
Table 4 - Recommended maximum logging speeds	88
Table 5 - Coefficients in Archie's formula determined from resistivity-porosity crossplots in well RV-25	89
Table 6 - Coefficients in Archie's formula determined from resistivity-porosity crossplots in well RV-28	89
Table 7 - Coefficients in Archie's formula determined from resistivity-porosity crossplots in well RV-32	90
Table 8 - Conclusion of the Archie's exponents (m) for wells RV-25, RV-28 and RV-32	90
Table 9 - Conclusion of the Archie's constants (a) for wells RV-25, RV-28 and RV-32	91
Table 10 - Mean values of resistivity, porosity and silica content in wells RV-25, RV-28 and RV-32 . .	91

LIST OF FIGURES

Figure 1	Elliðaáir geothermal field, Reykjavik	92
Figure 2	Temperature profiles of wells RV-25, RV-28 and RV-32	93
Figure 3	Interpreted subsurface geology including wells RV-25 and RV-28	94
Figure 4	Interpreted subsurface geology including wells RV-25 and RV-32	95
Figure 5	Normal configuration of resistivity log	96
Figure 6	Basic principle of resistivity measurement	97
Figure 7	Gamma ray emission spectra of radioactive elements	98
Figure 8	Real spectrograms of K, Th and U obtained from NaI(Tl) crystal detector	99
Figure 9	Efficiency curves of gamma ray detectors	100
Figure 10	Slowing down power of H, O and Si for different incident neutron energies	101
Figure 11	Distribution of the measurements about the mean value	102
Figure 12	Probable error as a function of counting rate	103
Figure 13	Hydrothermal minerals in well RV-39	104
Figure 14	Calibration curves for neutron-neutron log	105
Figure 15	Well size correction for 16" normal resistivity log	106
Figure 16	Well size correction for 64" normal resistivity log	107
Figure 17	Borehole absorption function used for well size correction of gamma ray log	108
Figure 18	Distribution of resistivity in well RV-25	109
Figure 19	Distribution of resistivity in well RV-28	110
Figure 20	Distribution of resistivity in well RV-32	111
Figure 21	Distribution of porosity in well RV-25	112
Figure 22	Distribution of porosity in well RV-28	113
Figure 23	Distribution of porosity in well RV-32	114
Figure 24	Distribution of silica content in well RV-25	115
Figure 25	Distribution of silica content in well RV-28	116
Figure 26	Distribution of silica content in well RV-32	117

1. INTRODUCTION

This report is a part of a project work done during the specialized training course of the United Nations University Geothermal Training Programme in 1987. The aim of the project work is to study geophysical log interpretation and analysis, the efficiency of neutron-neutron log to determine the porosity in the geothermal area. The project also includes the experiment of "source-to-detector" spacing effect of the neutron-neutron logging but that is not included in this report.

The geophysical logs in our project work include temperature, caliper, resistivity, natural gamma ray, and neutron-neutron logs.

The area of study was at the Elliðaár geothermal field, Reykjavík (Figure 1). The logs were run in wells RV-25, RV-28, and RV-32. Previous logging work was done in wells RV-36, RV-37, RV-39, and RV-41. The Elliðaár field is a low temperature field with the maximum temperature not exceeding 150°C. The logs were run to the maximum depth of 1,632 meters in well RV-25, 1,345 meters in well RV-28, and 1,352 meters in well RV-32. The temperature logs of these three wells are shown in Figure 2.

The Elliðaár field is one of the separate geothermal systems within a radius of 6 kilometers from the center of Reykjavík. The geothermal water from the wells is used for space heating facilities and operated by Reykjavík Municipal District Heating Service.

Geologically, the Elliðaár field is in Quaternary rocks ranging in age from 2.8 to 1.8 million years. Few series of hyaloclastites were accumulated during this period. An abundance of shallow level dykes and sheets provide secondary rock porosity or fracture porosity. Porous basaltic lavas and dolerite are commonly found in the drillholes in this

area and seem to perform as geothermal reservoirs.

According to the drillcuttings lithology, the main rock formations in these three wells are basaltic rock and hyaloclastite tuff. There are some interbedding sediments and dolerite intrusions. Basaltic breccia is found only in wells RV-25, and RV-28. Basalt is a term used for basaltic rock type containing SiO_2 of 45-52% by weight and its main minerals are plagioclase, pyroxene, olivine and iron oxides. Dolerite is a kind of intrusive rock having the same composition as the basaltic rock, its grain size is therefore larger than that of the basalt. Hyaloclastite tuff is a kind of rock containing rock fragments with glassy matrix. Hyaloclastite tuff found in the Elliðaár field is mostly of basaltic composition. The acid ones are usually found as thin layers interbedding with basaltic lava piles or sedimentary horizons. Basaltic breccia is a mixture of the crystalline basalt and basaltic tuff which its matrix is vesicular glass. Sediments conclude of conglomerate, tillite, and alluvial sediment. The interpreted subsurface geology of wells RV-25, RV-28 and RV-32 have been shown in Figures 3 and 4.

The recent study of hydrothermal alteration has been done in well number RV-39 by Ganda (1987). Since well RV-39 is located in the Elliðaár field (Figure 1) among with the wells of our project work, it is worthwhile to use the information of alteration minerals of this well for log analysis in this area. The effect of rock alteration to the log analysis will be discussed.

2. THEORY AND APPLICATION

2.1. Temperature Log

The temperature log tool used in our investigation is a so-called resistivity thermometer which is most frequently used in well logging at present. It is made using a resistance temperature detector (RTD), whose element consists of a temperature sensitive metal resistor. The metal is a corrosion proof alloy (the one used in the project work is Ni-Fe type). It has a linear positive response in the normal temperature range (0°C to 176°C), a low time constant, and a low Joule effect (or heating effect). The RTD is coupled into a voltage controlled oscillator in order to obtain a stable measured value. While logging, a measured value is sent from the measuring point in the well to a surface recorder through an electric cable. The measured value is pulsed signals, where the temperature is given by the frequency of the pulses and its frequency is finally converted to a voltage output to the recorder that provides the logging result. The pulsed logging is far less sensitive to electrical leaks in cable and cable head than DC (direct current) logging, and it is not affected by the changing resistivity of the cable due to temperature variation.

In our project work, the temperature logging was done in order to limit the depth of investigation due to temperature limitation of the logging tools, and to use its data for the correction of the resistivity log which will be described in chapter 7.2.

2.2. Caliper Log

Caliper log for measuring the hole diameter is of great importance for well size correction in well log analysis. There are several types of measuring sondes. The ordinary type, a three-arm caliper which the arms are linked to the

cursor of a potentiometer, such that any changes in the deflection of the arms reflect in resistance changes in the potentiometer, therefore, variations in hole diameter can be detected. A calibration allows for changes in resistance that means the changes in hole diameter can be scaled on the recorder chart. During logging, the probe is lowered to the bottom of the well, the arms is opened by an electric motor in the probe and the log is run continuously from bottom to top.

2.3. Resistivity Log

There are several methods of resistivity logging. One of these methods, the normal resistivity log, which was used in our project work, will be described.

The normal configuration (Figure 5) composes of four electrodes with two of them fixed on the logging sonde. The third electrode is placed at the surface, and the armour of the logging cable is used as the fourth electrode.

During logging, current is passed through the formation via current electrodes A and B, and voltage is measured between potential electrodes M and N. The measured voltage provides the resistivity determinations. For a current flow to occur between electrodes and the formation, the sonde must be run in holes containing electrically conductive mud or water. In order to obtain a good resistivity log, it is important that the electrode N has a good electrical contact to the ground.

In a homogeneous, isotropic formation of infinite extent, the equipotential surfaces surrounding a single current-emitting-electrode (A) are spheres. The voltage between an electrode (M) situated on one of these spheres and one at infinity is proportional to the resistivity of the homogeneous formation, and the voltmeter deflection corresponding to such voltage can be scaled in resistivity units. In the normal configuration, electrodes A and M are on the sonde. B and N

are, theoretically, located at an infinite distance away. In practice, B is the cable armour, and N is the mud pit far removed from A and M. The distance AM is called "spacing" (16" for short normal and 64" for medium or long normal) and the point of inscription for the measurement is at the midway between A and M.

Detailed principle of normal resistivity log is described as follows. In Figure 6, a single point electrode, A, sends current in an infinite, homogeneous medium, to a remote return B. The current will radiate uniformly in all directions, and the equipotential surfaces will be concentric spheres centered on A. If the potential at distance r from A is V(r), then the difference dV between two equipotentials dr apart is:

$$dV = (RI/4\pi r^2)dr \dots\dots\dots(2.3-1)$$

where I is the total current flowing in amperes, and R is the resistivity of the medium in Ohm-m (so that R dr/4πr² is the resistance in Ohms between two surfaces).

Integrating dV between r and infinity (zero potential):

$$V = \int_r^\infty \frac{RI}{4\pi r^2} dr = -RI/4\pi [1/r]_r^\infty$$

$$= RI/4\pi r \dots\dots\dots(2.3-2)$$

and from these, we obtain R:

$$R = (V/I)4\pi r \dots\dots\dots(2.3-3)$$

$$R = (4\pi r^2/I) (dV/dr) \dots\dots\dots(2.3-4)$$

For the normal configuration, the measuring electrode M is situated close to the current electrode A, (Figure 5a). A constant current I flows from A to the remote return B. The potential V_M of M is measured with respect to the reference electrode N (at zero potential) by mean of volt-

meter (Figure 5b). From equation 2.3-2:

$$V_M = RI/4\pi\bar{AM} \dots \dots \dots (2.3-5)$$

Neglecting borehole effects, i.e. we assume an infinite homogeneous medium. Since I is held constant, V_M is proportional to R:

$$R = 4\pi\bar{AM} (\Delta V/I) \dots \dots \dots (2.3-6)$$

In a non-uniform medium, the resistivity by the above relation is an apparent resistivity. The normal configuration resistivity will show the apparent resistivity variations of the medium surrounding the sonde, and will include the well itself. The determination of the true rock resistivity will therefore include elimination of the well effects (fluid resistivity and well size) as well as the effects of limited bed thickness of the adjacent lithological units.

The specific resistivity of the reservoir rock is the result of two different contributions, the resistivity of the rock matrix and the formation fluid. In igneous rocks, the matrix is generally a poor electrical conductor at geothermal temperatures, with typical specific resistivity values of the order of 10^4 - 10^6 Ohm-m. With medium conducting fluid like geothermal water (<50 Ohm-m), the electrical property of the fluid will define the resistivity of the reservoir rock. This value will therefore in general depend on the porosity as well as temperature and water salinity.

2.4. Natural Gamma Ray Log

Gamma ray is the electromagnetic radiation emitted from an atomic nucleus during radioactive decay. The natural gamma ray log is performed to measure the natural radioactivity of the rocks. The radiation is in fact emitted from three main series of source elements: ^{40}K , ^{232}Th or ^{238}U , and their decay products. There are two ways to measure their radioactivity. One is the measurement of total gamma ray

intensity, and the other is the measurement of a certain energy spectrum of the gamma radiation. In general, gamma rays emitted by the elements in the three decay series have a number of discrete energies. As shown in Figure 7, there are three corresponding gamma ray emission spectra. Each spectrum characterizes a decay series, each series has a spectral "signature" that enables its presence to be discerned. The ^{40}K is characterized by a single gamma ray emission at 1.46 MeV. The most distinctive gamma ray peak in the ^{232}Th series is at 2.62 MeV but there are many lower energy peaks. The peak at 1.76 MeV is used to recognize the ^{238}U series, and there are numerous other peaks. As a matter of fact, the observed spectrum is continuous rather than in a discrete form (Figure 8). The life history of the gamma radiation will be described as a gamma photon (Czubek, 1981). Each primary photon is scattered in the rock medium, undergoing usually several consecutive Compton scatterings, up to the moment when it is absorbed due to the photoelectric absorption. The simultaneous combination of these two phenomena during the photon transports through the rock media gives as a result the continuous photon energy spectrum, and as a matter of fact, in the rocks one has a superposition of such spectra due to the whole set of primary photon energies. This combined photon spectrum is impinging with the gamma detector in the gamma ray tool. There are two types of gamma ray detector, Geiger-Müller(GM) and scintillation counters. The GM-counter, which was used in our investigation, measures the total gamma ray intensity (combined spectrum). The efficiency curves of gamma ray detectors have been shown in Figure 9.

In igneous rock case, the presence of potassium (with radioactive ^{40}K isotope) is in the amount between 0 and 6%, uranium (mainly ^{238}U isotope) and thorium (^{232}Th isotope) are at the level between 0 and 30 ppm, with the usual Th/U of about 3 (Czubek 1981), and the content of uranium and thorium increases when one goes from the ultrabasic to the more acidic igneous rocks.

Recent investigation in Iceland shows that the gamma ray radioactivity in Icelandic volcanic rock is related to the silica content in the rock. Geochemical evidence supports this correlation as the content of radioactive isotopes increases from basic to acidic composition. In a geological environment like in Iceland, where the rock is mainly tholeiitic basalt, the natural gamma ray log generally shows low gamma intensity with a few peaks due to more acidic units in the formation piles. The natural gamma ray log is, therefore, used to indicate the acidic rock, and as a guideline to correlate the rock formations between wells.

2.5. Neutron-Neutron Log

Neutrons are electrically neutral particles, each having a mass almost identical to the mass of hydrogen atom. High-energy neutrons are continuously emitted from the radioactive source which is mounted on the sonde. These neutrons collide with nuclei of the formation materials in what may be thought of as elastic collision. A neutron loses some of its energy with each collision. The life time of these neutrons can be divided into four phases (Table 1): fast, slowing down, diffusion and capture. The fast neutrons of energies between 4 and 6 MeV are emitted continuously from the chemical source. They travel initially at some 10,000 km/s and have a high penetrating power. Following the fast neutron phase, the neutrons are rapidly slowed down by elastic collision with nuclei. The energy lost at each encounter depends on the angle of incidence, and the mass of target nucleus. The mechanics of elastic collisions predicts that the maximum energy will be lost when a target nucleus has a mass equal to that of the incident neutron. Thus, the neutron slow-down is strongly affected by hydrogen atom (H), the single proton of the nucleus having very nearly the same mass as a neutron. This explains why the average energy loss by collision between neutrons and hydrogen is 50% (Table 2). The probability of a collision occurring with a particular

element depends, obviously, on the number of its atoms present in a given volume of formation. However, another parameter must be considered, the elastic interaction cross-section. This is a characteristic of each type of atom. It has the dimensions of area and can be considered as the effective surface area presented by the nucleus to the on-coming neutron. It is not, however, simply related to the physical size of the nucleus and depends, for instance, on the energy of the neutron. It can be summarized by saying that the total slowing down power, SDP, of a certain element in the formation is given by the proportionality:

$$SDP = N\sigma_c\xi \dots\dots\dots (2.5-1)$$

where: N = concentration of atom per cm³;
 σ_c = average collision cross-section;
 ξ = energy lost per collision;

Figure 10 shows the slowing down power of H, O and Si for different incident neutron energies. As at moderate porosity, hydrogen is relatively highly abundant, and its atoms are at least a factor of 10 more effective at slowing down neutrons than the other common elements, it follows that the slowing-down phase is very dependent on the concentration of hydrogen. Table 3 shows that only 18 collisions in average are required for hydrogen to slow a neutron down from 2 MeV to a thermal energy, while other common elements require several hundred. The neutrons continue to be slowed down until their mean kinetic energies are equal to the vibration energies of the atoms in thermal equilibrium. A cloud of the thermal neutrons forms around the source. It is unevenly distributed in space because of the inhomogeneous nature of the borehole and formation. Collisions between the vibrating neutrons and nuclei continue and there is a general spreading or diffusion of the cloud outwards into the formation, where the concentration of the thermal neutrons is low. Some diffusion of neutrons back towards the borehole may also occur. Occasionally, during this diffusion phase, a

nucleus will capture a neutron, resulting in its total absorption. The nucleus becomes momentarily excited and on returning to its ground-state, emits one or several gamma rays or some other radiation.

For practical reasons, all neutron logging tools operate in the long-spacing configuration, with a source to detector spacing in excess of 30 cm or 12". There are several types of the tools. The one used in the project work is the neutron thermal-neutron log. It is a measure of the as yet uncaptured thermal neutron density in the formation. A ^3He detector is used, the helium having a large capture cross-section for the thermal neutrons. An α -particle is produced in the detector at each neutron detection. Higher energy (epithermal, etc.) neutrons do not interact with the helium because, its capture cross-section becomes negligible above the thermal energy level.

The source of neutrons is an intimate mixture of beryllium and one of the α -emitters. α -particles are produced by radioactive isotopes such as $^{226}\text{Radium}$, $^{239}\text{Plutonium}$ or $^{241}\text{Americium}$. They are allowed to bombard beryllium, and neutrons are emitted at high energy. The Americium-Beryllium (Am-Be) type was used in our investigation. The Am-Be source emits 10^7 neutrons/second of mean energy 4.5 MeV, with almost no gamma radiation.

It should be pointed out, however, that the neutrons do not distinguish between protons which belong to formation water or water bound in minerals. This is of particular interest in geothermal logging, as hydrothermal alteration is a process of forming minerals with bound water and the water content of secondary minerals which form frequently in pores in geothermal rock is often high.

3. MAIN ENVIRONMENTAL EFFECTS AND SOME LOGGING PARAMETERS

Only the main effects to the neutron-neutron, natural gamma ray, and resistivity logging will be described.

3.1. Hole Diameter

The larger the hole, the greater the volume of fluid around the logging tool, and stronger its effect on the log reading. Above the certain hole sizes, there may be a little or no signal from the formation. Different hole diameters provide different log reading on the same formation. In our investigation, the neutron-neutron, natural gamma ray and resistivity logs all are affected by the influence of hole diameter. The caliper log is, therefore, important for well size correction.

3.2. Mud Type and Mud Density

The effects of mud seem to be negligible in wells RV-25, RV-28, and RV-32, which are filled with hot geothermal water, with the temperature not exceeding 130°C, and with low salinity (the measured Cl⁻ content of the fluid in well RV-32 is 36.9 ppm). The mud salinity affects conductivity (resistivity), and hydrogen index, among others. The density of mud influences the absorption of gamma rays.

3.3. Bed Thickness

In theory, each bed should be distinguished from its neighbors by its own particular reading on each of the logs. This is indeed seen in practice when the beds are thick. Thin beds present a different picture, and on certain logs, it will be barely possible to pick out the bed boundaries, on others not at all. Two factors must be taken into account, one related to the logging tool design, the other to the fact that measurement is made while the tool is moving. Bed boundaries on logs are not perfectly sharp, but appear as a

more or less gradual transition between the lower and the higher reading. The steepness of the transition depends on the bed resolution of the logging tool. The bed resolution depends on a number of factors, and will be difference for each tool: (a) the thickness of the beds; (b) the tool geometry and type of measurement being made, in as much as they affect the volume of investigation (relative bed thickness); (c) the contrast between readings in the bed in question and its immediate neighbors; and (d) a few cases, ancillary or parasite tool responses, (such as the blind zone and inverse deflection characteristic of the conventional resistivity measurements, the normal and lateral) which may mask or distort bed thickness, and give erroneous values. "Thin" beds (that is, beds thinner than the spacing of the logging tool) may still be discerned on the log. The measured signal, however, is an average of contributions from all beds within the volume of investigation, and the true log value in a thin bed is rarely obtained, even after correction.

3.4. Logging Speed

The resistivity logging is not affected by the normal logging speed, but the radioactive logs are. Since natural and induced radioactive phenomena are random by nature (Figure 11), it is necessary to accumulate count data over a period of time and compute the mean in order to obtain a representative reading. This accumulation or sampling period corresponds to the "time constant" of conventional (capacitative-type) measuring equipment. Figure 11 shows that for random statistical variations, 50% of the sample data will lie within $\pm 0.67N/\sqrt{2NT}$ (the probable error) of the mean, where T is a time constant, and N is the mean counting rate. It is therefore necessary to choose a high time constant when the mean counting rate is low. T is typically 1-6 sec for most logging purposes. N is of the order $10-10^3$ cps. Figure 12 shows how the relative probable error, expressed as a percentage of mean counts, decreases as the

counting rate increases ($T = \frac{1}{2}$ sec). The time constant is chosen according to the counting rate level and measurement precision desired but it should be chosen to keep the standard deviation less than 2.5% of the mean reading wherever practical, which implies that NT should be over 400 and T must be increased when counting rate is low. The logging speed is usually adjusted such that the tool travels 1 ft (0.3 m) in one time constant period, as shown in Table 4. Vertical resolution of 2-3 ft (0.6-0.9 m) may be attained under these conditions. Table 4 show the maximum logging speeds recommended for some of the logging services. Obviously, for combinations of several tools, the maximum speed of the lowest survey must be respected. For our case, the neutron-neutron log was run by the time constant of 4 sec with the logging speeds of 12 m/min. The natural gamma ray was run by 6 sec of time constant, and with the logging speed of 8 m/min.

3.5. Hydrothermal Alteration Effect

The recent study of the hydrothermal alteration history in well RV-39 has been done by Ganda (1987). The alteration of this well is classified as four zones: 1) Iron oxides-chalcedony zone for the depth interval from 0 to 600 m, 2) Chlorite-Epidote-Prehnite zone for the depth interval 1,030 to 2,095 m (bottom), 3) Laumontite zone for the depth interval 420 to 2,095 m, and 4) Thomsonite-Chabasite zone for the depth interval 64 to 1,200 m. Figure 13 shows the hydrothermal minerals in well RV-39. The rocks at depth interval from 1,030 to 2,095 m (bottom) are strongly altered, whereas other intervals are also affected by alteration. This indicates the high amount of bound-water minerals in the rocks that reflects to the neutron-neutron log response as mentioned in chapter 2.5.

4. LOGGING EQUIPMENT AND FIELD PROCEDURE

Generally, all logging equipment consists of three parts: downhole sonde, transmission line, and registration unit. Such units vary in sophistication. A downhole sonde can be one sensor or a very complicated electronic instrument, and the registration unit can be a mini-computer or simply a note book and a pencil. A logging cable is used as a transmission line, which contains one, four or seven conductors with the bearing unit, and with armour wound on the outside of the conductors. On the lower end of the cable is a cable head, and different sondes can be connected to the cable. At the surface, the logging cable is connected to slip ring which makes it possible to obtain continuous registration while the cable drum rotates and the sonde is moving in the well. As most of the instrument functions of logging tools depend on logging speed, it is necessary to have a cable drum motorized to achieve constant logging speed. Hydraulic draw-work is usually preferred at least for logging deep wells (>1,000 meters). There are different surface instruments for each sonde. Logging data is recorded on an analog recorder, where the recorder paper is fed by the deptometer or by the computer.

The logging tools used in our investigation are from Gearhart-Owen Industries Inc. (now Gearhart Inc.). The modules used for our logging work included Line Power Module (LPM), Rate Meter Module (RMM), Differential Temperature Module (DTM), and Electric Log Module (ELM). The function of these modules are described as follows.

LPM: With this module, the current needed for the probes can be adjusted according to the specifications and types of each probe which is, in our case, 50 mA for temperature and caliper logs, 60-70 mA for neutron-neutron and natural gamma ray log. This module can also pick up the Casing Collar Locator (CCL) signal and give it to a pen on the recorder.

RMM: This module converts the frequency to a DC voltage which is given to a pen on the recorder. This voltage is 50-100 mV maximum and is adjustable as well as the time constant suitable for the log. The module also has a pulse-former which produces one well-shaped pulse for each pulse coming from the temperature or caliper probe. This well-shaped pulses are used for the DTM afterward. There is also a 100 Hz built-in oscillator for the purpose of proper setting of the pen.

DTM: This module receives the pulses from the RMM and converts the frequency to temperature reading on a digital display. Some differential temperature modules are built for the temperature reading in °F, then the module simply divides the frequency with 20, that is, frequency divided by 20 is equivalent to the temperature reading in °F. Our temperature probe is designed to produce 20 Hz for each increasing 1°F. The DTM used in our case displays the temperature in °C and the conversion which is frequency divided by 36 plus 17.7 will be equivalent to the temperature reading in °C. Besides, the DTM gives a DC voltage to a pen on the recorder which is proportional to the changes in the frequency with times. This is a very useful feature because very slight changes (<0.1°C) in temperature can be clearly seen on the log.

ELM: This module is for either resistivity or self potential log. For our purpose, normal 16" and 64" resistivity, the desired amount of current is generated to the logging circuit while logging or calibrating. The converter in this module is used to control the frequency of the square wave logging current. The measurements are commonly made using square wave of AC instead of DC to prevent the influence of polarization at the electrodes. This polarization generates a new current between the electrodes against the logging current. There is an internal resistor for calibration purpose which gives the certain resistance to calibrate the pen deflection on the recorder chart.

The field procedure of each method are described as follows:

Temperature log (modules used: LPM, RMM, and DTM): First of all, the temperature probe was calibrated in a calibration bath and all the electronic circuit components were adjusted by the electronic engineer of the Borehole Geophysics Department. Before running the temperature probe down into the wells, the pen deflection on the recorder was set in such a way that for the temperature value of 0°F (or -17.7°C), the output frequency is 0 Hz, whereas the probe is designed to produce 20 Hz for each increasing 1°F, and the deflection of the recording pen is adjusted to the 0 cm position on the recorder chart. For 302°F (or 150°C) which is equivalent to 6,040 Hz the pen deflection is up against the 24 cm position on the chart. This adjustment can be done by the help of 100 Hz built-in oscillator inside the RMM. Temperature log was run with controlled logging speed of 25 m/min and the temperature values were noted on the recording chart every 10 meters.

Caliper log (modules used: LPM, and RMM): Before running the log, the RMM was used to find the proper setting of the pen to obtain an appropriate range on the recorder chart. The range was set to detect 6" to 26" width of the wells which corresponds to some certain frequencies of the pulse signals. The 100 Hz built-in oscillator is needed for this setting. After logging the simple device for calibration was used. The device is aluminium bar having holes at certain distances away, from 2" to 16", from an end of the bar. The bar can hold one arm of the probe in a certain radius, each radius corresponds to a deflection on the recorder chart. Thus, every 2" of diameter from 4" to 32" can be marked on the recorder chart. Our caliper log was run by controlled logging speed of 15 m/min.

Natural Gamma Ray log (module used: LPM, and RMM): The natural gamma ray log was run simultaneously with 13" neutron-neutron log. The logging speed for the natural gamma

ray log must be rather slow. In our case, it was run by the speed of 8 m/min (refer to chapter 3.4) and the time constant of 6 sec was used. Before running the log, the RMM was used to set a range of the pen deflection on the recorder chart. Each pulse frequency or counting rate corresponds to a certain pen deflection and, therefore, the range of expected counting rate (for Icelandic rocks, it is normally from a few counts up to about 30) could be scaled on the recorder chart. The calibration was done (see to chapter 5.1).

Neutron-Neutron log (module used: LPM, and RMM): The proper setting for the pen deflection on the recorder chart of the neutron-neutron log was done in the same way as of the natural gamma ray log. The calibration was done (see chapter 5.2). The logging speed of neutron-neutron log was 12 m/min in our investigation. But for running with the natural gamma ray log, the logging speed of natural gamma ray log which is slower must be chosen.

Resistivity log (module used: ELM): The 16" and 64" normal resistivity. The logs (16" and 64") can be run simultaneously by using the same sonde with different circuits. The calibration was done by generating 5 mA current through the logging circuit which has a calibration resistor located inside the ELM. The deflection of recording pens (16" and 64") controlled by voltage output from the module were scaled on the recorder chart.

For our logging work, the temperature log was the first log of investigation. Caliper log was the second and followed by 13" neutron-neutron simultaneously with natural gamma ray log, the 15" neutron-neutron, 17" neutron-neutron, and finally the resistivity log. The depth of each wells were referred to the reference point for zero depth which is located at the surface. The depth of investigation are always shallower than the drilled depth of the wells due to collapsing or caving.

5. STANDARD CALIBRATION

"Calibration" which is described in this chapter means to set standard of the logging result in order to obtain the standard values for the purpose of quantitative analysis. Only the calibration for the natural gamma ray, and neutron-neutron logs will be described.

5.1. Calibration of Natural Gamma Ray Log

The intensity of natural gamma rays depends on the concentration of ^{40}K , ^{238}U , and ^{232}Th in the rock and the absorption of the fluid in the well. The gamma ray intensity is originally recorded in counting rate. By the reason described above, the tool needs to be calibrated. The gamma ray tool used in our investigation was calibrated before logging by secondary standard provided by the manufacturer of the tool. A radioactive source of $20\ \mu\text{Ci}\ ^{226}\text{Ra}$ is placed at a certain distance away from the tool. The gamma ray recorded is equivalent to 120 API GU for the reading value obtained over the background (no the radioactive source).

5.2. Calibration of Neutron-Neutron Log

The counting rate of the neutron-neutron log depends on the concentration of neutrons captured by the neutron detector. The calibration was done by using the secondary standard (which is a so-called "calibrator") provided by the manufacturer of the tool. The calibrator which is made from synthane plastic, passes through a flux of thermal neutron of approximately 1,000 API NU when placed over the tool at a certain position between the source and the detector.

Porosity in our investigation wells is expressed as limestone porosity. The difference between limestone porosity and the porosity of igneous rocks should not be larger than 3% as shown by Czubek (1981). It is, therefore, considered reasonable to use the limestone porosity calibration curve or

our case. Calibration curves for the neutron-neutron log used for the calculation of porosity are provided by the manufacturer of the tool. In our case, the calibration curves (Figure 14) was used (see chapter 6.3).

6. WELL SIZE CORRECTION

As described in chapter 3.1, different well sizes influence the log response. Neutron-neutron, natural gamma ray, resistivity 16" and 64" logs are influenced by variable well size. Well size correction for neutron-neutron, natural gamma ray, and resistivity logs was, therefore, done in our investigation in order to obtain more precise result. Correction for each log is based on a particular correction curve.

6.1. Correction of Resistivity Log

Figures 15 and 16 show the correction curves published by Gearhart-Owen Inc. (now Gearhart Inc.). As can be seen in Figure 16, the influence of well size on 64" normal resistivity is very small for moderate well diameter and $R_0/R_W < 500$. The same is true for the 16" normal resistivity if the well diameter is less than 10 cm (4 inches). However, for large resistivity values, the well size effect is much more pronounced for the 16" normal resistivity than for the 64" normal resistivity. The internal consistency of the resistivity logs can be checked by comparing the measured values of the two normal resistivities with the correction curves presented in Figure 15.

6.2. Correction of Natural Gamma Ray Log

The drilling fluid acts as an extra absorbent for the natural gamma intensity around the probe. We call the true gamma intensity I_0 , and the recorded intensity I . The relationship between these intensities is:

$$I_0 = CF \times I \dots \dots \dots (6.2-1)$$

where CF is a correction factor. This correction factor is related to the so called borehole absorption function A_p in the following way (Czubek 1981):

$$CF = 1/[1-A_p(\mu,R)] \dots\dots\dots (6.2-2)$$

Figure 17 shows $A_p(\mu,R)$ as function of R_s/R ; where the following parameters are involved:

- R = radius of the borehole
- R_s = radius of the probe = 2.14 cm
- μ = effective mass absorption coefficient for the drilling fluid, which in case of the natural radioactivity of rocks is taken to be $\mu = 0.03\rho$, where ρ is the density of the fluid in the well.

This means that CF is a function of R alone. By using the function shown in figure 17, the following expression for CF can be obtained:

$$CF = [1/(1.586-0.3937\log R)] + [32.0/R^2] \dots\dots\dots (6.2-3)$$

where R is given in mm. The correction factor is equal to 1.0 if $2R_s = 42$ mm which is the diameter of the probe used. The expression shown above has been used for the well size correction of the natural gamma ray.

6.3. Correction of Neutron-Neutron Log

The effect of the well size on the counting rate in the neutron-neutron log is generally such that the logarithm of the counting rate is a linear function of the well diameter. If I_{nn} is the neutron intensity and D is the diameter of the well, then we can write:

$$\log I_{nn} = a \times D + b \dots\dots\dots (6.3-1)$$

where a and b are particular constants for a given probe construction. The empirical value of the neutron-neutron probe used in our investigation:

$$a = -0.0015/\text{mm}$$

as been deduced from numerous investigations in wells in Krafla Geothermal field. This value is also in reasonable agreement with calibration curves published by the manufacturer of the probe (GOI, 1978). For a fixed diameter of the well D_0 of the well, we can write :

$$\log I_{nn}(D_0) = a \times D_0 + b \dots \dots \dots (6.3-2)$$

and by dividing $I_{nn}(D_0)$ we obtain :

$$I_{nn}(D_0) = X \times I_{nn} \dots \dots \dots (6.3-3)$$

where :

$$X = 10^{a(D_0 - D)}$$

A neutron-neutron log corrected for the well size is based on the equations described above.

The method described above that corrects for the well diameter before using the calibration curves was not used in our case. The calibration curves have been used to make a set of curves of $\log I_{nn}$ versus well diameter for different porosities. These curves are then used with interpolation in a computer program to calculate the porosity in one step from measured neutron intensity (I_{nn}) in API NU and caliper in mm. (Figure 14).

7. DATA PROCESSING

Computer is needed for processing of log data due to convenience and quick reasons. All the log results were originally analog, therefore, they had to be digitized to obtain the values possible for processing by the computer afterward. This was done by a digitizer.

7.1. Depth Correction

The error in depth of investigation always happens in logging operation. It is due to stretch of cable, backlash in paper drive system, slippage of paper on sheave, or accidental errors. A computer program called "DEPTH-COVARIANCE" is used to figure out this error. The program is based on the influence of variable log values, which any positive or negative changes in one will reflect in changes of the other. In practice, variable well size can influence the correlation between the resistivity and the neutron-neutron log responses considerably more than the real log response from the formations. The program computes a best value that can be used to set new depths. In our case, the caliper log is used as the reference. For the natural gamma ray log which was run with the same probe as the neutron-neutron log, its new depth is then set respected to the neutron-neutron log. After this correction, we obtained the better logs to be analyzed afterward.

7.2. Data Processing for Resistivity Log

After depth correction, the 16" and 64" normal resistivity log data were processed by three computer programs. The original data were apparent resistivity values, that is they are composed of the true rock resistivity, and the resistivity of the mud (or fluid). This apparent resistivity is the function of temperature. The three computer programs work as follows:

RTW Program: The program requires the input apparent resistivity file, caliper file, temperature file, and the resistivity of the mud at 23°C. The temperature log data should be taken at about the same time as the resistivity, and is used to calculate the resistivity of the fluid. The program corrects for the resistivity of the mud to obtain the apparent rock resistivity.

RTC0 Program: The program requires the input corrected resistivity file from the RTW program, and temperature file. The program computes for the true rock resistivity at 30°C.

RTC1 Program: The program requires the input corrected resistivity file from the RTC0 program, and undisturbed rock temperature file. The program computes for the true rock resistivity at equilibrium temperature, which is used in data analysis.

7.3. Data Processing for Natural Gamma Ray Log

The original natural gamma ray log data was in API GU after it had been digitized. A program called "SILICA" was used to correct for well size. The program requires the input original natural gamma ray file, and caliper file. This program also calculates for the silica content in the rocks. The data obtained from this program are corrected natural gamma ray in API GU, and silica content.

7.4. Data Processing for Neutron-Neutron Log

The original neutron-neutron log data was in API NU after it had been digitized. A program called "PORURK" was used to correct for the well size and it computes for the porosity in %, afterward. This program requires the original neutron-neutron file, and caliper file. The data obtained is porosity of rocks in %.

All the computer programs used for well size correction and calibration are based on the correction and calibration curves as described in chapter 5 and 6. But for the

resistivity log, the temperature factor is taken into consideration due to its effect to the resistivity of the mud.

7.5. Crossplots and Histograms

In our case, CROSSPLOT program is applied for the determination of m and a values in Archie's formula by resistivity-porosity crossplot (see to chapter 8.3). The program computes for the slope of a fitted straight line which represents the value of $-m$, and an intersection point on the $\log(R_0/R_w)$ axis represents the value of a . The program requires an input file of resistivity (in our case, corrected 16" resistivity files from RTC0 divided by fluid resistivity at 30°C were used) for y-axis, and a porosity file from PORURK for x-axis. The output files obtained are a plot file and a regression file which provide two sets of slopes and intersections on y-axis values from the two fitted lines based on deviation on x and y axes and it also computes for a value of correlation coefficient which indicates how close to the fitted line the scattering points of data are. The determination of m and a are calculated from the average of these two slopes.

Histograms are produced from a program called "STAT". The program computes for the frequency of values in desired certain intervals from an input file. The output files provide the relative comparison of all the counted values in these ranges.

7.6. Plotting Programs

Some plotting programs were used in final processing. The lithology and geophysical logs shown in Appendix-1, 2 and 3 were plotted by a program called "LOGPLOT". A program called "XPLOT" was used to plot the output files from the CROSSPLOT and STAT programs as shown by crossplot results (Appendix-3, 4, and 5) and the histograms.

8. RESULTS AND ANALYSIS

The log results have been shown in Appendix 1, 2, and 3 for wells RV-25, RV-28, and RV-32 respectively. Prior to any analysis of the log data, the conclusion of each logging method will be described as follows:

Resistivity log is used to determine the resistivity of the rocks. It normally shows the good relation to the neutron-neutron log.

Neutron-neutron log is used to determine the amount of hydrogen containing in the rocks either from the water in pores or the bound water in minerals.

Natural gamma ray log is used to determine the silica content in rocks for Icelandic igneous rock case.

8.1. Resistivity

In general, the log values obtained from 64" resistivity log should be larger than the ones from 16" resistivity log. But the situation is reversed in our case for all the wells which most of the 64" resistivity log values have been found less than the 16" resistivity ones. It is, theoretically, affected by the "bed thickness" that the beds are thinner than the spacing of the 64" resistivity log. Moreover, in our case, several intervals in all the wells show the resistivity values less than the resistivity of fluids (approximately 45 Ohm-m at 23°C). This should indicate the rock alteration as supported by the alteration data mentioned in chapter 3.5, and the 64" resistivity log values are therefore less than the values from 16" resistivity log.

The log analysis for resistivity in wells RV-25, RV-28 and RV-32 is based on the 16" resistivity log value which is however considerably more precise.

8.1.1. Distribution of Resistivity in Well RV-25

The mean value of the formation resistivity by the resistivity in well RV-25 is 33.9 ± 3.0 Ohm-m (standard deviation). As the range of resistivity values is large, it is more convenient to present the distribution of the resistivity on a logarithmic scale. The distribution of resistivity in well RV-25 can be divided into four groups as shown in Figure 18. Each group is marked by a number. Group 2 is however unclear. Group 3 and group 4 should represent the main rock types in the well which are basalt and hyaloclastite tuff whereas group 1 and group 2 should represent the altered rocks which have the resistivity values less than the fluid resistivity.

8.1.2. Distribution of Resistivity in Well RV-28

The mean value of the formation resistivity in well RV-28 is 49.0 ± 2.3 Ohm-m. The mean value is quite higher than in wells RV-25 and RV-32 and it should indicate less alteration effect. Figure 19 shows two distinct groups. Group 1 showing the resistivity values lower than the fluid resistivity should represent the alteration zones, and group 2 should represent the main rock types in the well i.e. basalt and hyaloclastite tuff. Most of dolerite and basaltic breccia have the resistivity values between 40 and 60 Ohm-m as shown by the resistivity log presented in Appendix-2.

8.1.3. Distribution of Resistivity in Well RV-32

The mean value of the formation resistivity in well RV-32 is 34.5 ± 3.1 Ohm-m. The distribution of resistivity can be divided into four groups as shown in Figure 20. Group 1 and group 2 show the resistivity values less than the fluid resistivity, again they should represent the alteration zones. Group 3 and 4 should represent dolerite and hyaloclastite tuff which are the main rock types in this well.

8.2. Porosity

Since fractured porosity has been found intensive in Icelandic igneous rocks, the distribution of porosity is not only controlled by the primary matrix porosity in rocks but also the fractures. Besides, the porosity from the neutron-neutron log determines not only the hydrogen content from water in pores but it includes the hydrogen from bound water in minerals. In consideration of the first case, the way of analysis should be based on the fact that different rock types provide different fracturing behaviors which implies difference in porosity.

8.2.1. Distribution of Porosity in Well RV-25

The mean value of porosity in well RV-25 is $24.9 \pm 9.6\%$ (standard deviation). Figure 21 shows two groups of porosity distribution. Group 1, the peak is broad but should however represent basalt and hyaloclastite tuff which are the main rock types in this well whereas group 2 which is unclear distinguished from group 1 should indicate hyaloclastite tuff in some intervals that show higher porosity, as it is also shown on the porosity log presented in Appendix-1.

8.2.2. Distribution of Porosity in Well RV-28

The mean value of porosity in well RV-28 is $25.9 \pm 9.1\%$. The distribution of porosity shown in Figure 22 can be divided into three groups. Group 2 and group 3 should represent the main rock types of this well i.e. basalt and hyaloclastite tuff whereas group 1 should represent dense formations which are mostly basalt in some intervals shown on the porosity log in Appendix-2.

8.2.3. Distribution of Porosity in Well RV-32

The mean value of porosity in well RV-32 is $21.5 \pm 10.9\%$. There are 3 groups of porosity distribution (Figure 23). As

also shown on the porosity log presented in Appendix-3, Group 1 should represent dolerite which is the main rock type in this well whereas group 2 and group 3 should represent the combination of various rock types, mostly hyaloclastite tuff, basaltic breccia. Since the mean porosity in this well is the lowest value comparing with wells RV-25 and RV-28, and the main rock type is dolerite which is far less abundant in the other two wells, it should be able to state that dolerite provides the lowest porosity in these wells for overall consideration.

8.3. Resistivity-Porosity Relation

Archie's formula, a well-known formula explaining the relation between formation resistivity factor and porosity, can be written in the following form:

$$F = R_0/R_W = a \times \phi^{-m}$$

where: F = formation resistivity factor

R_0 = formation resistivity

R_W = resistivity of fluid

a = constant (usually about 1 in sedimentary rocks)

ϕ = porosity

m = cementation factor

It has been shown that the exponent m in Archie's formula is close to 1 for fractured crystalline rocks, whereas the value 2 seems to be valid for non-fractured rocks. For Icelandic basalt, in most cases, the value of m is close to 1 (Stefánsson and Tulinius, 1983).

The determination of m and a is obtained from a conventional crossplot on log-log scales, R_0/R_W against ϕ . In our case, R_0/R_W at 30°C is used. The equations explaining the determination of m and a are described as follows:

From: $R_0/R_W = a \times \phi^{-m}$

we obtain:

$$\log(R_0/R_W) = \log(a) - m \times \log(\phi)$$

where R_0 is represented by resistivity of rock at 30°C and R_W is the resistivity of fluid at 30°C (44 Ohm-m for all the wells of our investigation).

For each scattering data point from the crossplot, a straight line is fitted to the data points, and an exponent m and a constant a in Archie's formula are determined. The intersection of the fitted line on the $\log(R_0/R_W)$ indicates a value, and its slope represents the value of m .

The resistivity-porosity relation in wells RV-25, RV-28 and RV-32 has been studied separately for each geological unit based on the lithology log available and neglecting low resistivity zones that are considered as the alteration zones.

The results from resistivity-porosity crossplots have been presented in Appendix-4, 5 and 6 for wells RV-25, RV-28 and RV-32 respectively. The results in most cases show low values of the correlation coefficients which indicates scattering in crossplot, but the coefficients m and a , however, show moderate consistency for each rock unit. It is difficult to state that the low values of correlation coefficients indicate unusable data since some consistency have been pronounced. At least, they imply some useful points of view for analysis.

8.3.1. Resistivity-Porosity Crossplots in Well RV-25

Two depth intervals of basalt in RV-25 have been selected for analysis. Basalt-1 represents the depth interval 100-330 meters, basalt-2 represents the depth interval 830-1,630 meters. Hyaloclastite tuff has been selected from depth interval 850-1,550 meters, dolerite from depth interval

1,190-1,450 meters, and fine-grained sediment from depth interval 200-300 meters. In case of basaltic breccia, all intervals are in the low resistivity zones, it is therefore neglected by the reason mentioned above.

Table 5 shows the coefficients in Archie's formula determined from resistivity-porosity crossplot results in Well RV-25 (presented in Appendix-4). In basalt-1, the value of m has been found close to 1, with the a value not close to 1. This indicates fractured porosity. For basalt-2, the value of m equivalent to 1.75 (close to 2) seems to indicate matrix porosity but the value of a is too high that disagree with the a value of matrix porosity which is about 1. Hyaloclastite has been found in the similar case as basalt-2, with high a and m values. Dolerite and fine-grained sediment have been found to provide fractured porosity as well as the basalt-1 that the values of m are close to 1 and the a values not close to 1.

8.3.2. Resistivity-Porosity Crossplots in Well RV-28

Basalt from two depth intervals has been selected, depth interval 100-390 meters for basalt-1 and 750-1,230 meters for basalt-2. Hyaloclastite tuff is also from two depth intervals, depth interval 100-420 meters for hyaloclastite tuff-1, and 1,050-1,080 meters for hyaloclastite-2. Dolerite is from depth interval 850-1,000 meters, fine-grained sediment from depth interval 250-380 meters, basaltic breccia from depth interval 770-1,350 meters.

Table 6 shows the coefficients in Archie's formula determined from resistivity-porosity crossplot results in Well RV-28 (presented in Appendix-5). In basalt-1, basalt-2, hyaloclastite tuff-1, fine-grained sediment and basaltic breccia, their coefficients m and a indicates fractured porosity. For hyaloclastite tuff-2, as well as the hyaloclastite tuff in Well RV-25, shows the high values of m and a , and also the disagreement in each other. In case of dolerite, the

coefficients likely indicate fractured porosity although the m value is quite high. This is due to consideration with wells RV-25 and RV-32.

8.3.3. Resistivity-Porosity Crossplots in Well RV-32

Basalt in well RV-32 was selected from depth interval 140-230 meters. Hyaloclastite tuff is from depth interval 580-780 meters, dolerite from depth interval 820-1,280 meters, and fine-grained sediment from depth interval 100-230 meters. For basaltic breccia and coarse-grained sediment, most of which are in the low resistivity zones and therefore neglected.

Table 7 shows the coefficients in Archie's formula determined from resistivity-porosity crossplot results in well RV-32 (presented in Appendix-6). The values of coefficients m and a for basalt, hyaloclastite tuff, dolerite and fine-grained sediment all indicate fractured porosity. The consistency in m and a values for various rock units in this well is higher comparing with wells RV-25 and RV-28.

8.3.4. Correlation of Archie's Coefficients among Wells RV-25, RV-28 and RV-32

Table 8 and 9 show the conclusion of the Archie's coefficients for wells RV-25, RV-28 and RV-32. The coefficients m and a for basalt in all the wells show the m values close to 1, whereas the a values rather close to 2, except for basalt-2 in well RV-25, showing the m close to 2 and a close to 3. Hyaloclastite tuff in all the wells provides the highest values of m and a , except for hyaloclastite tuff-1 in well RV-28 that shows the m close to 1 and a close to 2. Dolerite has been found to have the values close to 1.5 for the m , and 2.5 for the a . Fine-grained sediment shows the m close to 1, and the a for RV-25 and RV-32 close to 2, but in RV-28 is about 1.4. For the overall consideration, in most cases, the rock units are of fractured porosity, and no distinct

indication of matrix porosity has been found.

8.4. Silica

The relationship between the gamma ray intensity and the SiO₂ content of Icelandic rocks has been found that for the tholeiitic trend, there is a linear relationship between the gamma ray intensity and the silica content of the rocks. The empirical relation:

$$\text{SiO}_2 = 0.264 \times I_0 + 40.6\%$$

has been found applicable for crystalline rocks in many locations in Iceland. The SiO₂ is in percent and I₀ is the gamma intensity in API GU corrected for the well diameter.

8.4.1. Distribution of Silica Content in Well RV-25

The mean value of silica content in well RV-25 is 48.6 ± 2.7% (standard deviation). The silica distribution shows one distinct peak having silica content of 46-50% (Figure 24). It represents the rock of basaltic composition. It can be basalt, hyaloclastite tuff, or dolerite. There are some silica layers showing high silica content up to 68% (maximum). This indicates intermediate-acid rocks, or silica-rich alteration layers. According to the natural gamma ray log presented in Appendix-1, the high gamma ray peaks have been found in dolerite and hyaloclastite tuff units. However, andesite (52-64% of SiO₂ content) has been found from the drillcuttings in Well RV-39 at depth interval approximately 1,700-2,000 meters, but no logging measurement.

8.4.2. Distribution of Silica Content in Well RV-28

The mean value of silica content in well RV-28 is 48.5 ± 1.7%. Figure 25 shows one distinct peak as well as in well RV-25. The peak indicates the silica content of 46-50% corresponding to the basaltic composition. High silica content of about 74-76% that represents acid rocks has been found in the natural gamma ray log presented in Appendix-2.

This gamma ray peak is in a basalt unit. The intermediate or acid rocks are, however, not found in the lithology log.

8.4.3. Distribution of Silica Content in Well RV-32

The mean value of silica content in well RV-32 is $50.7 \pm 2.3\%$. The distribution of silica as well as in wells RV-25 and RV-28, shows one distinct peak (Figure 26) representing the rocks of basaltic composition. The silica content in well RV-32 shows higher values than the ones in wells RV-25 and RV-28. In this consideration, dolerite is the main rock type in this well and far less abundant in the other two wells, it should therefore indicate that dolerite obtain higher silica content than the other rock types of basaltic composition in all of these wells. There are some hyaloclastite tuff and dolerite units in the well showing moderately high gamma ray as shown in the natural gamma ray log presented in Appendix-3. The maximum silica content of 64% indicating intermediate rocks is not shown in the lithology log.

9. DISCUSSION

The lithology logs in most cases shows large bed thickness which there might be some small interbeddings of different rock units. Some log values selected for crossplot analysis might not represent the true rock units, although they are carefully selected. The disagreement on the Archie's coefficients between the two hyaloclastite tuff units in well RV-28 should be a reason. Some difficulties arose when analyzing the coefficients m and a separately for each well, but some distinct implications have been found when they were grouped and correlated among each others.

The resistivity log results show the less value of the formation resistivity than the fluid resistivity in many intervals of these wells. In this consideration, other than the influence of rock alteration, the parasite tool responses might occur due to poor contact of the potential electrode at the mud pit.

The neutron-neutron log used in our investigation is one type of single detector, thus the corrected log data is only based on the calibration curves. If compensated neutron-neutron log (double detectors) was used instead, error in calculation for the well size correction would be reduced, resulting in more precise log data. Besides, it also reflects in better results in determination of the coefficients m and a in Archie's formula.

Several intervals, the porosity from the neutron-neutron log have been found very high (>30%) either in low resistivity zones or normal zones. From the result and analysis the main rock porosity is fractured, but the alteration effect producing bound-water in minerals must be taken into consideration.

The silica distribution from the natural gamma ray log has been found well corresponding to the lithology log that

indicates the main rock type of basaltic composition. There are some peaks on the natural gamma ray log presented in Appendix-1, 2 and 3. They indicate high silica content corresponding to intermediate-acid rocks which are not found in lithology log. In this consideration, the high silica content are probably of some silica-rich layers caused by accumulation of free silica in those layers. Density log might be useful to distinguish the free silica from the primary silica in the rocks themselves by the difference in density between basic and acid rocks.

10. CONCLUSIONS AND RECOMMENDATIONS

1. The log results have been found to be reliable.
2. The mean values of resistivity, porosity and silica content distribution in wells RV-25, RV-28 and RV-32 have been concluded in Table 10.
3. The coefficients m and a in Archie's formula from cross-plots, R_0/R_w against ϕ , in most cases indicates fractured porosity for all the wells of investigation. The range of m value is about 1-1.5, and a value about 1.5-2.5 for basalt, dolerite, fine-grained sediment, and basaltic breccia.
4. Hyaloclastite tuff in all wells, except hyaloclastite tuff-1 in well RV-28, provide the relatively highest values of m and a , and the values are considerably unreliable.
5. The values of m and a show moderate consistency for each rock unit.
6. Resistivity log indicates the alteration zones in these wells. The crossplot analysis has been neglected to use the data from these alteration zones.
7. The compensated neutron-neutron log is recommended for more precise log results.
8. Silica content from the natural gamma ray log indicates the main rock types in these three wells being in basaltic composition (45-52%).
9. Density log is recommended to determine the high gamma ray peaks.
10. "Thin bed thickness" strongly influences the 64" resistivity log response.
11. The mean value of resistivity distribution in RV-28 is higher than RV-25 and RV-32 due to less alteration effect.
12. Dolerite, the main rock unit in well RV-32, shows relatively the lowest porosity in that well, and it shows higher silica content than the other rock units of basaltic composition.
13. The geophysical logs and lithology log are well correlated in the large scale.

ACKNOWLEDGEMENTS

My gratitude is expressed to the UNU Geothermal Training Programme for acceptance of my participation in the specialized training course. My thanks to Hilmar Sigvaldason, my adviser for his great supervising, to Helga Tulinius for her useful informal lecture, knowledge about computer and revision of this report, to Sugiarto Ganda for consultation about hydrothermal alteration in well RV-39, to Jón-Steinar Guðmundsson for some special advice and guidelines on writing reports, to the UNU Geothermal Training Programme staff for their kind assistance of the office work. My thanks are also extended to the staff of the Borehole Geophysics Department for the great valuable training during the course. And special thanks are due to UNU fellows 1987 for the good time cooperation during doing the report.

NOMENCLATURE

A	=	current electrode in resistivity log investigation.
\overline{AM}	=	distance between the current electrode A and the potential electrode M in resistivity log investigation (m).
A_p	=	borehole absorption function (dimensionless).
a	=	particular constant for neutron-neutron probe (dimensionless).
a	=	constant in Archie's formula (dimensionless).
b	=	particular constant for neutron-neutron probe (dimensionless).
CF	=	correction factor of the natural gamma ray log (dimensionless).
D	=	well diameter (mm).
D_0	=	fixed well diameter (mm).
I	=	electrical current magnitude (ampere).
I_{nn}	=	neutron intensity (API NU).
I_0	=	true gamma ray intensity (API GU).
M	=	potential electrode in resistivity log investigation.
m	=	exponent in Archie's formula (dimensionless).
N	=	concentration of atoms (atoms/cm ³).
N	=	mean counting rate (cps).
R	=	radius of the borehole (cm).
R	=	apparent resistivity (Ohm-m).
R_s	=	radius of the neutron-neutron probe (cm).
R_w	=	fluid resistivity (Ohm-m).
R_0	=	formation resistivity (Ohm-m).
r	=	distance between the current electrode and the potential electrode in resistivity log investigation (m).
T	=	time constant (sec).
V	=	electrical potential (volt).
V_M	=	electrical potential at position M (volt).
α	=	alpha.
μ	=	effective mass absorption coefficient for drilling

		fluid (g/cm ³).
ξ	=	energy loss per collision (MeV/collision).
ρ	=	fluid density (g/cm ³).
σ_C	=	average collision cross-section (cm ²).
ϕ	=	porosity (%).

Units

API GU	=	American Petroleum Institute gamma ray unit.
API NU	=	American Petroleum Institute neutron unit.
cm	=	centimeter.
cm ²	=	square centimeter.
cm ³	=	cubic centimeter.
cps	=	counts per second.
eV	=	electron volt.
ft	=	foot.
g	=	gram.
Hz	=	Hertz.
MeV	=	mega-electron volt.
km/s	=	kilometers/second.
m	=	meter.
mA	=	milliampere.
min	=	minute.
mm	=	millimeter.
mV	=	millivolt.
Ohm-m	=	Ohm-meter.
ppm	=	parts per million.
sec	=	second.
°C	=	degree Centigrade.
°F	=	degree Fahrenheit.
%	=	percent.
μ Ci	=	3.7×10^4 disintegrations/second of the radioactive decay.

Abbreviations

AC	=	alternating current.
API	=	American Petroleum Institute.
CCL	=	casing collar locator.
DC	=	direct current.
DTM	=	differential temperature module.
ELM	=	electric log module.
GOI	=	Gearhart-Owen Industries Inc.
GM	=	Geiger-Müller.
GU	=	gamma ray unit.
LPM	=	line power module.
NU	=	neutron unit.
RMM	=	rate meter module.
RTD	=	resistance temperature detector.
SDP	=	total slowing down power of atom.

REFERENCES

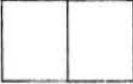
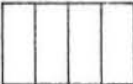
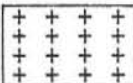
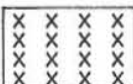

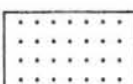
- Czubek, J. A., (1981a): Some Aspects of Nuclear Well Logging in Igneous Rocks, National Energy Authority, Reykjavik, Iceland, 77 pp.
- Ganda, S., (1987): Alteration History in Well RV-39, Reykjavik, Iceland, UNU report (inprep).
- GOI, (1975): ELM202 Electric Log Module Installation Manual, Gearhart-Owen, Industries, Inc., Texas, U.S.A., 17 pp.
- GOI, (1977): GR-CCL-NEUTRON Logging System Operator's Manual, Section-2, Gearhart-Owen, Industries, Inc., Texas, U.S.A., pp. 17-31.
- GOI, (1978): Formation Evaluation Data Handbook, Gearhart-Owen, Industries, Inc., Texas, U.S.A., 237 pp.
- OMEGA, (1986): Complete Temperature Measurement Handbook and Encyclopedia, Omega Engineering, Inc., Stamford, Connecticut, U.S.A., pp. T5-T22.
- Schlumberger, (1972): Log Interpretation Volume 1 Principles, Schlumberger Limited, New York, U.S.A., 113 pp.
- Serra, O., (1984): Fundamental of Well-Log Interpretation 1. The acquisition of logging data, Elsevier Science Publishing Company Inc., New York, U.S.A., 423 pp.
- Serra, O., (1986): Fundamental of Well-Log Interpretation 2. The interpretation of logging data, Elsevier Science Publishing Company Inc., New York, U.S.A., 684 pp.
- Sethi, D.K. and Fertl, W.H., (1980): Geophysical Well Logging Operations and Log Analysis in Geothermal Well Desert Peak No. B-23-1, informal report, Dresser Atlas, Dresser Industries, Inc., Houston, Texas, U.S.A., 74 pp.
- Stefánsson, V. and Steingrímsson, B., (1981): Geothermal Logging 1 - An Introduction to Techniques and Interpretation, National Energy Authority, Reykjavik, Iceland, 117 pp.

Stefánsson, V. and Tulinius, H., (1983): Geophysical Logs from Lopra-1 and Vestmanna-1, report No.OS83088/JHD18, National Energy Authority, Reykjavik, Iceland, 123 pp.

Tómasson, J., Thorsteinsson, Þ., Kristmannsdóttir, H. and Friðleifsson, I.B., (1977): Reykjavík Area Geothermal Exploration 1965-1973, National Energy Authority - Reykavík District Heating Service, Reykjavík, Iceland, 109 pp.

APPENDIX 1 - Lithology and geophysical logs in well RV-25

RV-25 : LITHOLOGICAL EXPLANATION

	Fresh basalt
	Altered basalt
	Dolerite intrusion
	Basaltic breccia
	Hyaloclastite tuff
	Fine-grained sediments

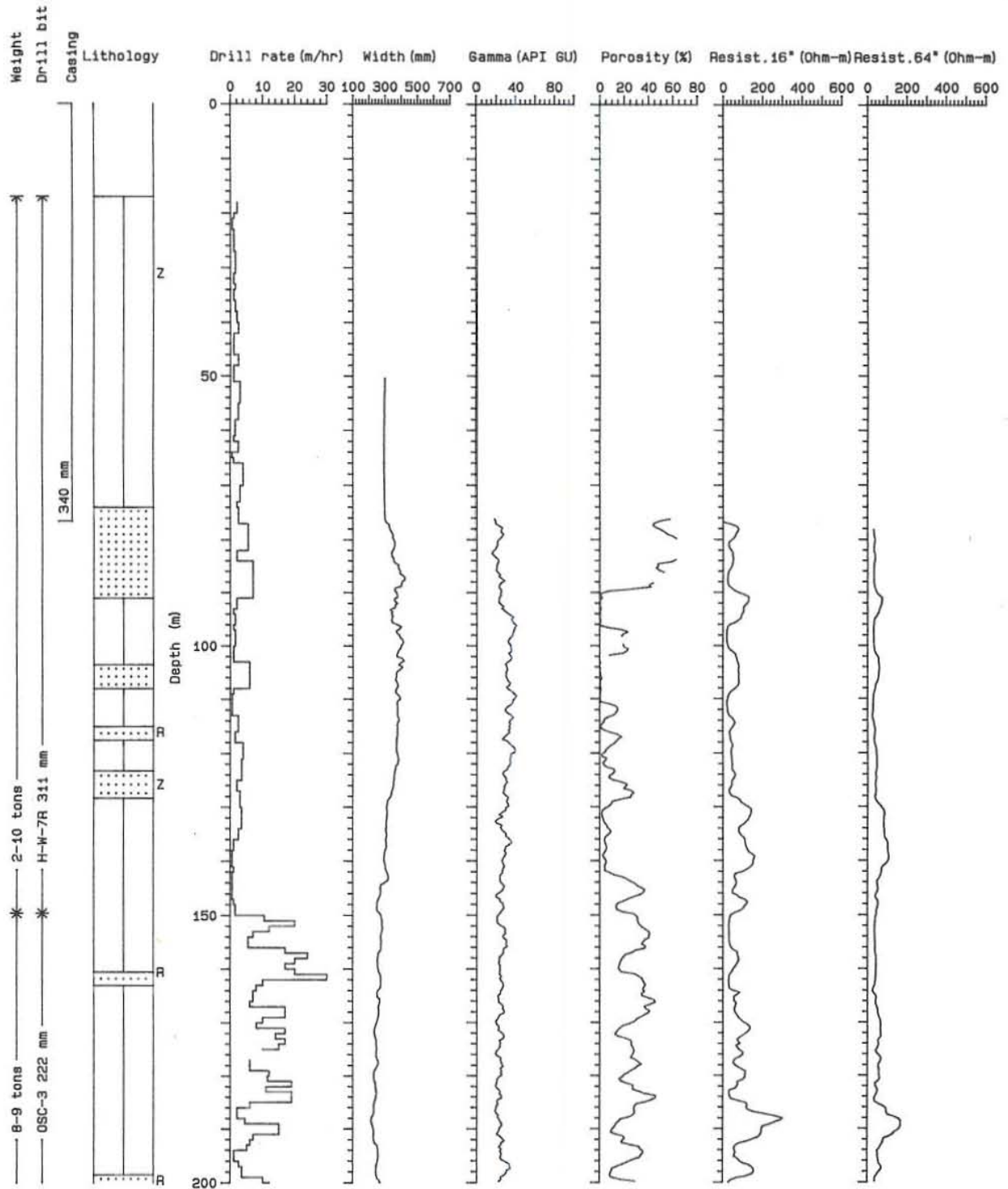
R : Red intercalation

Z : Zeolite

E : Epidote

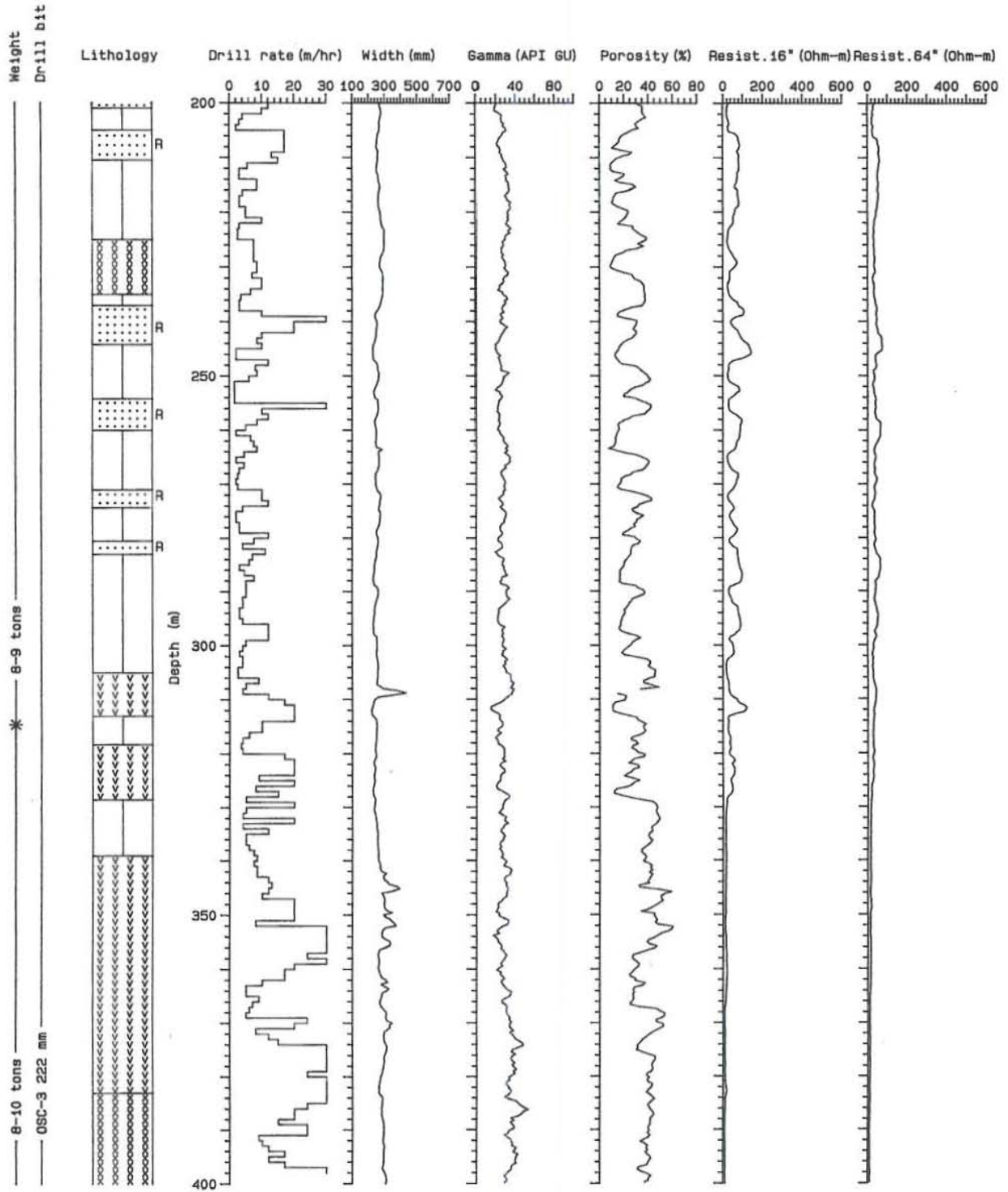
REYKJAVÍK WELL NUMBER RV-25

LITHOLOGY AND GEOPHYSICAL LOGS : DEPTH INTERVAL 0 TO 200 METERS



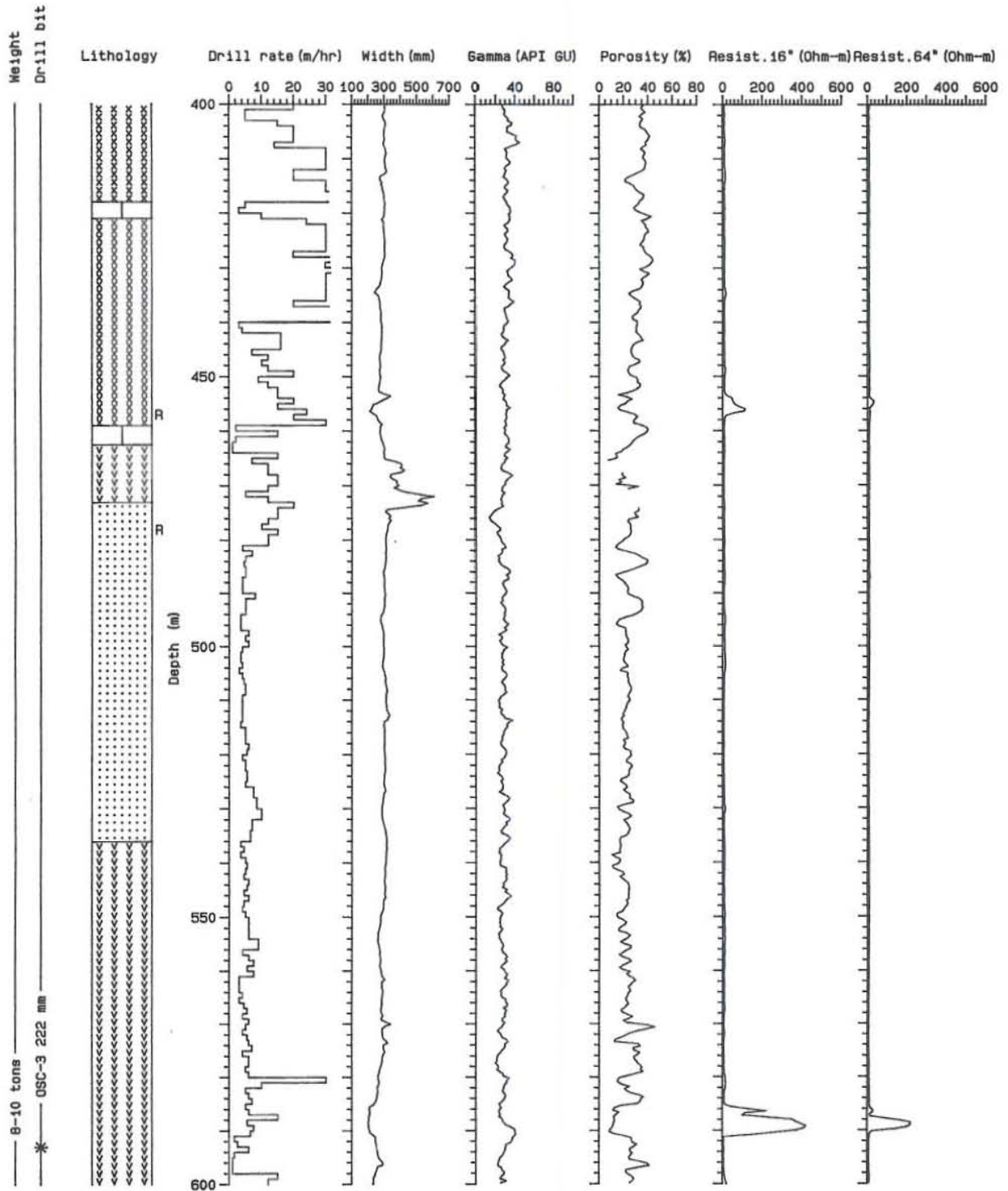
REYKJAVÍK WELL NUMBER RV-25

LITHOLOGY AND GEOPHYSICAL LOGS : DEPTH INTERVAL 200 TO 400 METERS



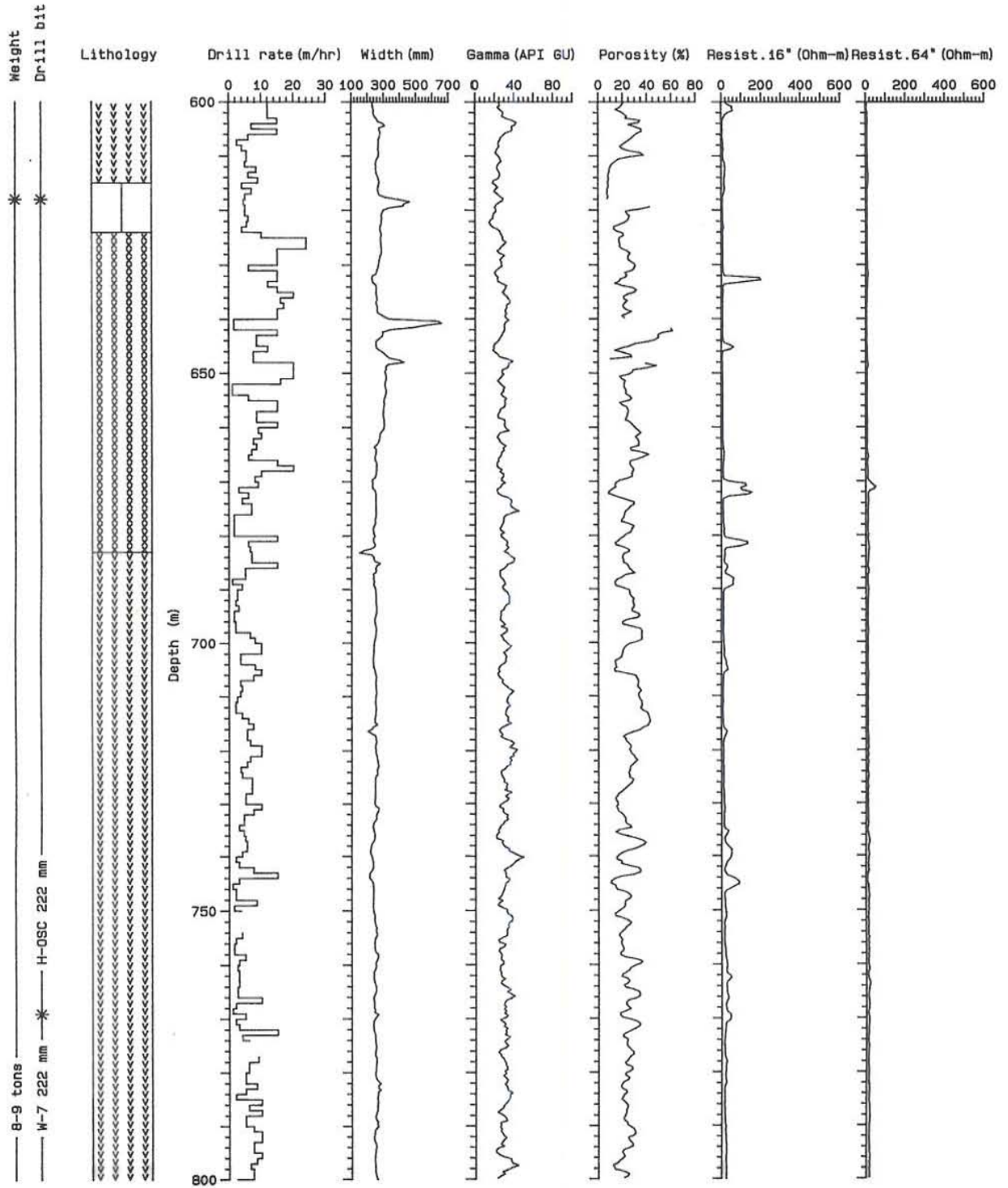
REYKJAVÍK WELL NUMBER RV-25

LITHOLOGY AND GEOPHYSICAL LOGS : DEPTH INTERVAL 400 TO 600 METERS



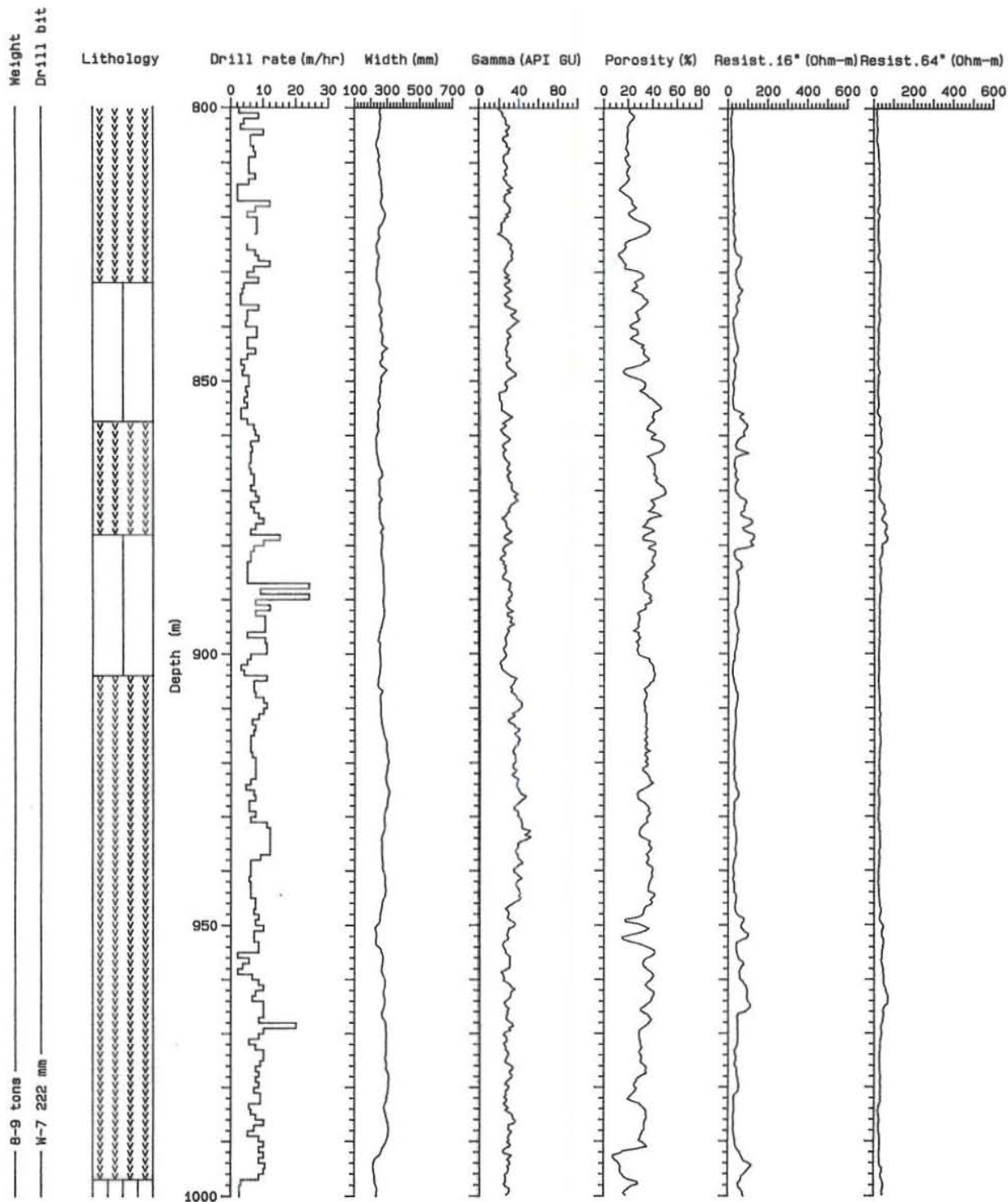
REYKJAVÍK WELL NUMBER RV-25

LITHOLOGY AND GEOPHYSICAL LOGS : DEPTH INTERVAL 600 TO 800 METERS



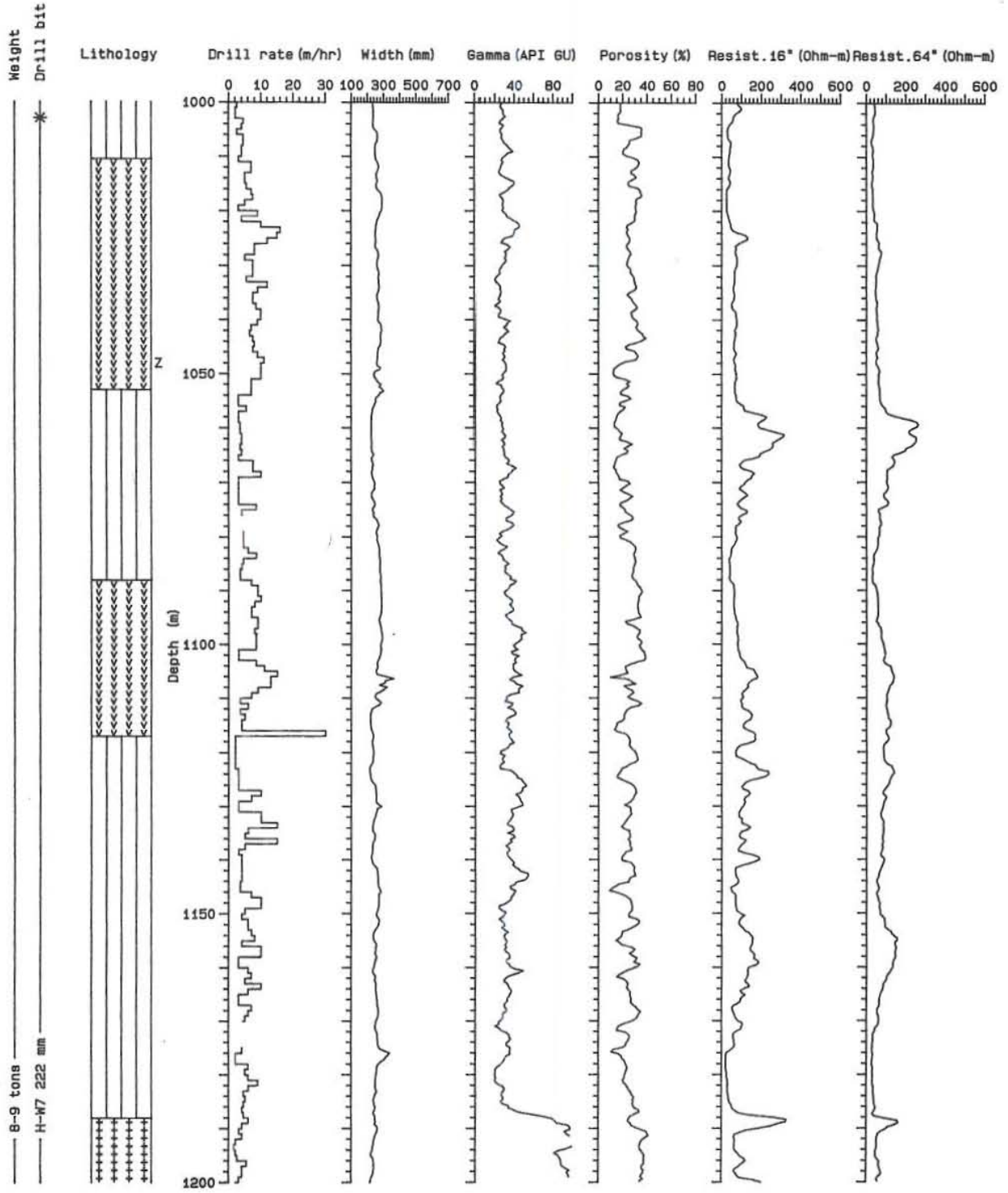
REYKJAVÍK WELL NUMBER RV-25

LITHOLOGY AND GEOPHYSICAL LOGS : DEPTH INTERVAL 800 TO 1000 METERS



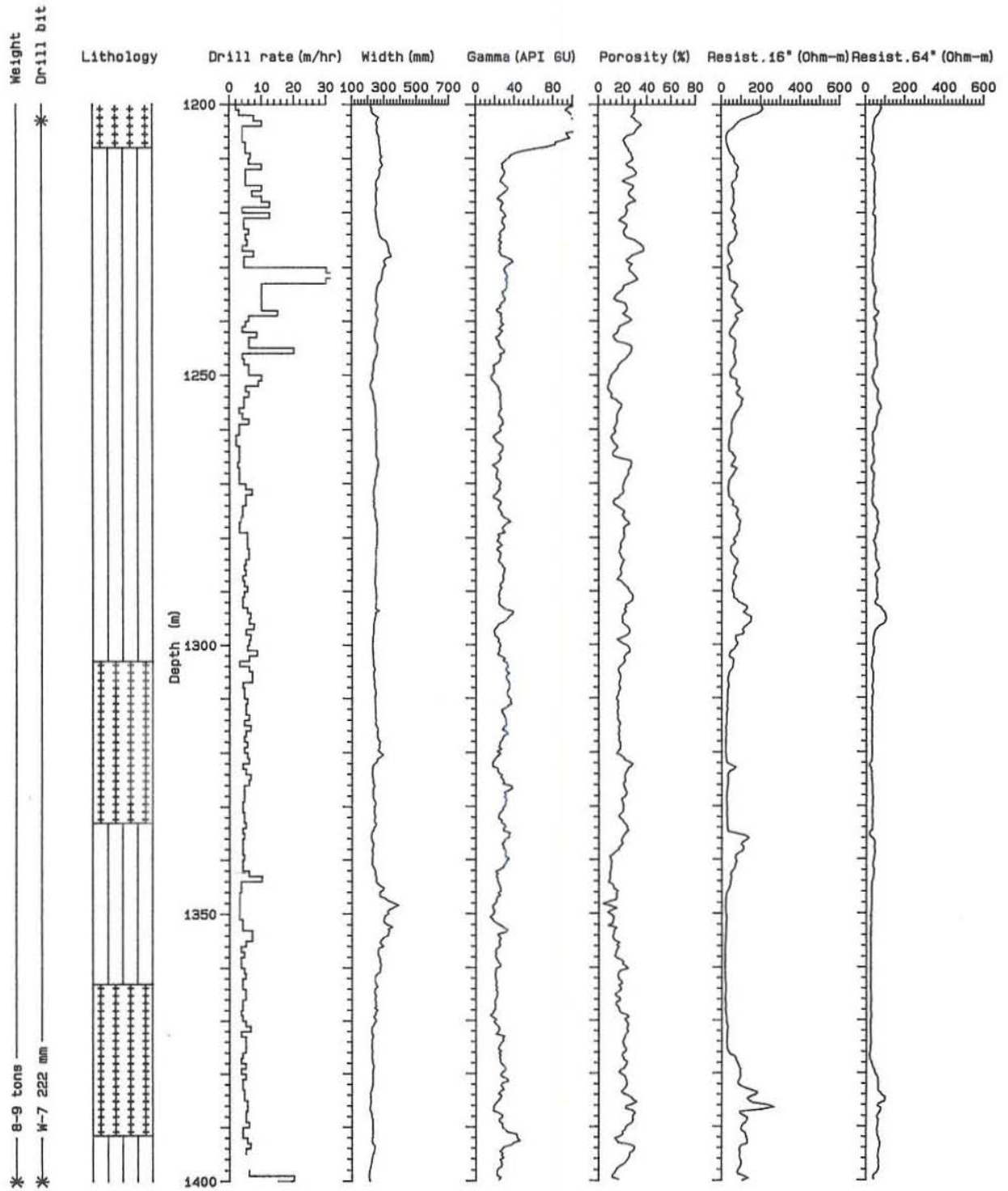
REYKJAVÍK WELL NUMBER RV-25

LITHOLOGY AND GEOPHYSICAL LOGS : DEPTH INTERVAL 1000 TO 1200 METERS



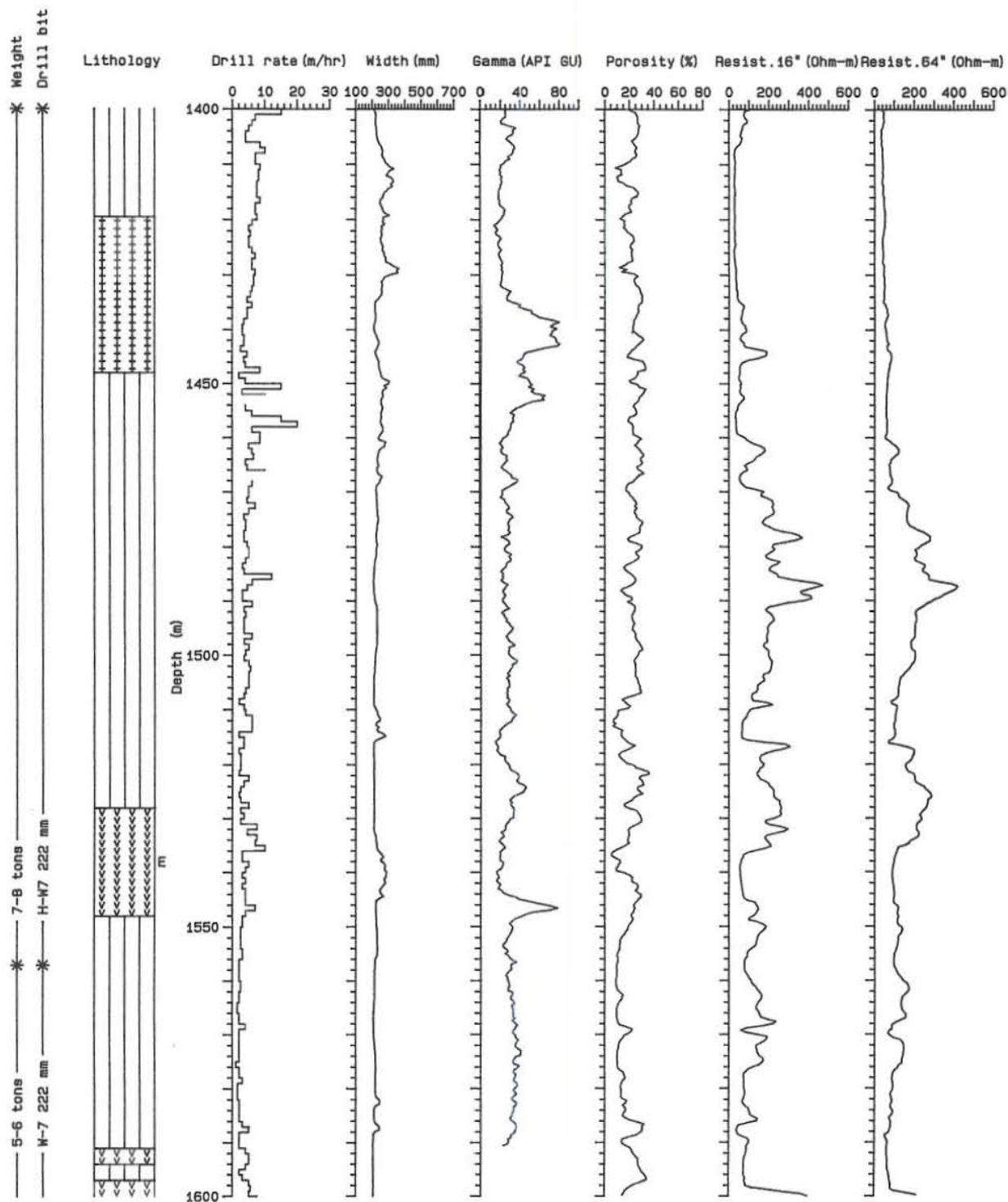
REYKJAVÍK WELL NUMBER RV-25

LITHOLOGY AND GEOPHYSICAL LOGS : DEPTH INTERVAL 1200 TO 1400 METERS



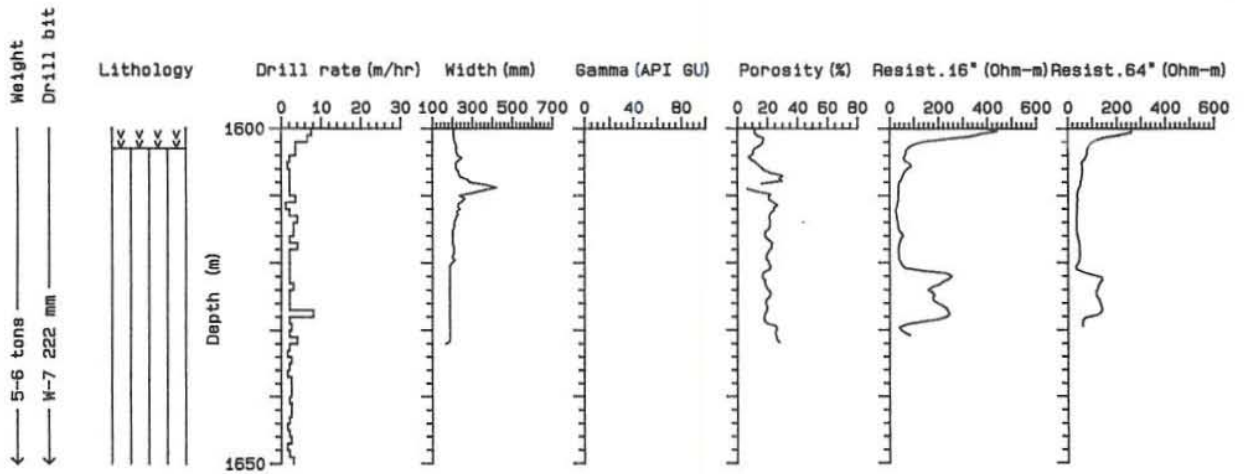
REYKJAVÍK WELL NUMBER RV-25

LITHOLOGY AND GEOPHYSICAL LOGS : DEPTH INTERVAL 1400 TO 1600 METERS



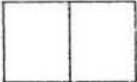
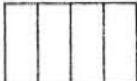
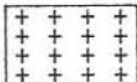
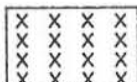



REYKJAVÍK WELL NUMBER RV-25

LITHOLOGY AND GEOPHYSICAL LOGS : DEPTH INTERVAL 1600 TO 1650 METERS



APPENDIX 2 - Lithology and geophysical logs in well RV-28

RV-28 : LITHOLOGICAL EXPLANATION

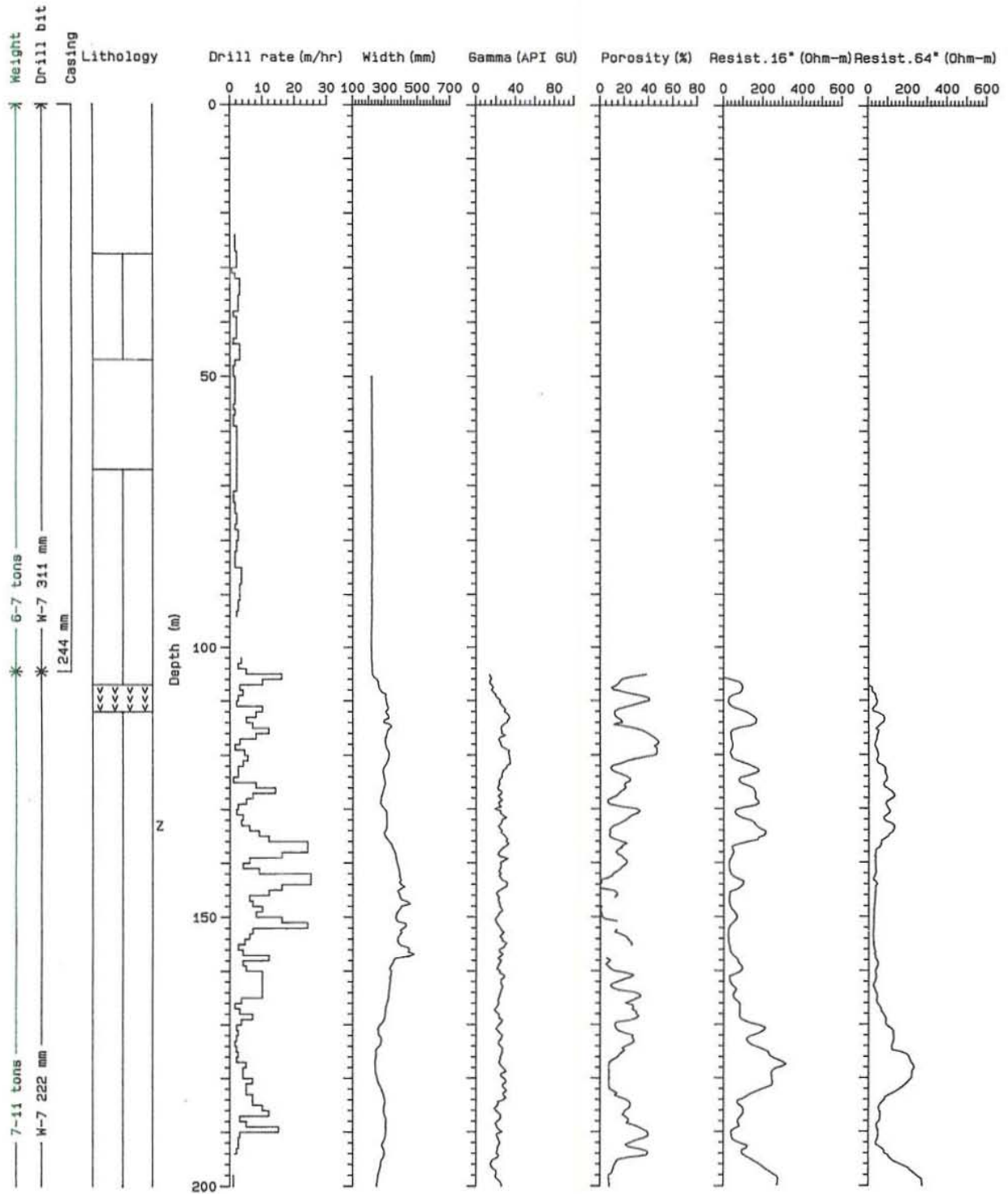
	Fresh basalt
	Altered basalt
	Dolerite intrusion
	Basaltic breccia
	Hyaloclastite tuff
	Fine-grained sediments
	No cuttings

R : Red intercalation

Z : Zeolite

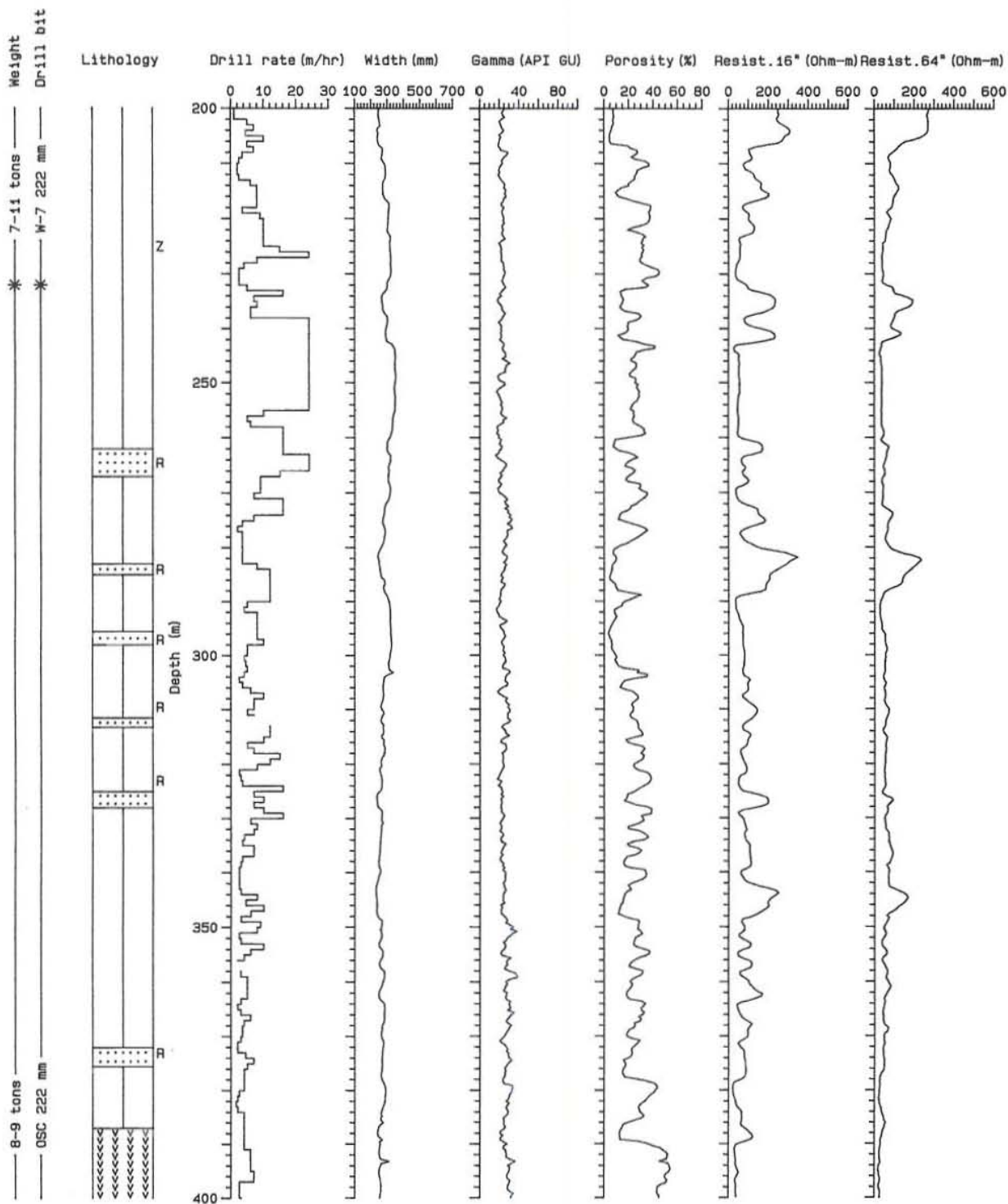
REYKJAVÍK WELL NUMBER RV-28

LITHOLOGY AND GEOPHYSICAL LOGS : DEPTH INTERVAL 0 TO 200 METERS



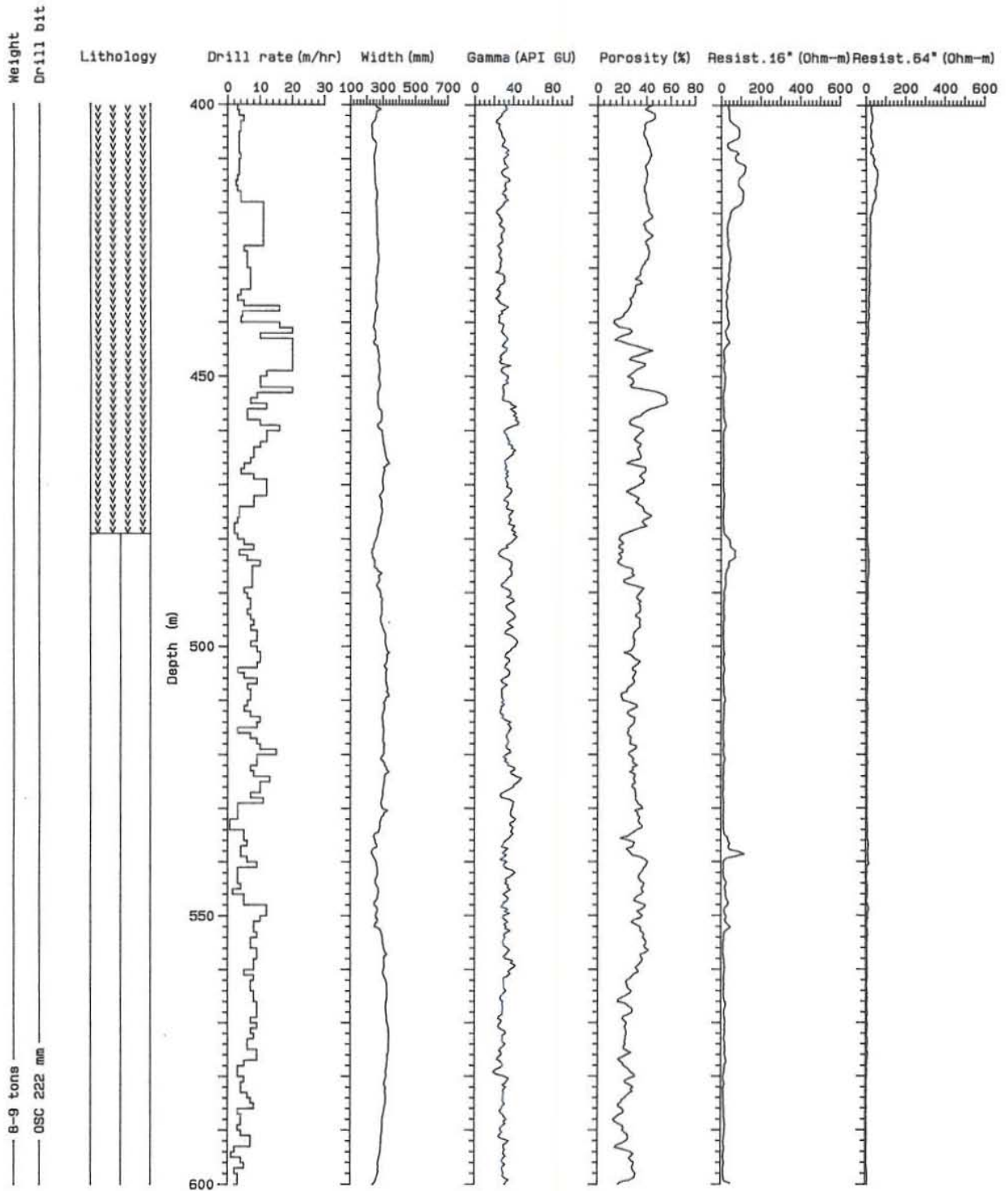
REYKJAVÍK WELL NUMBER RV-28

LITHOLOGY AND GEOPHYSICAL LOGS : DEPTH INTERVAL 200 TO 400 METERS



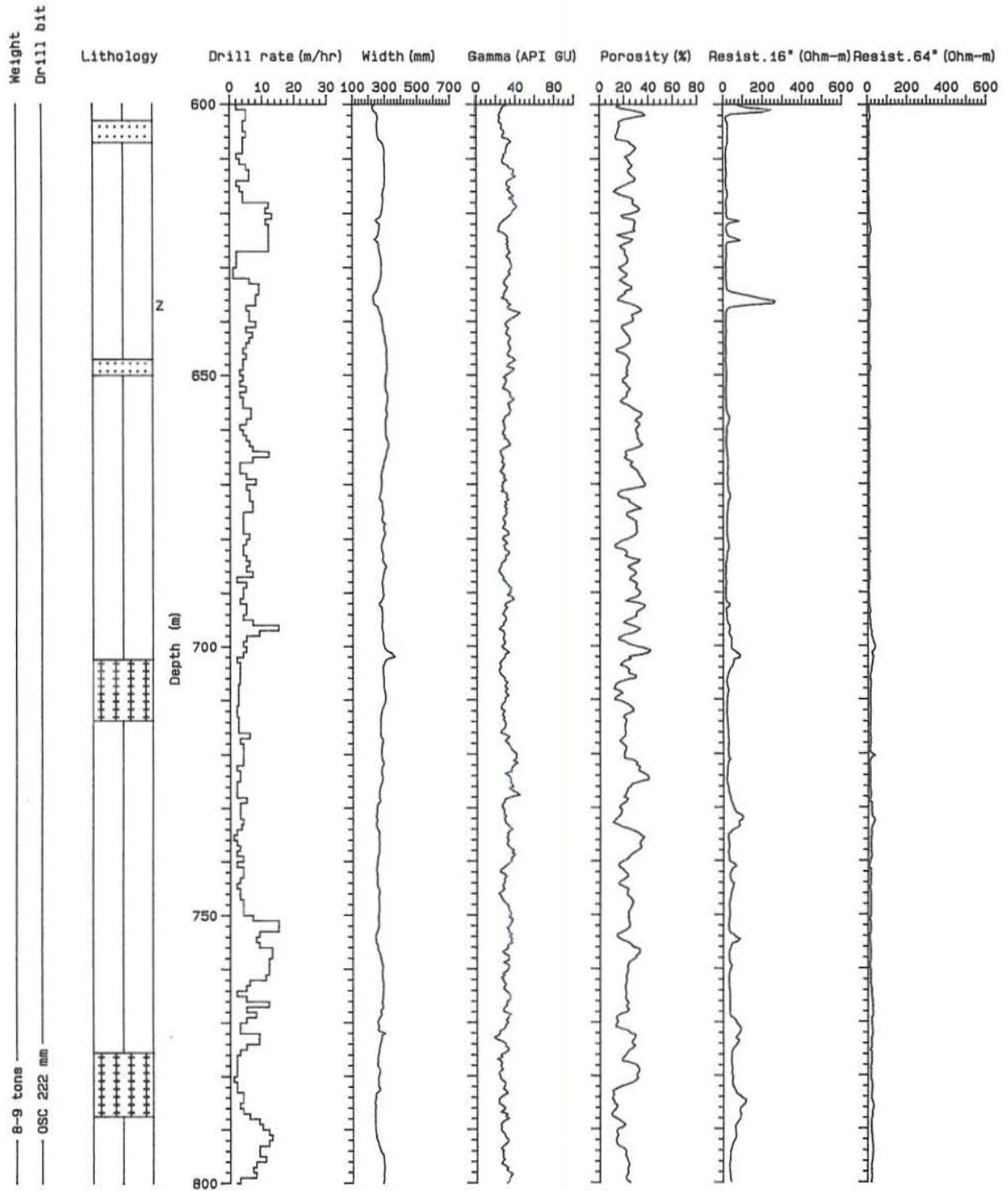
REYKJAVÍK WELL NUMBER RV-28

LITHOLOGY AND GEOPHYSICAL LOGS : DEPTH INTERVAL 400 TO 600 METERS



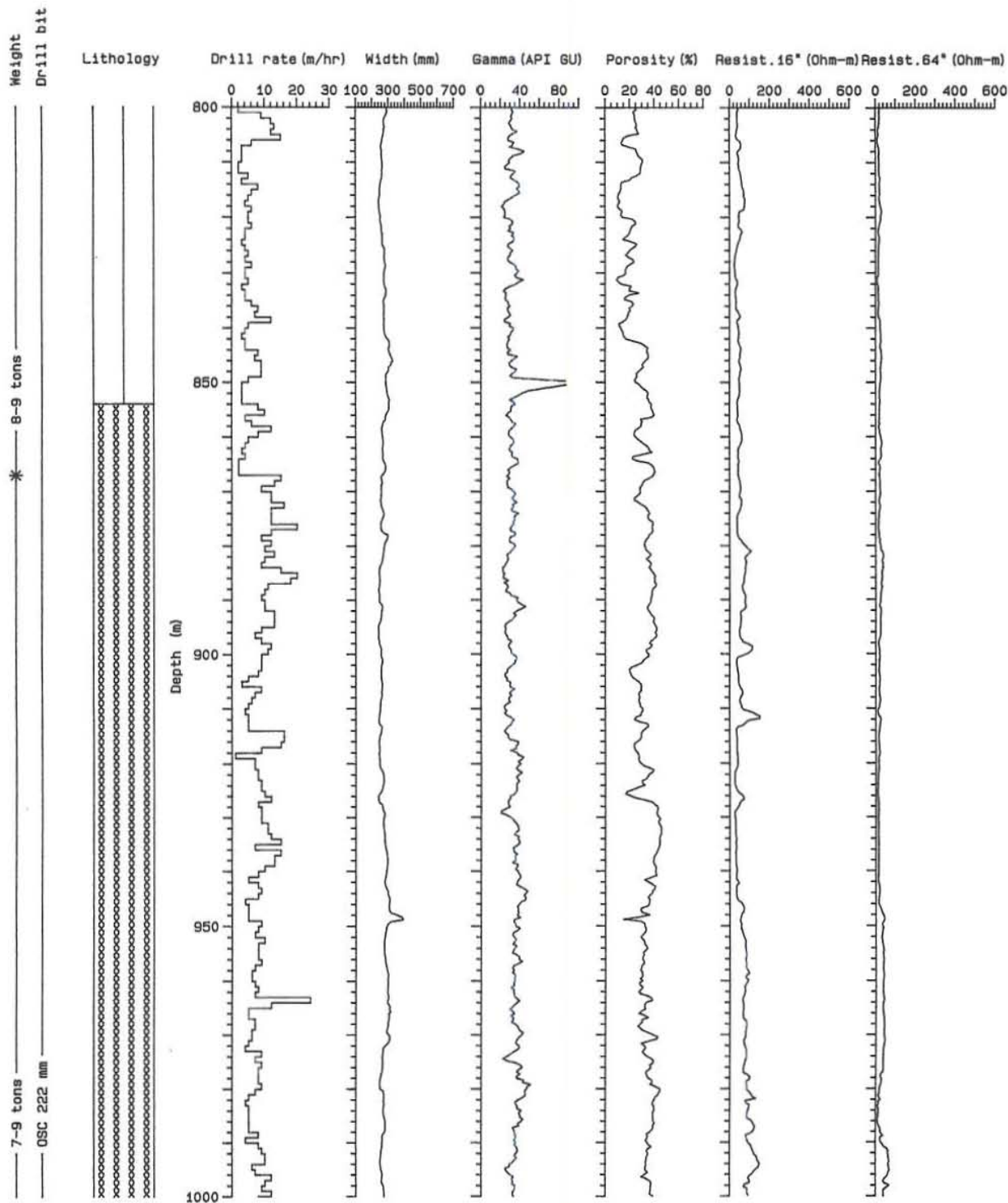
REYKJAVÍK WELL NUMBER RV-28

LITHOLOGY AND GEOPHYSICAL LOGS : DEPTH INTERVAL 600 TO 800 METERS



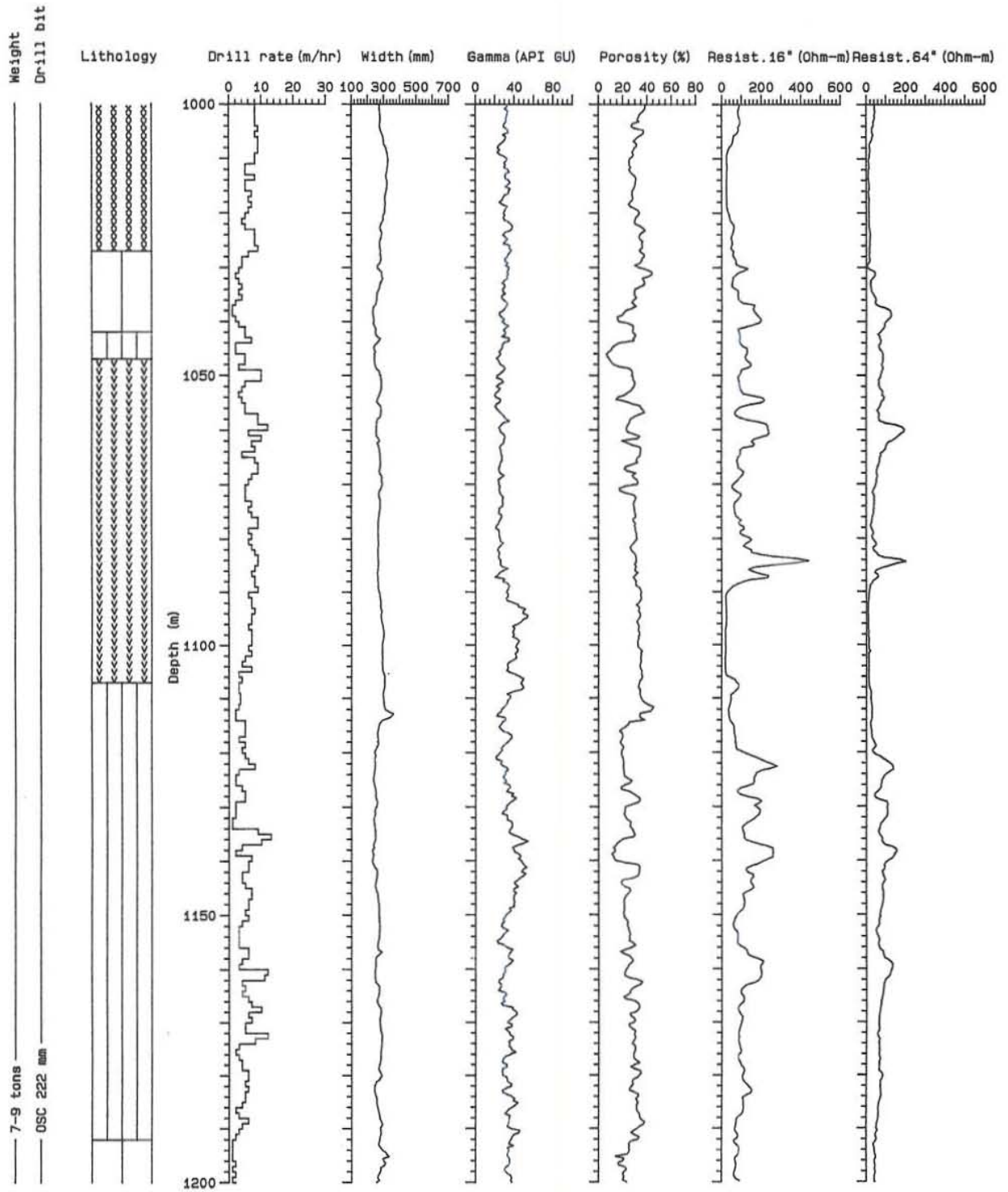
REYKJAVÍK WELL NUMBER RV-28

LITHOLOGY AND GEOPHYSICAL LOGS : DEPTH INTERVAL 800 TO 1000 METERS



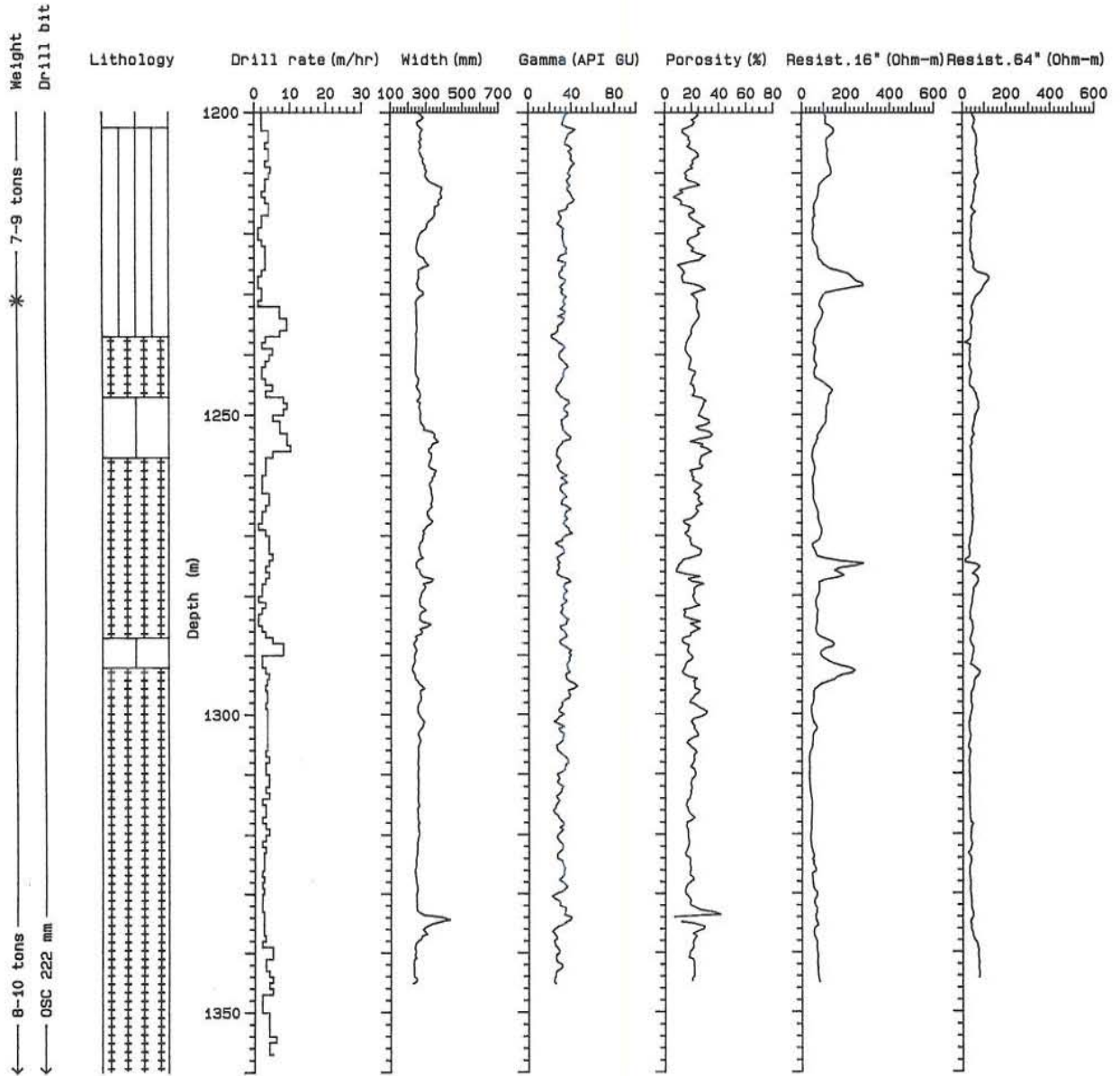
REYKJAVÍK WELL NUMBER RV-28

LITHOLOGY AND GEOPHYSICAL LOGS : DEPTH INTERVAL 1000 TO 1200 METERS





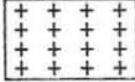

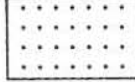


REYKJAVÍK WELL NUMBER RV-28

LITHOLOGY AND GEOPHYSICAL LOGS : DEPTH INTERVAL 1200 TO 1360 METERS



APPENDIX 3 - Lithology and geophysical logs in well RV-32

RV-32 : LITHOLOGICAL EXPLANATION

	Fresh basalt
	Altered basalt
	Dolerite intrusion
	Hyaloclastite tuff
	Fine-grained sediments
	Coarse-grained sediments
	No cuttings

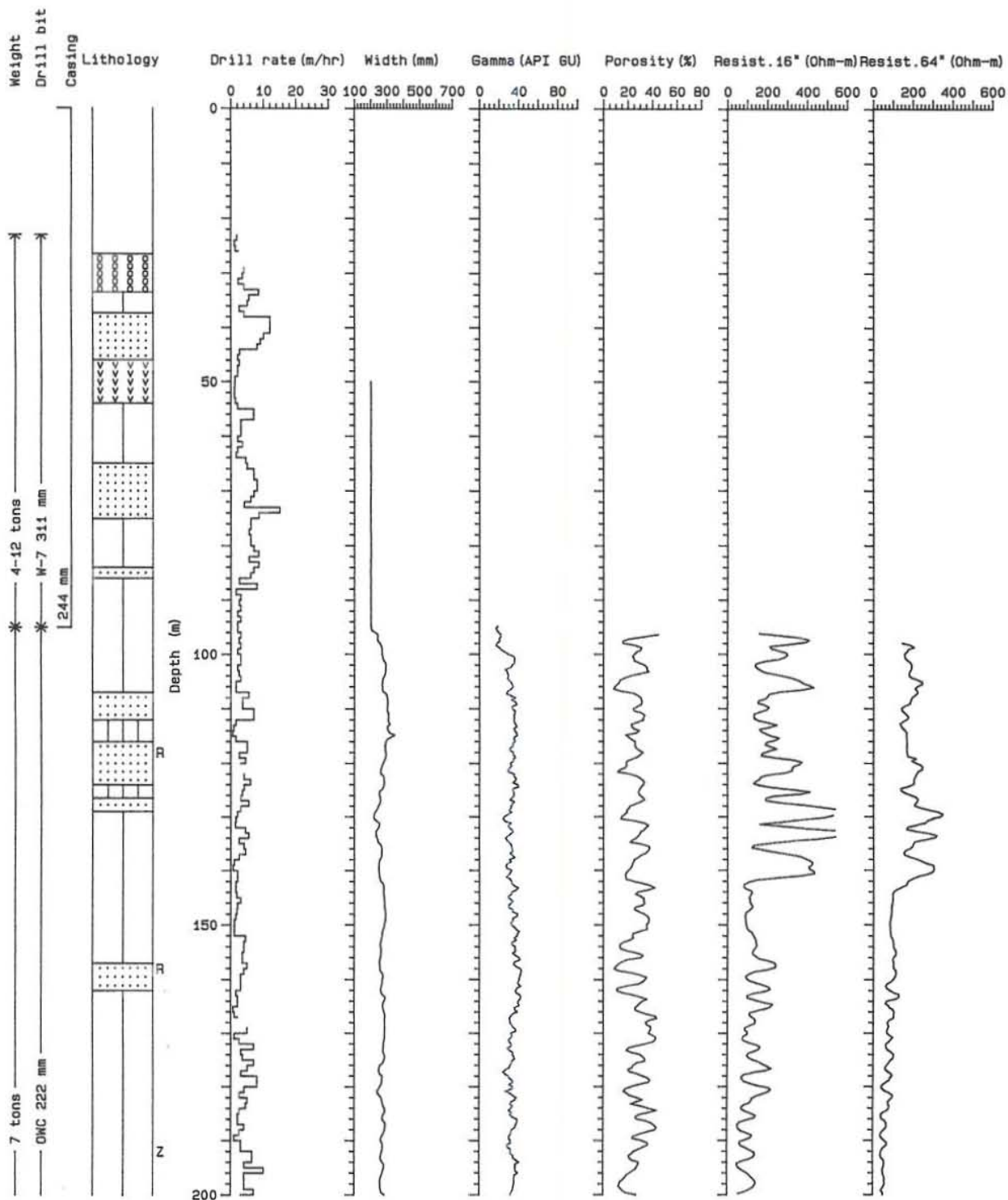
R : Red intercalation

Z : Zeolite

E : Epidote

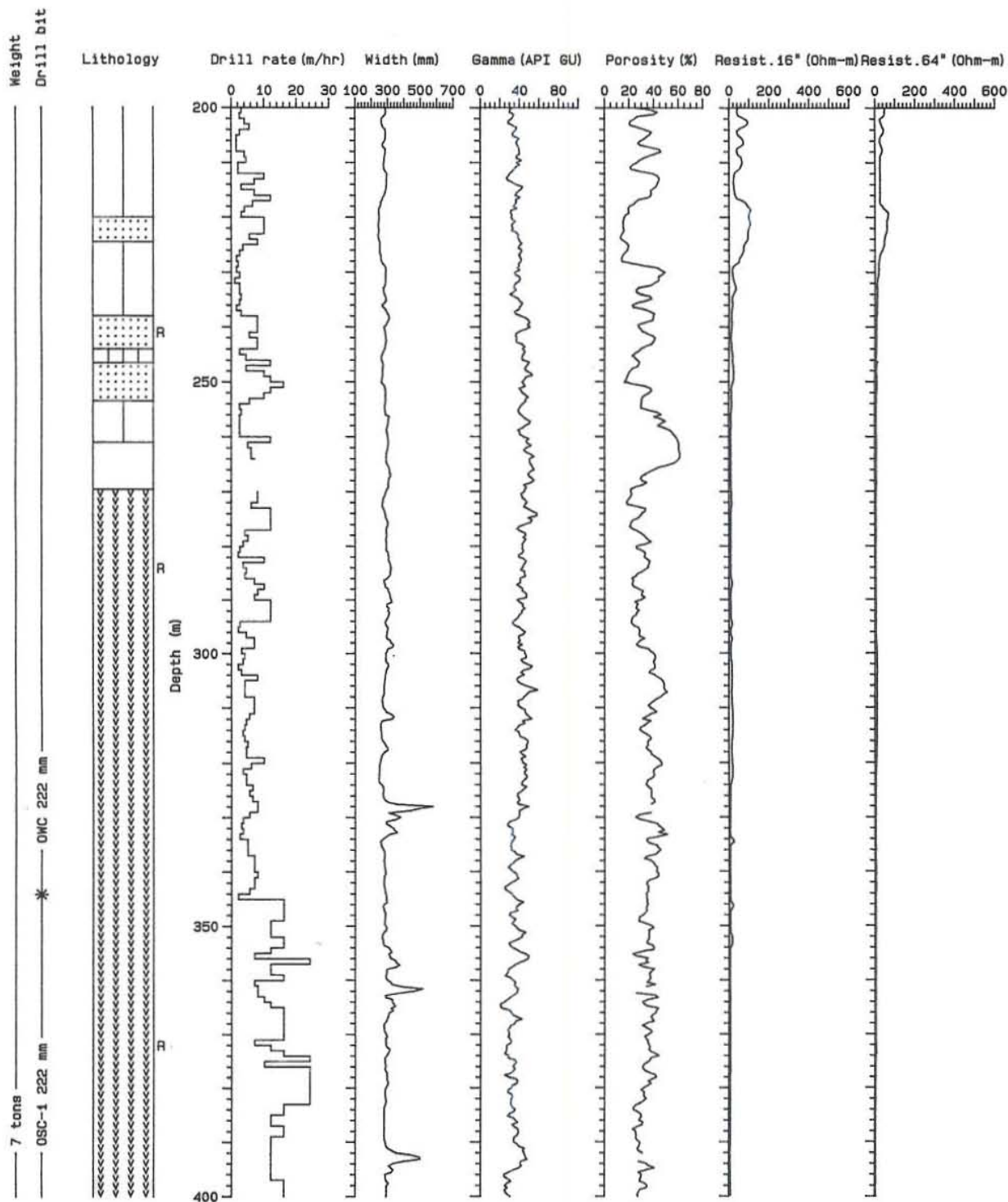
REYKJAVÍK WELL NUMBER RV-32

LITHOLOGY AND GEOPHYSICAL LOGS : DEPTH INTERVAL 0 TO 200 METERS



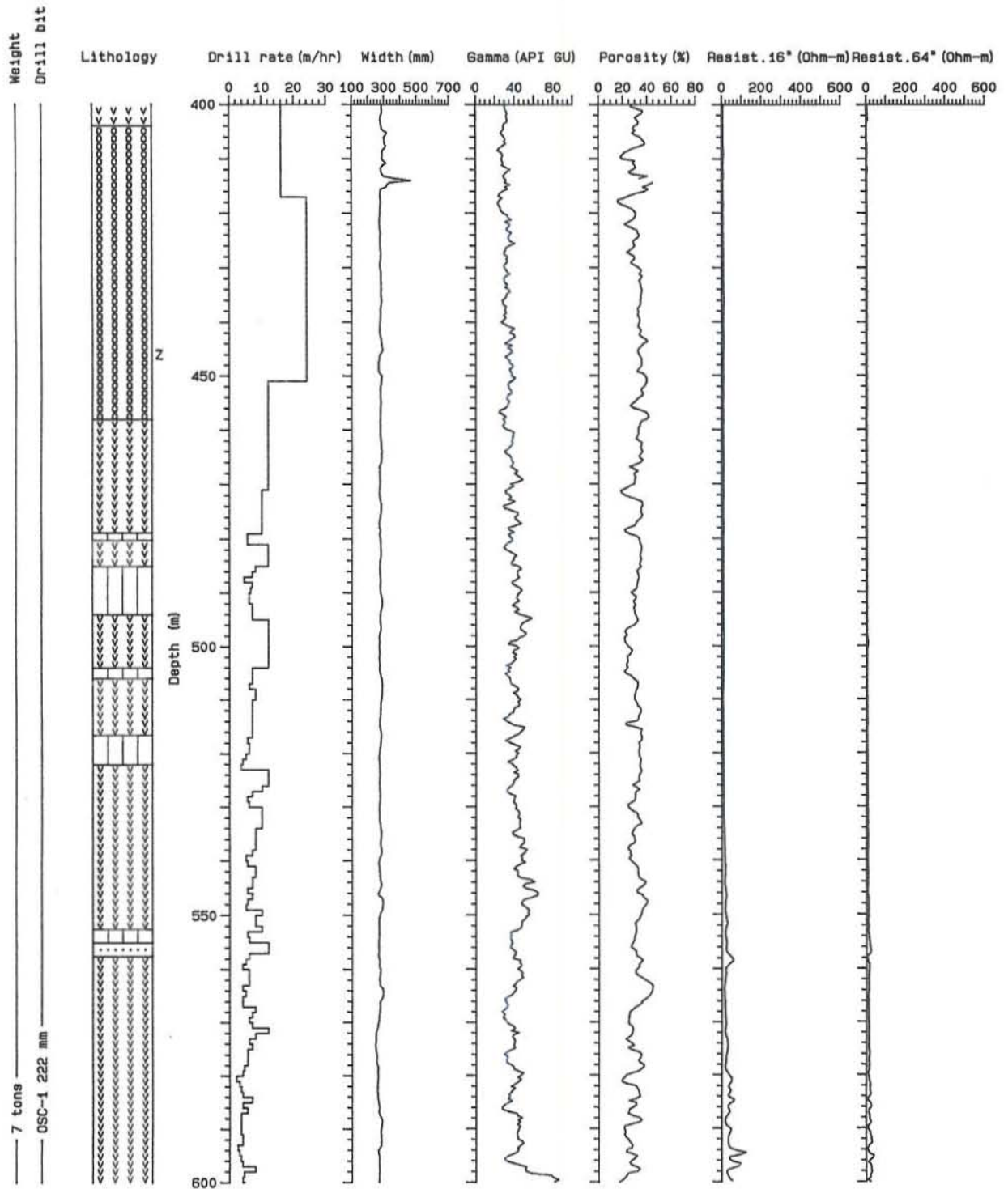
REYKJAVÍK WELL NUMBER RV-32

LITHOLOGY AND GEOPHYSICAL LOGS : DEPTH INTERVAL 200 TO 400 METERS



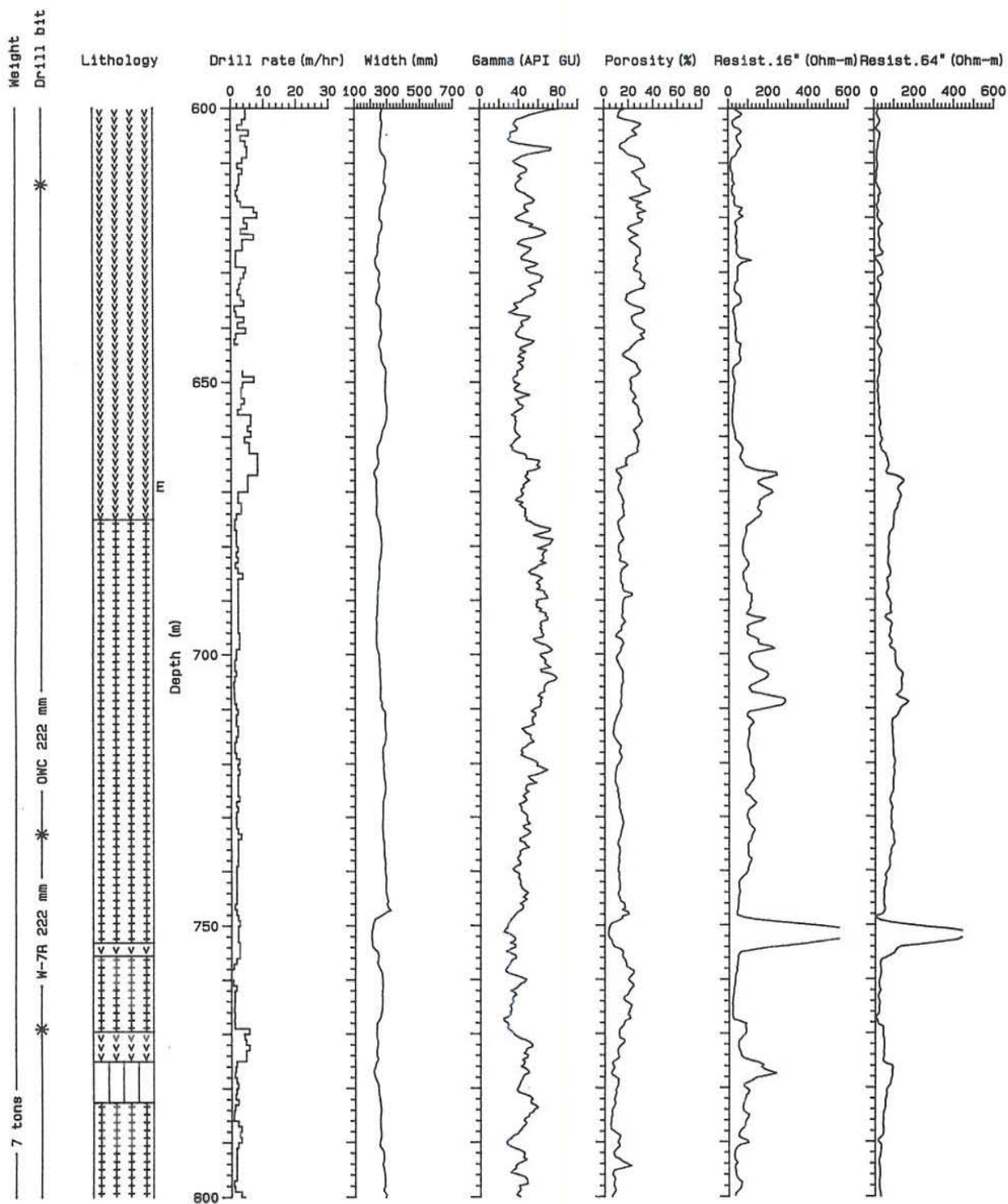
REYKJAVÍK WELL NUMBER RV-32

LITHOLOGY AND GEOPHYSICAL LOGS : DEPTH INTERVAL 400 TO 600 METERS



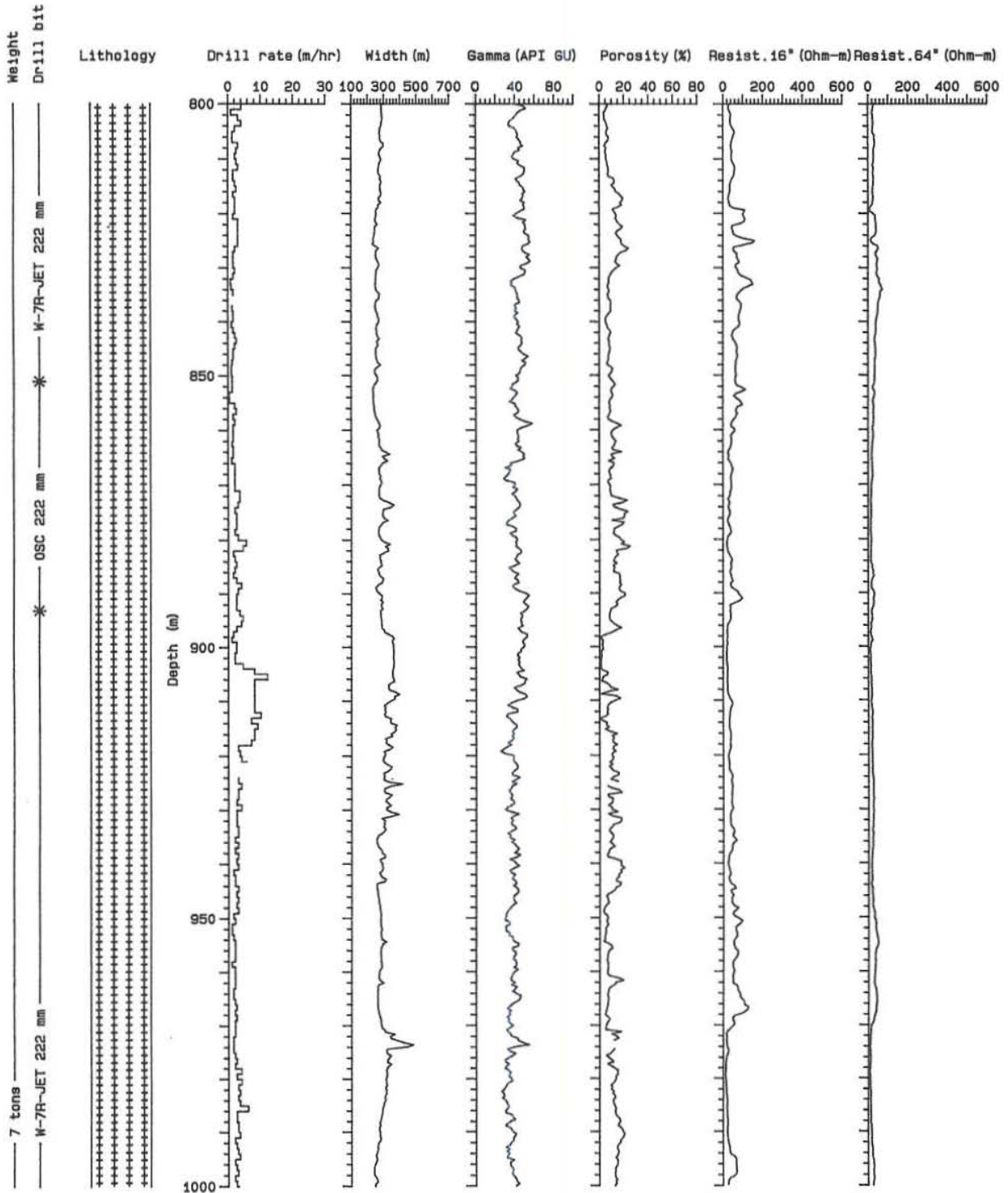
REYKJAVÍK WELL NUMBER RV-32

LITHOLOGY AND GEOPHYSICAL LOGS : DEPTH INTERVAL 600 TO 800 METERS



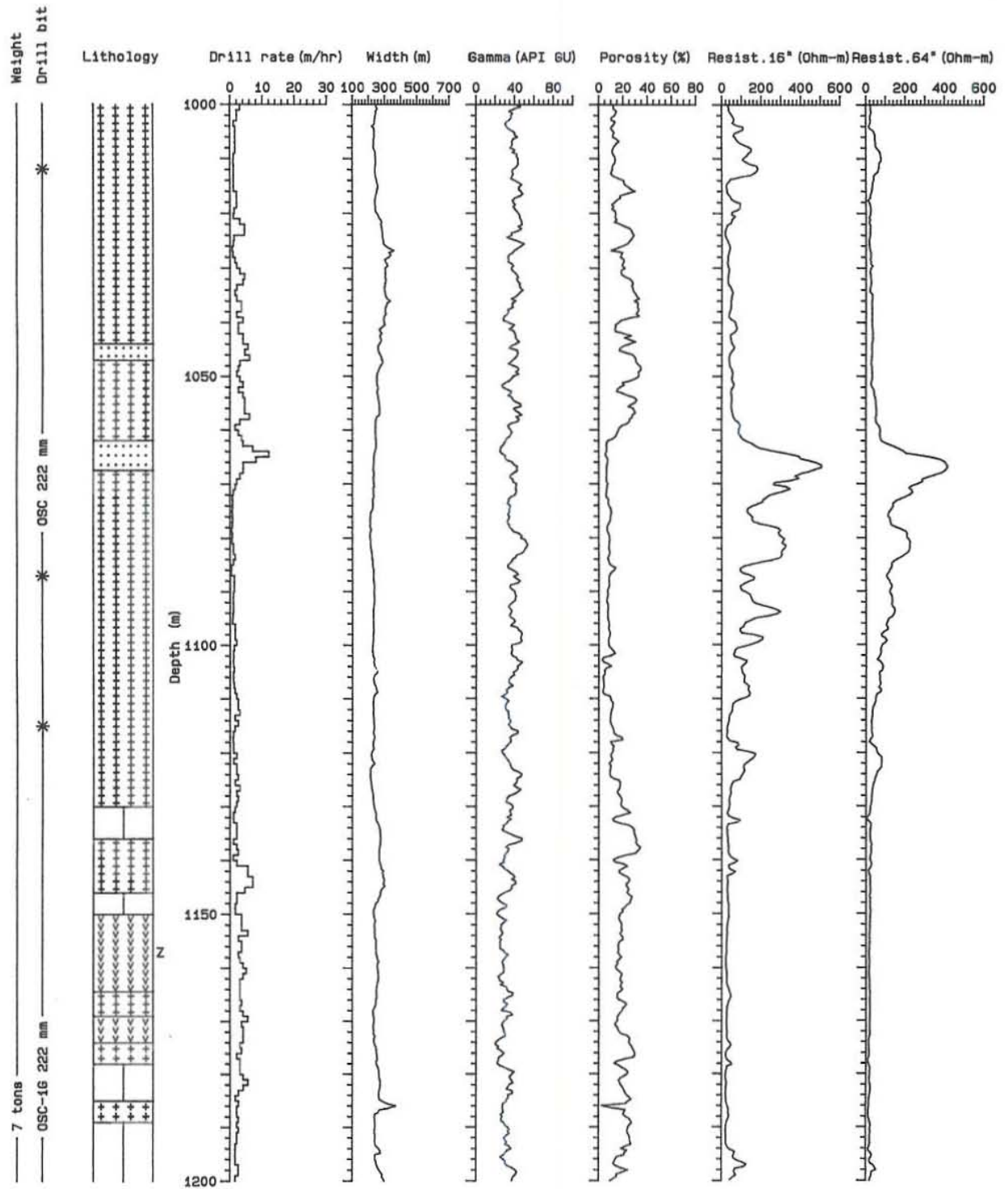
REYKJAVÍK WELL NUMBER RV-32

LITHOLOGY AND GEOPHYSICAL LOGS : DEPTH INTERVAL 800 TO 1000 METERS



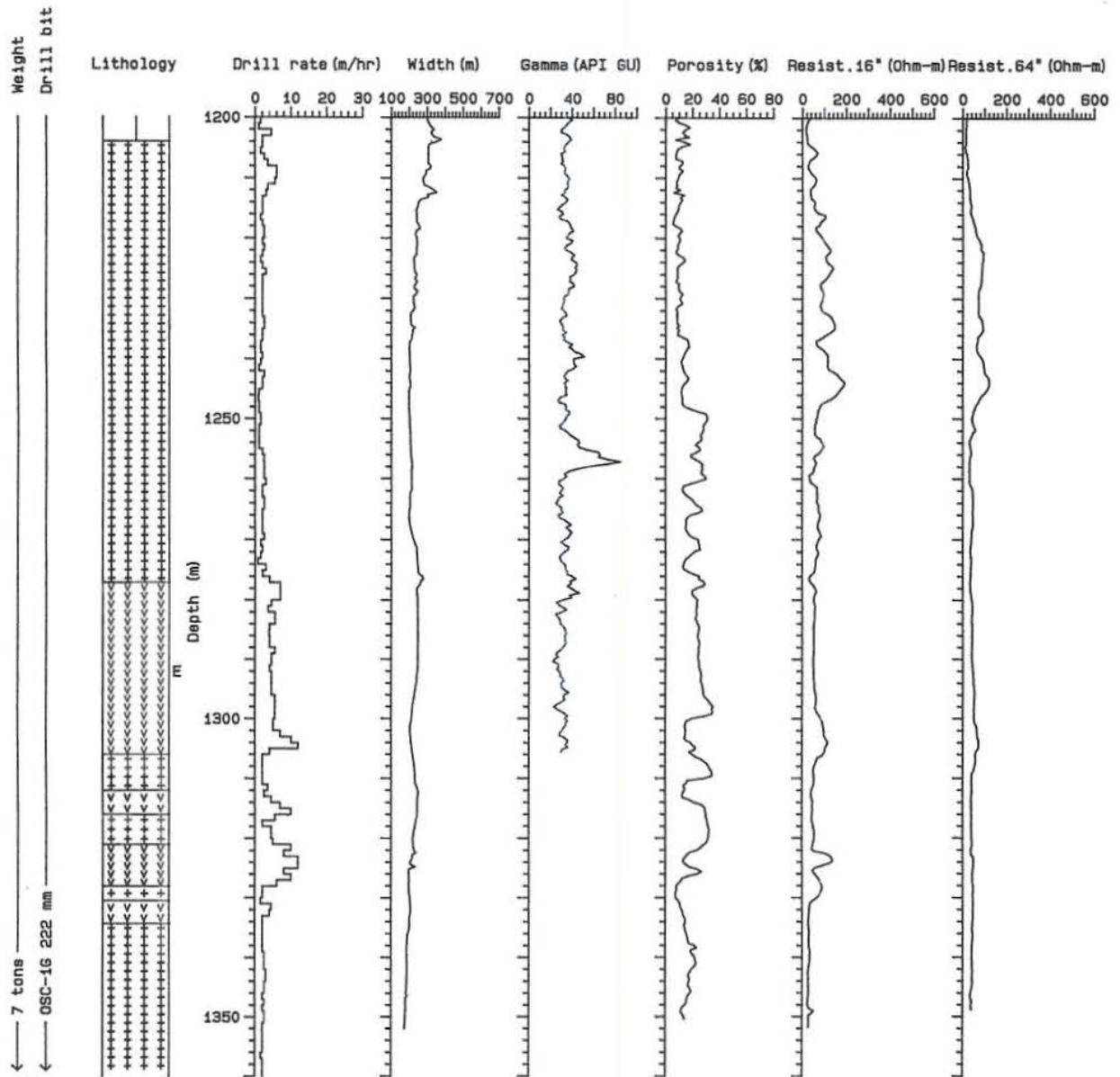
REYKJAVÍK WELL NUMBER RV-32

LITHOLOGY AND GEOPHYSICAL LOGS : DEPTH INTERVAL 1000 TO 1200 METERS



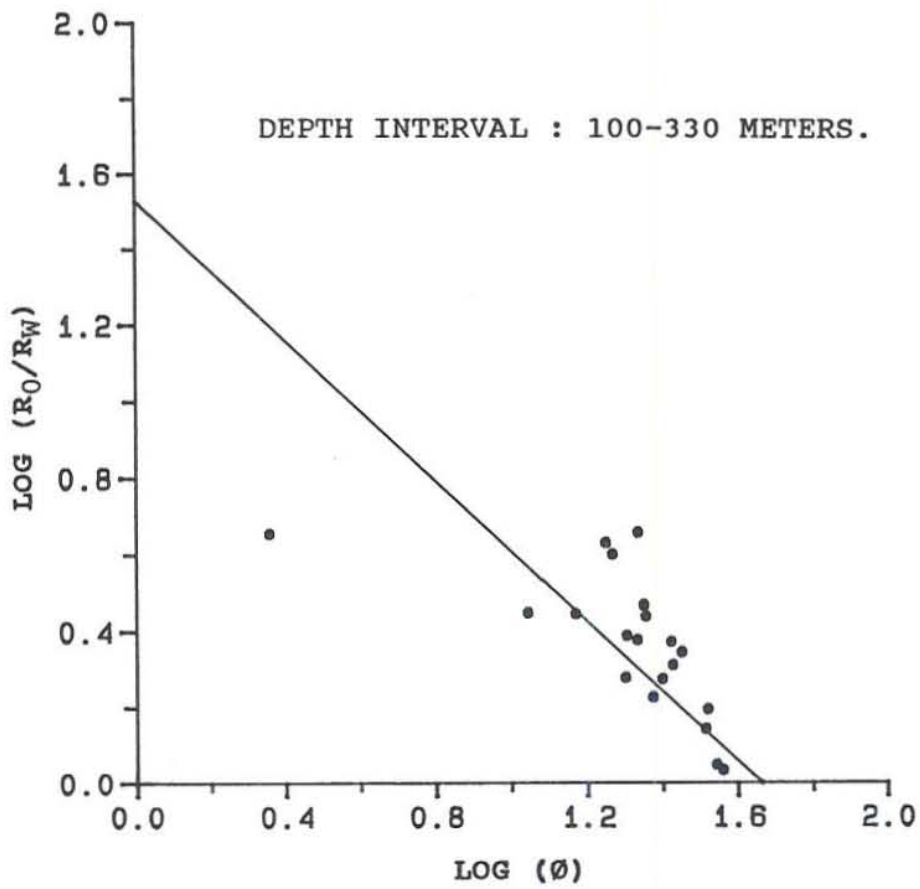
REYKJAVÍK WELL NUMBER RV-32

LITHOLOGY AND GEOPHYSICAL LOGS : DEPTH INTERVAL 1200 TO 1360 METERS

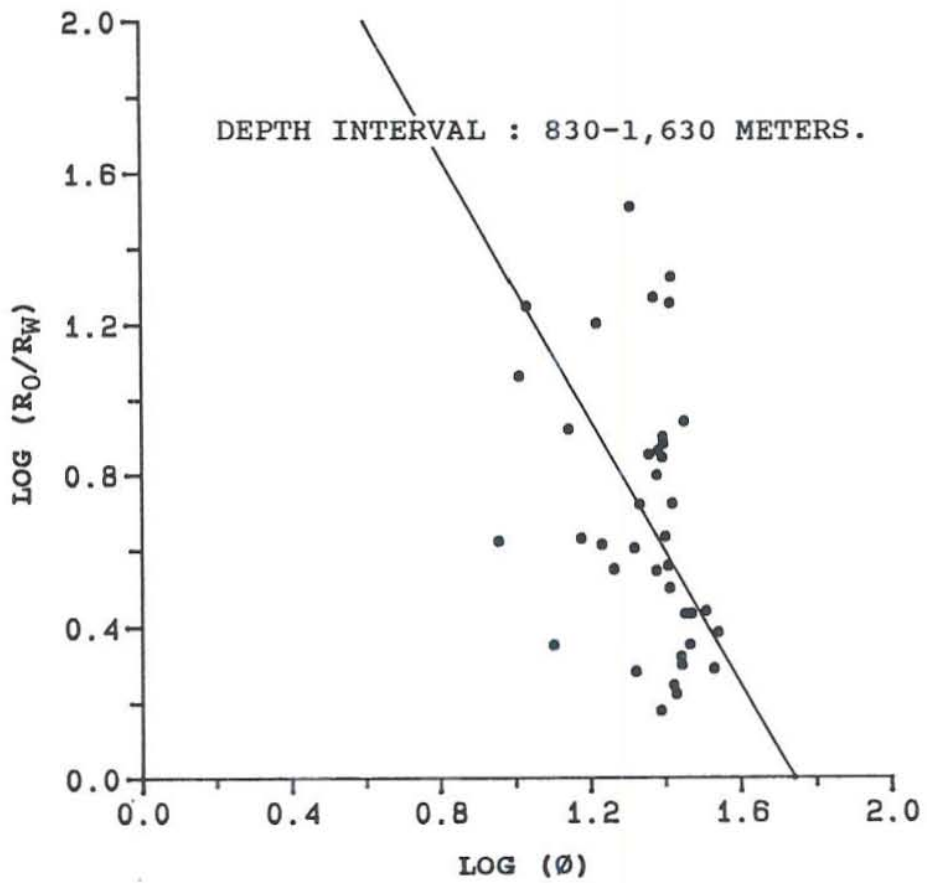


APPENDIX 4 - Resistivity-porosity crossplots in well RV-25

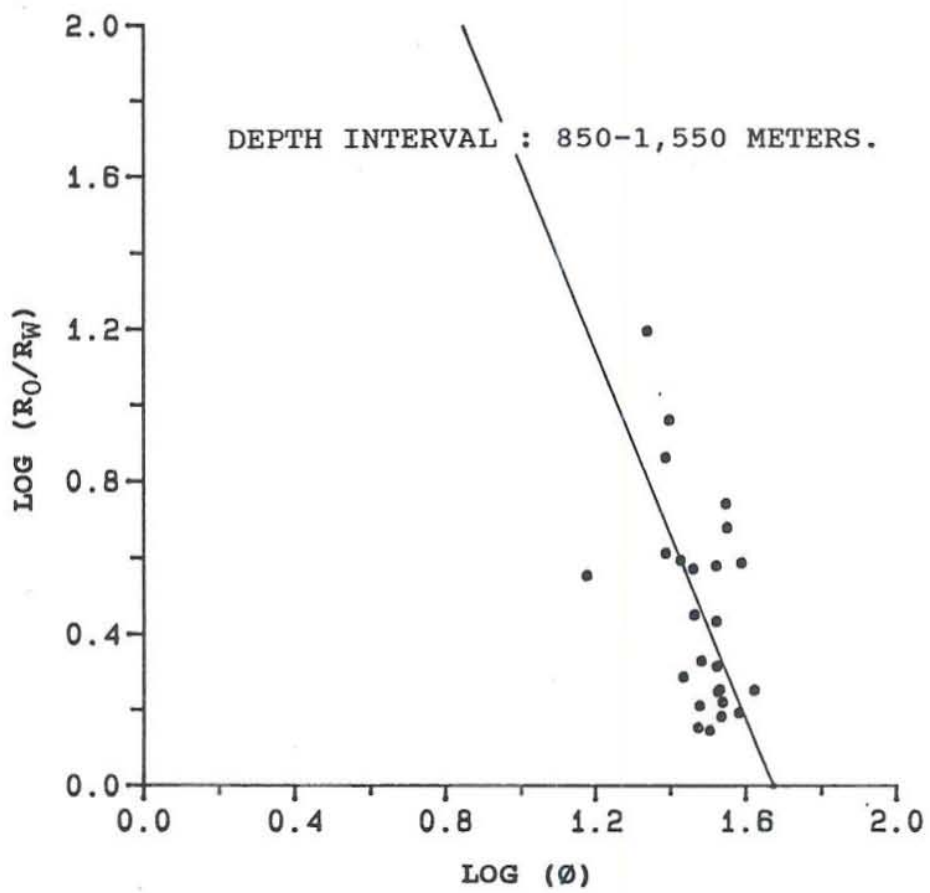
RV-25: Basalt-1



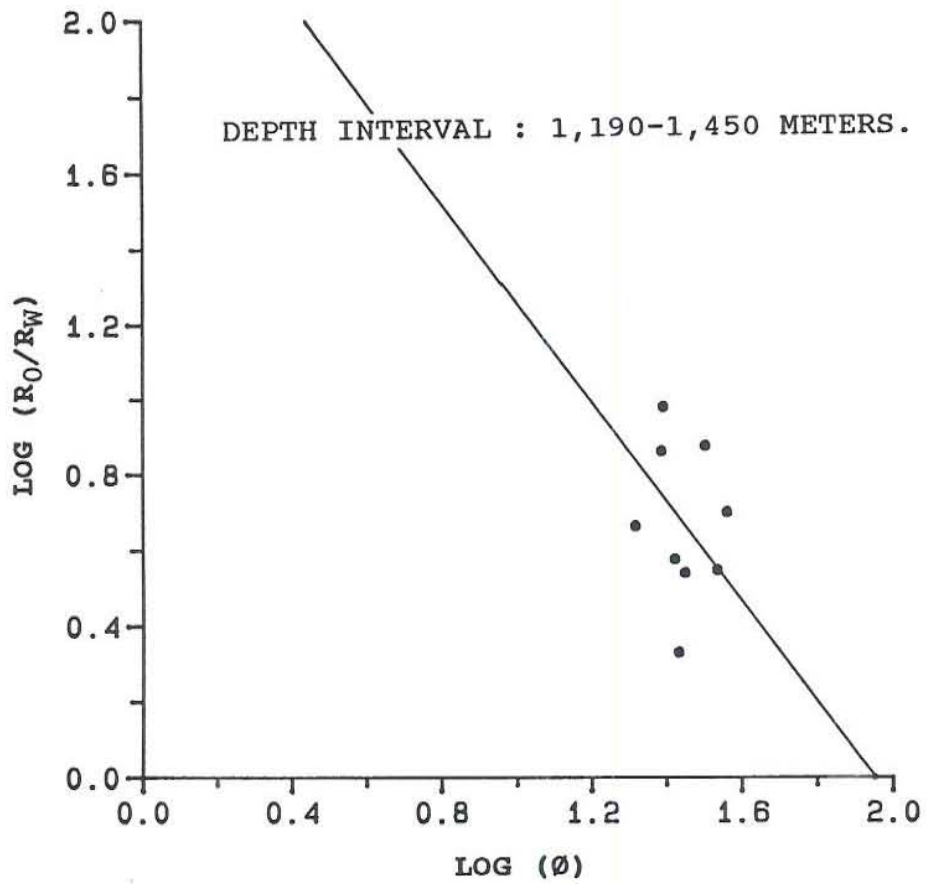
RV-25: Basalt-2



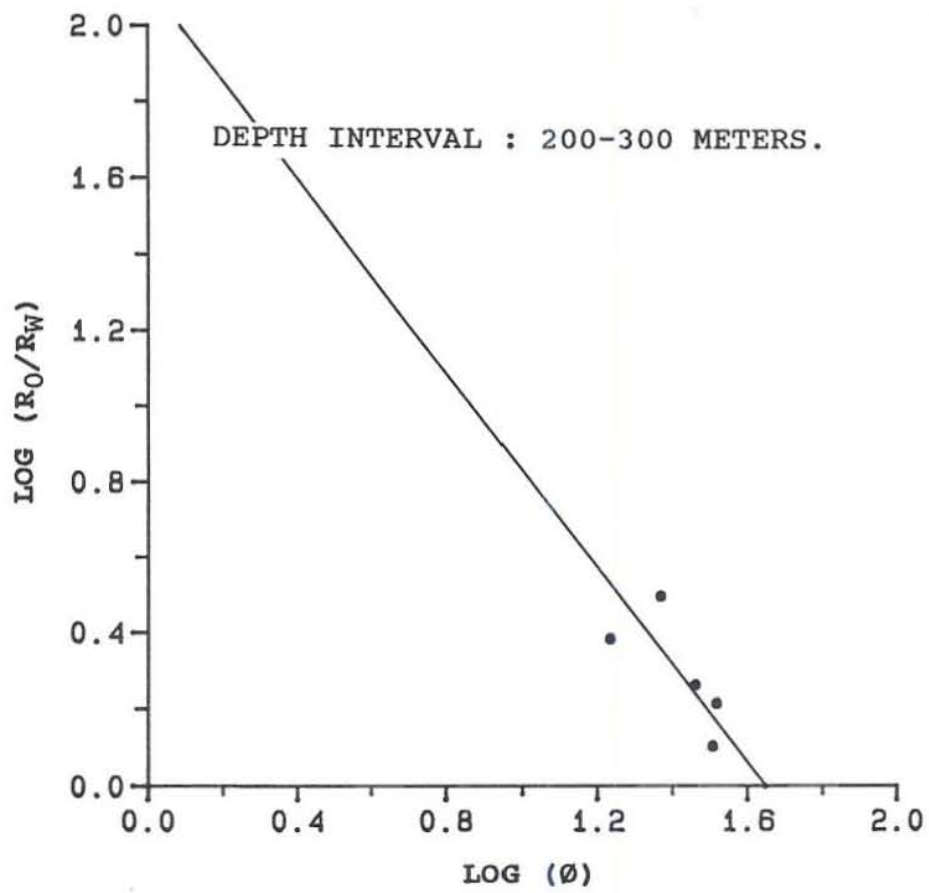
RV-25: Hyaloclastite tuff



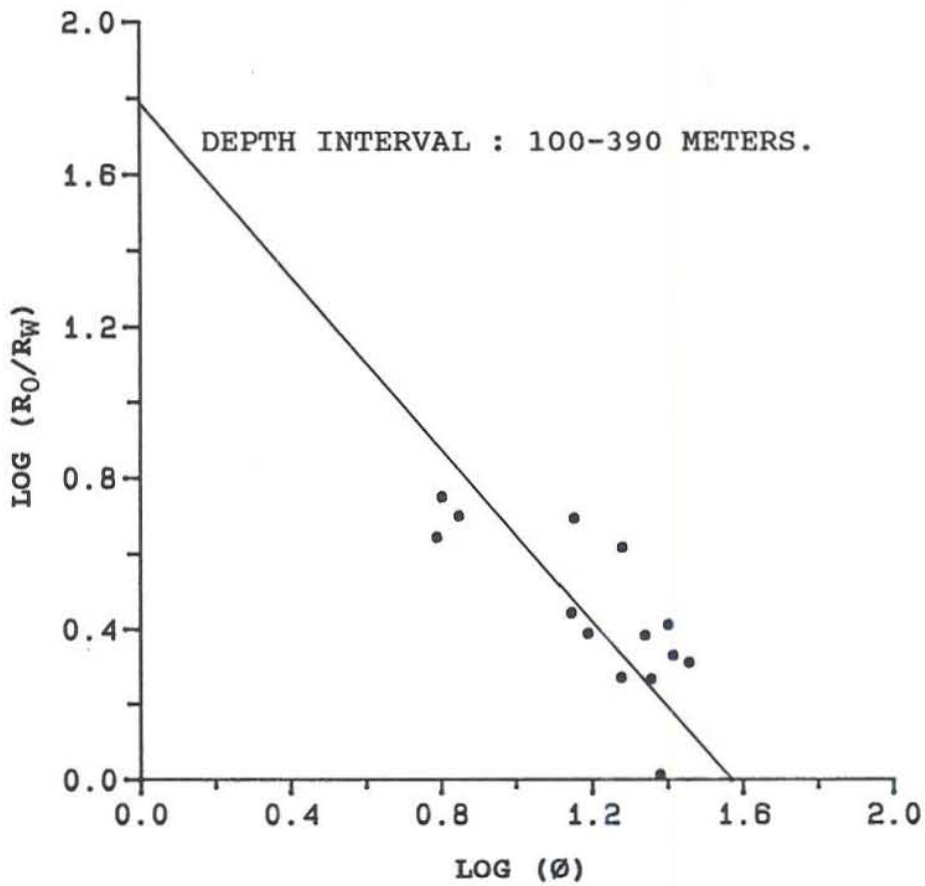
RV-25: Dolerite



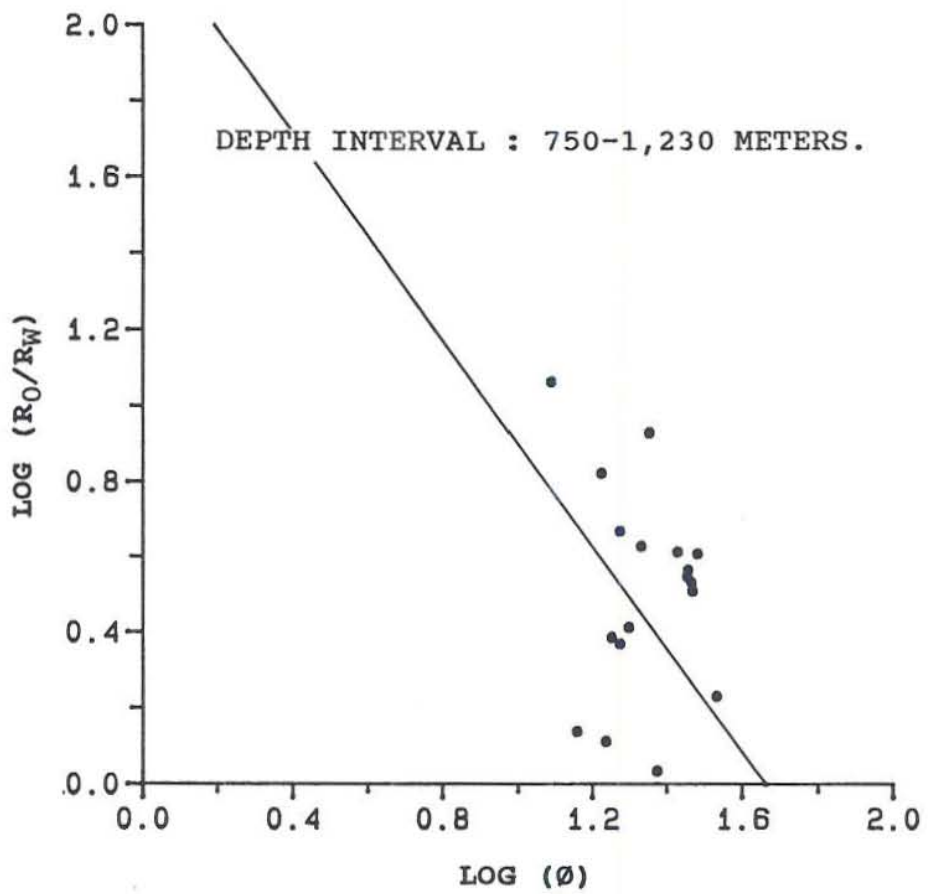
RV-25: Fine-grained sediment



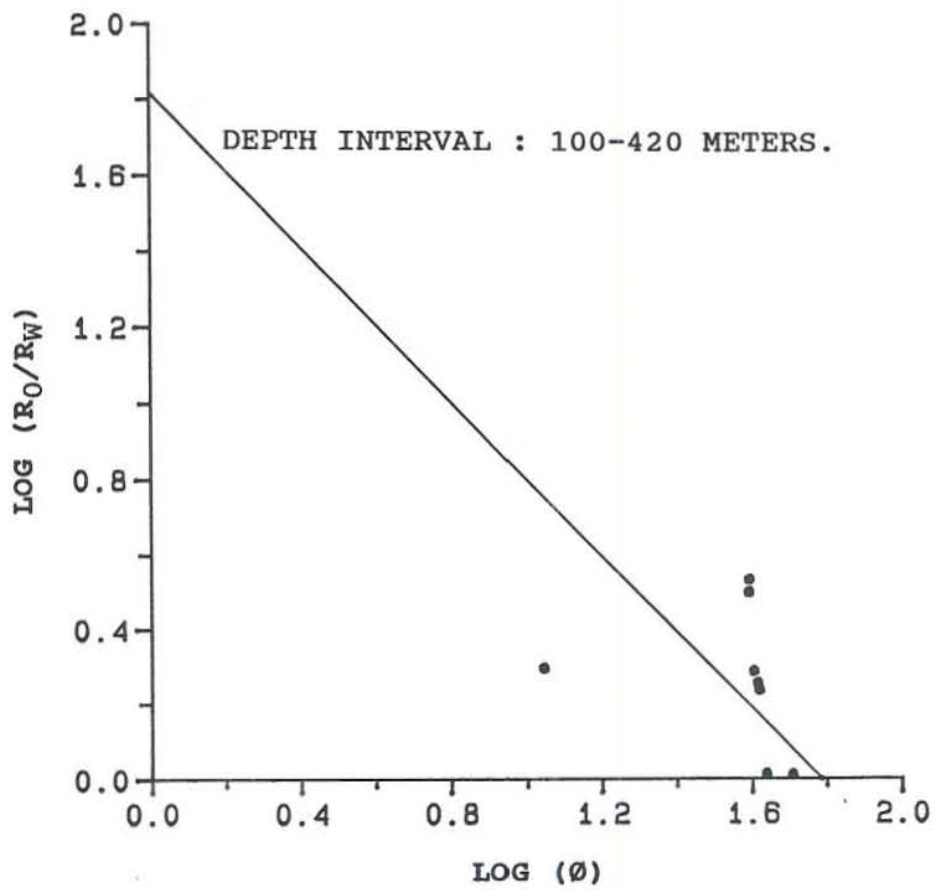
RV-28: Basalt-1



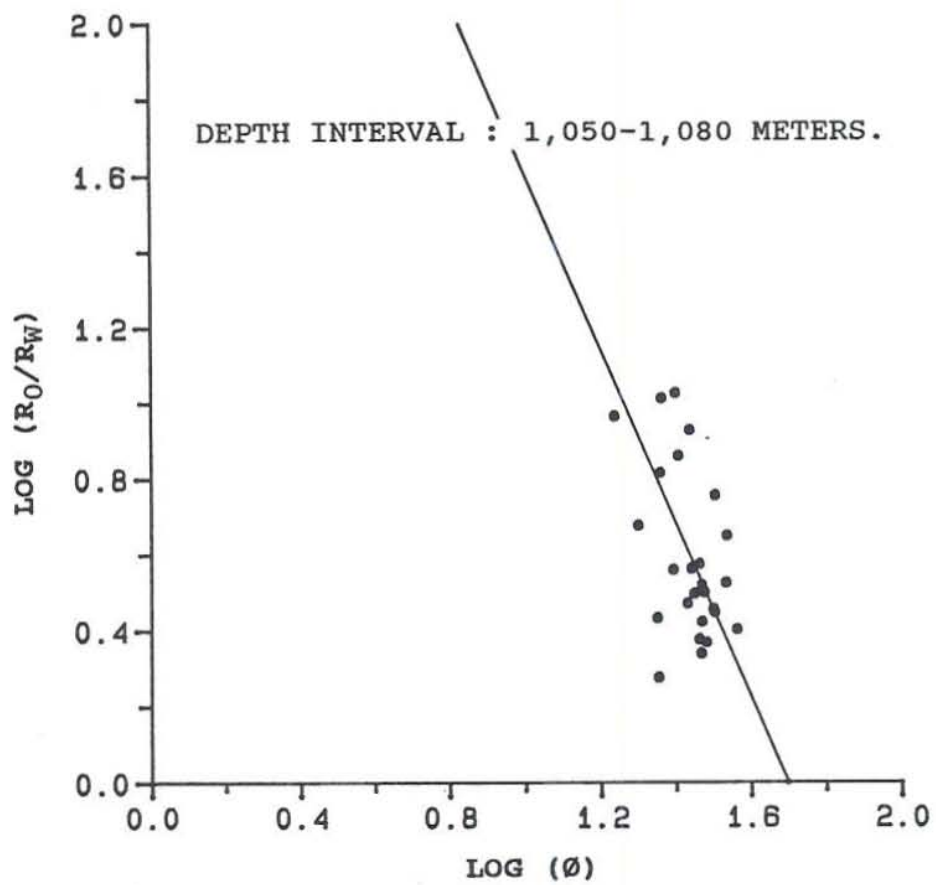
RV-28: Basalt-2



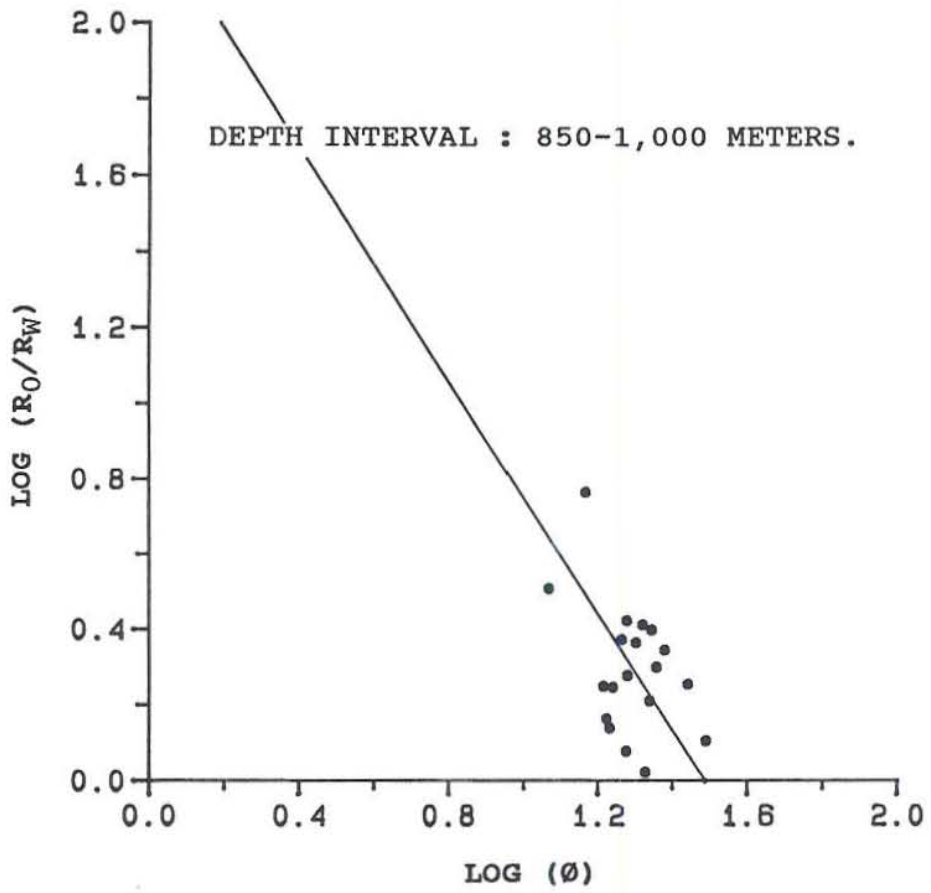
RV-28: Hyaloclastite tuff-1



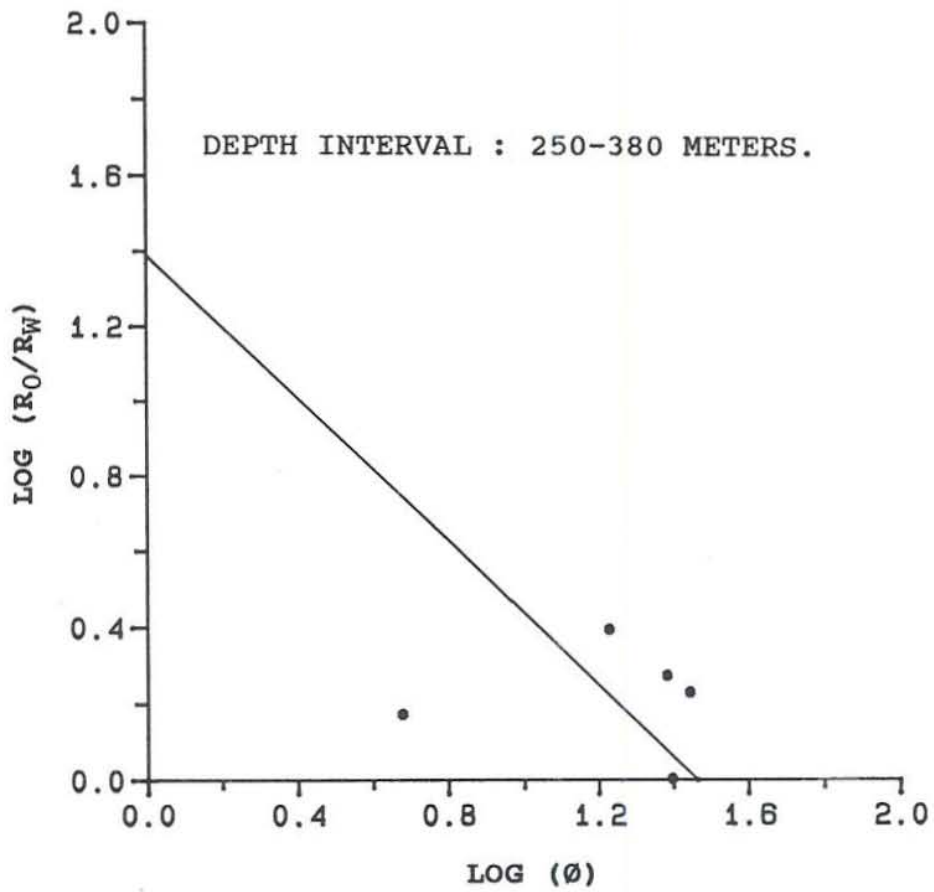
RV-28: Hyaloclastite tuff-2



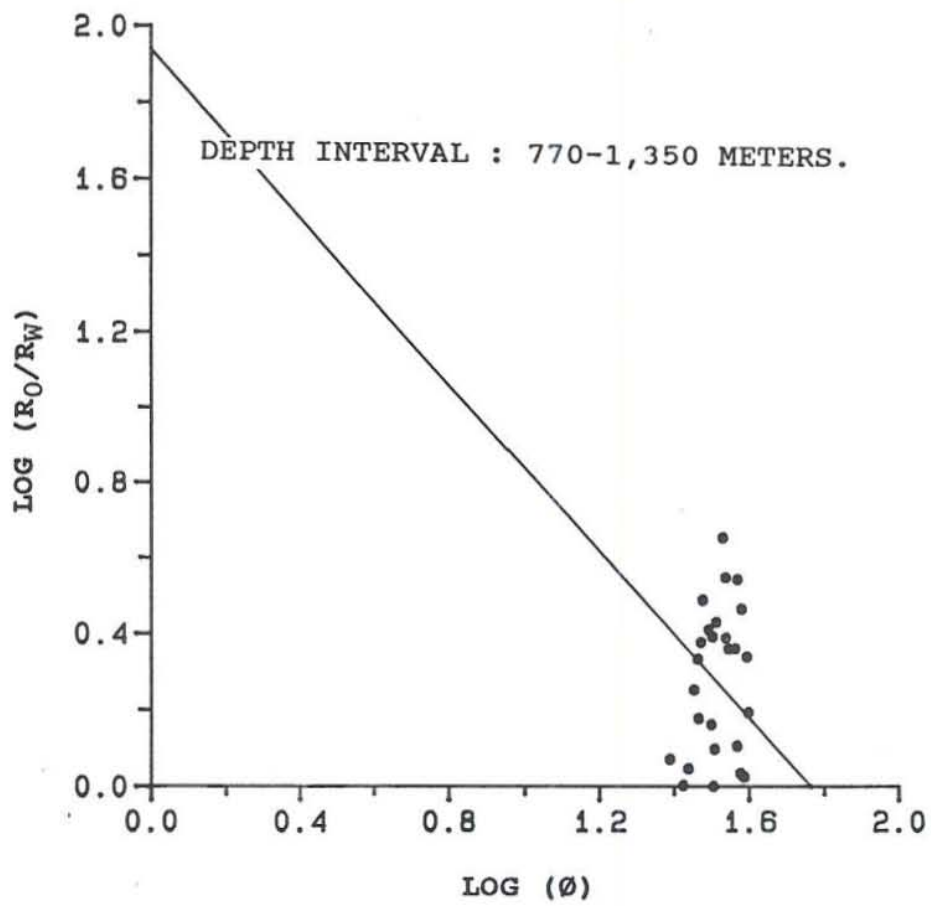
RV-28: Dolerite



RV-28: Fine-grained sediment

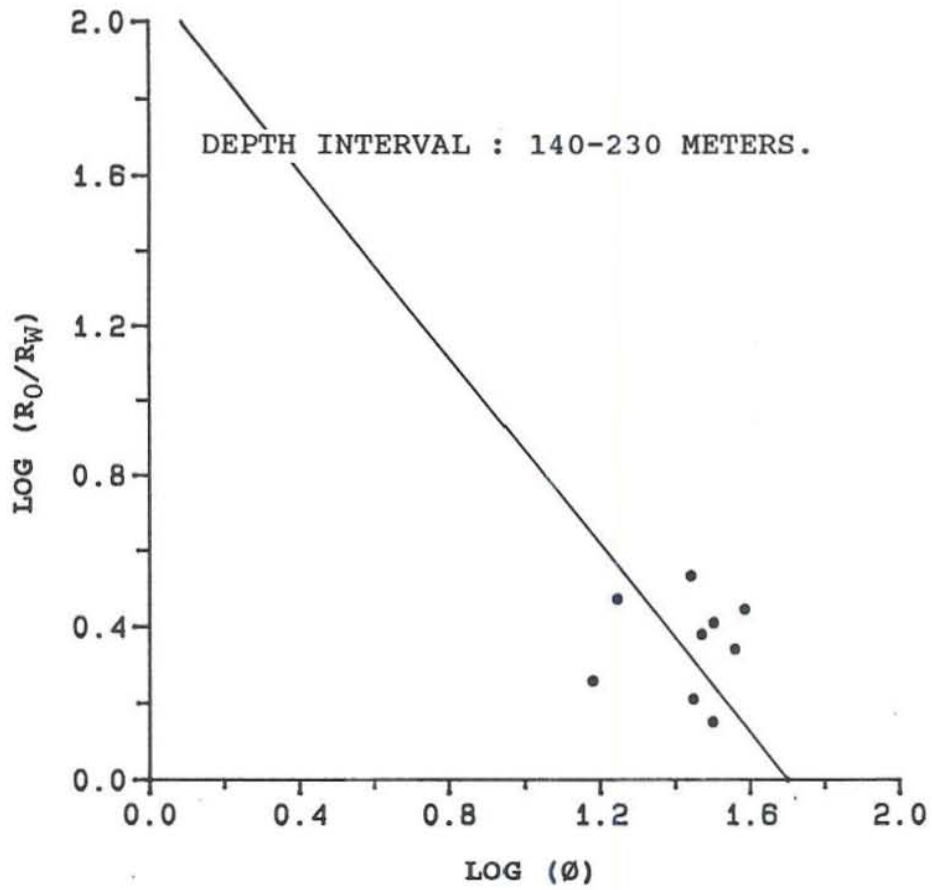


RV-28: Basaltic breccia

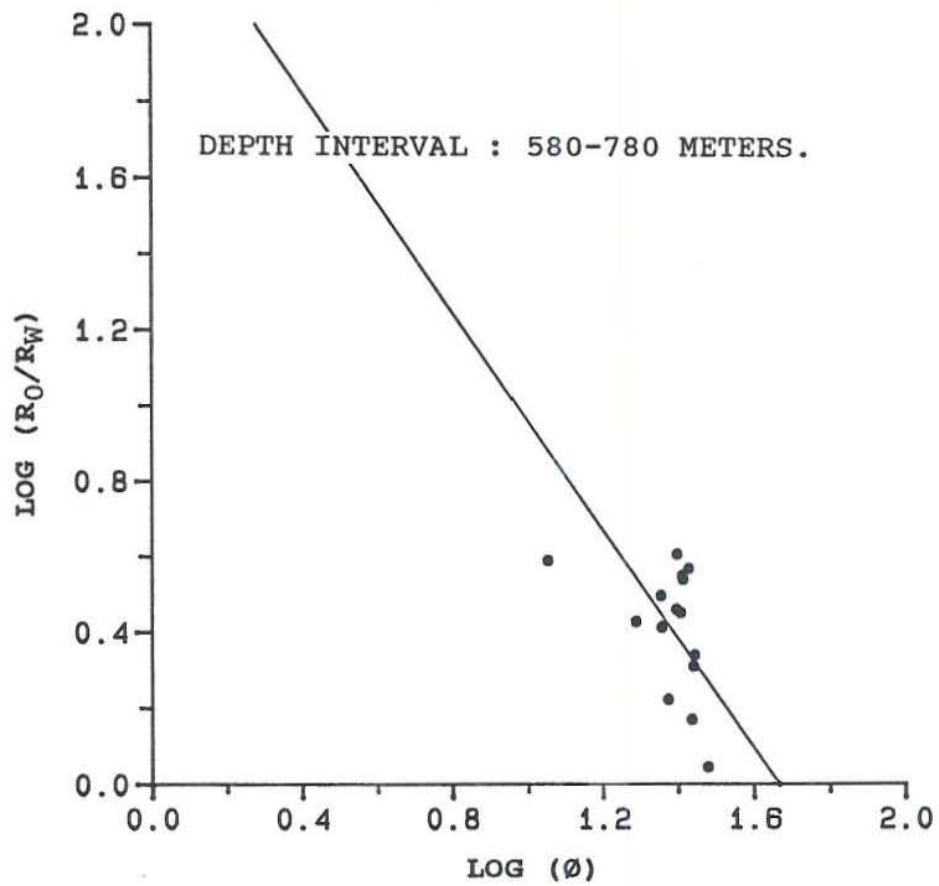


APPENDIX 6 - Resistivity-porosity crossplots in well RV-32

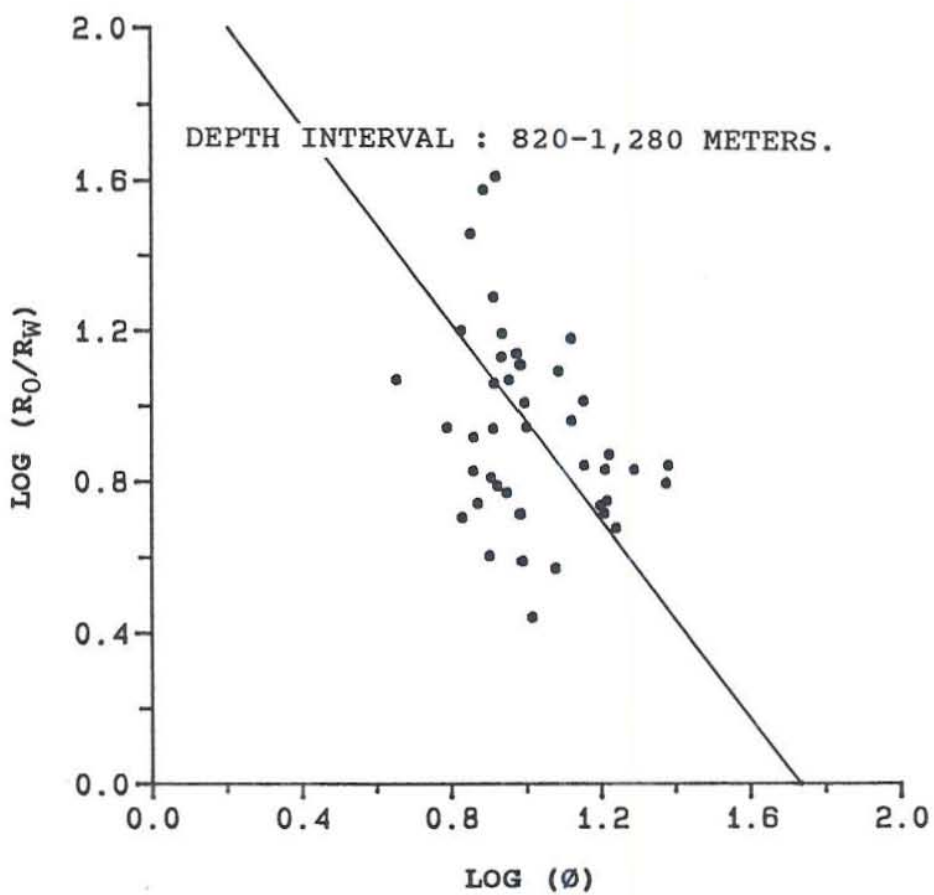
RV-32: Basalt



RV-32: Hyaloclastite tuff



RV-32: Dolerite



RV-32: Fine-grained sediment

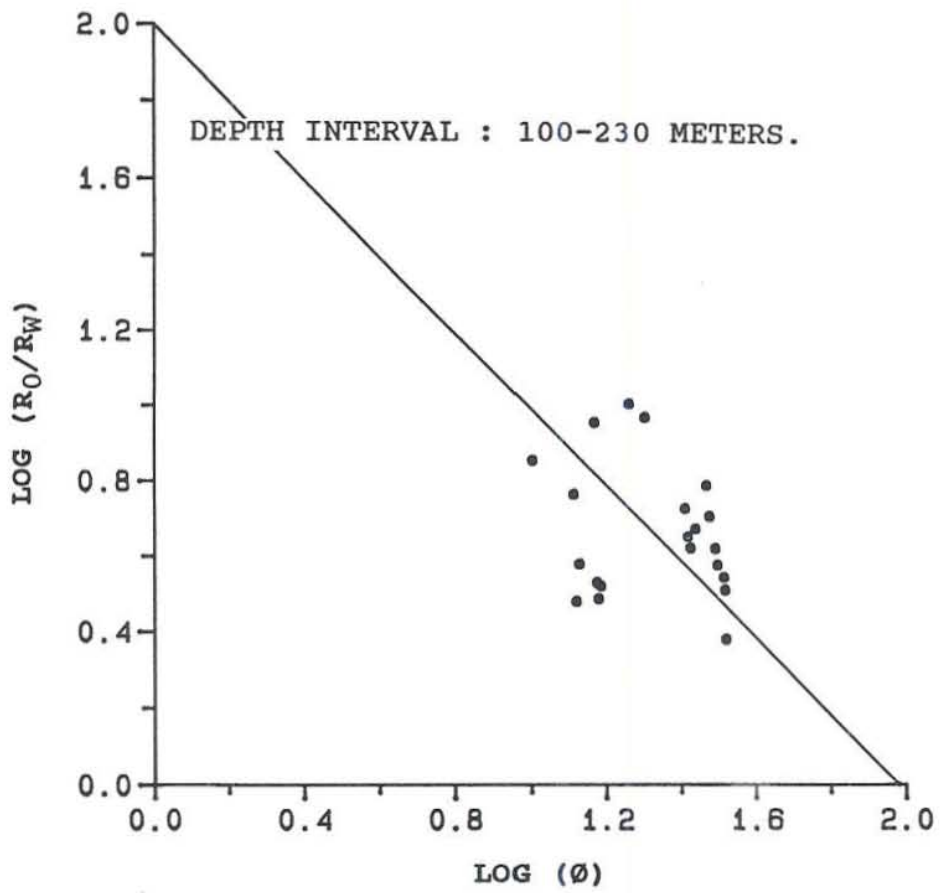


Table 1 - Schematic classification for phases of neutron life

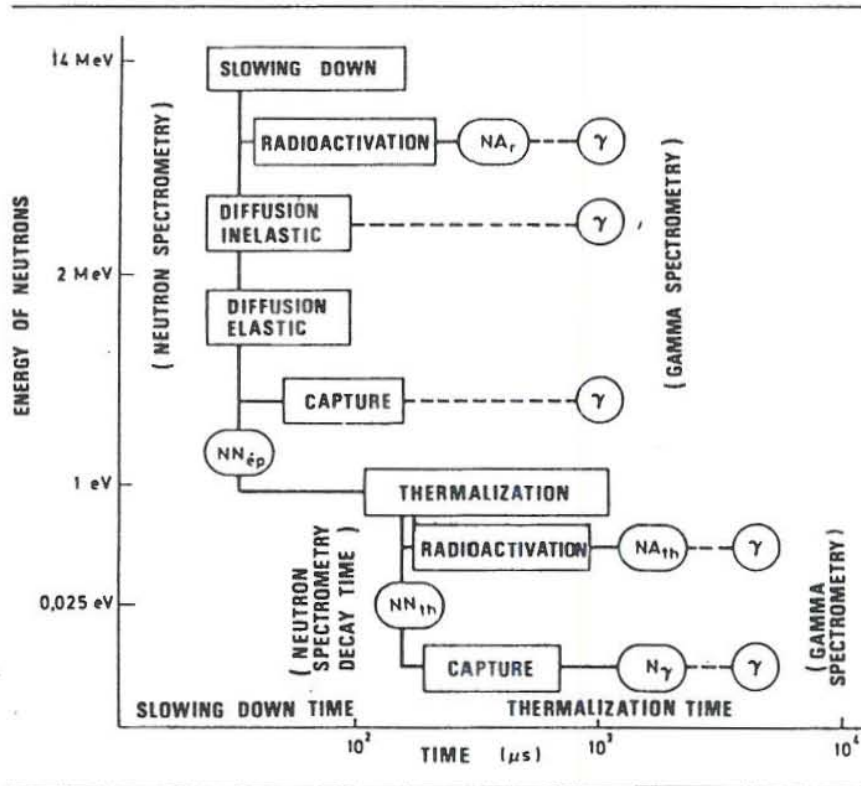


Table 2 - Thermal neutron cross-section for some principal elements

Elements	Cross-section in barns ($= 10^{-24} \text{ cm}^2$) for neutrons ($v = 2200 \text{ m/s}$)	Energy of emitted gamma rays (MeV)	Probability of emission	Mean loss of energy by collision
Gadolinium	40,000			
Bore	771			
Lithium	71			
Chlorine	33.4	7.77	0.1	
		7.42	0.08	
		6.12	0.06	
		5.01	0.04	
Potassium	2.2			
Barium	1.2			
Iron	2.56			
Sodium	0.534			
Sulphur	0.49	5.43	0.84	
		4.84	0.20	
Calcium	0.44	6.42	0.83	0.04
		5.89	0.11	
Hydrogen	0.332	2.23	1.0	0.5
Aluminium	0.232	7.72	0.35	
		3.02	0.16	
		2.84	0.13	
		6.40	0.19	0.06
Silicon	0.16	4.95	1.0	
		4.20	0.19	
		3.57	0.94	
		2.69	0.65	
		8.16	0.09	
Magnesium	0.064	3.92	0.83	
		3.45	0.16	
Carbon	0.0034	3.83	0.39	0.14
		4.95	0.49	
		4.05	0.15	
Oxygen	0.0002	3.05	0.36	
				0.11

* From Handbook of Chemistry and Physics, 62 edition (1981-1982). Chemical Rubber Publishing Co., Cleveland, Ohio, U.S.A.

Table 3 - Slowing down power of elements

Element	Number of collisions needed to reduce the energy of neutrons from 2 MeV to 0.025 eV
Hydrogen	18
Carbon	114
Oxygen	150
Silicon	257
Chlorine	329
Calcium	368

* Nuclear Physics, Irving Kaplan.

Table 4 - Recommended maximum logging speeds

Survey	Maximum logging speed			
	(ft/min)	(m/min)		
SP	100	30		
Induction	100	30		
Laterolog	50	15		
Microlaterolog	35	10		
Neutron	} TC = 2 sec	30	9	
GR		} TC = 3 sec	20	6
Density			} TC = 4 sec	15
TDT				
Sonic	70	20		
Amplitude	35	10		

Table 5 - Coefficients in Archie's formula determined from resistivity-porosity crossplots in well RV-25

RV-25 rock unit	exponent (m)	constant (a)	correlation coefficient
Basalt-1	0.92	1.53	-0.46
Basalt-2	1.75	3.05	-0.31
Hyaloclastite tuff	2.42	4.05	-0.47
Dolerite	1.32	2.58	-0.13
Fine-grained sediment	1.28	2.11	-0.74

Table 6 - Coefficients in Archie's formula determined from resistivity-porosity crossplots in well RV-28

RV-28 rock unit	exponent (m)	constant (a)	correlation coefficient
Basalt-1	1.14	1.79	-0.81
Basalt-2	1.36	2.26	-0.13
Hyaloclastite tuff-1	1.02	1.82	-0.27
Hyaloclastite tuff-2	2.31	3.92	-0.44
Dolerite	1.54	2.29	-0.42
Fine-grained sediment	0.95	1.39	-0.04
Basaltic breccia	1.10	1.94	-0.03

Table 7 - Coefficients in Archie's formula determined from resistivity-porosity crossplots in well RV-32

RV-32 rock unit	exponent (m)	constant (a)	correlation coefficient
Basalt	1.24	2.11	-0.30
Hyaloclastite tuff	1.44	2.40	-0.43
Dolerite	1.31	2.27	-0.32
Fine-grained sediment	1.01	2.00	-0.24

Table 8 - Conclusion of the Archie's exponents (m) for wells RV-25, RV-28 and RV-32

Exponent (m)	RV-25	RV-28	RV-32
Basalt-1	0.92	1.14	1.24
Basalt-2	1.75	1.36	-
Hyaloclastite tuff-1	2.24	1.02	1.44
Hyaloclastite tuff-2	-	2.31	-
Dolerite	1.32	1.54	1.31
Fine-grained sediment	1.28	0.95	1.01
Basaltic breccia	-	1.10	-

Table 9 - Conclusion of the Archie's constants (a) for wells RV-25, RV-28 and RV-32

Constant (a)	RV-25	RV-28	RV-32
Basalt-1	1.53	1.79	2.11
Basalt-2	3.05	2.26	-
Hyaloclastite tuff-1	4.05	1.82	2.40
Hyaloclastite tuff-2	-	3.92	-
Dolerite	2.58	2.29	2.27
Fine-grained sediment	2.11	1.39	2.00
Basaltic breccia	-	1.94	-

Table 10 - Mean values of resistivity, porosity and silica content in wells RV-25, RV-28 and RV-32

Mean value	Resistivity (Ohm-m)	Porosity (%)	Silica (%)
RV-25	33.9 ± 3.0	24.9 ± 9.6	48.6 ± 2.7
RV-28	49.3 ± 2.3	25.9 ± 9.1	48.5 ± 1.7
RV-32	34.5 ± 3.1	21.5 ± 10.9	50.7 ± 2.3

Figure 1 - Elliðaár geothermal field, Reykjavik

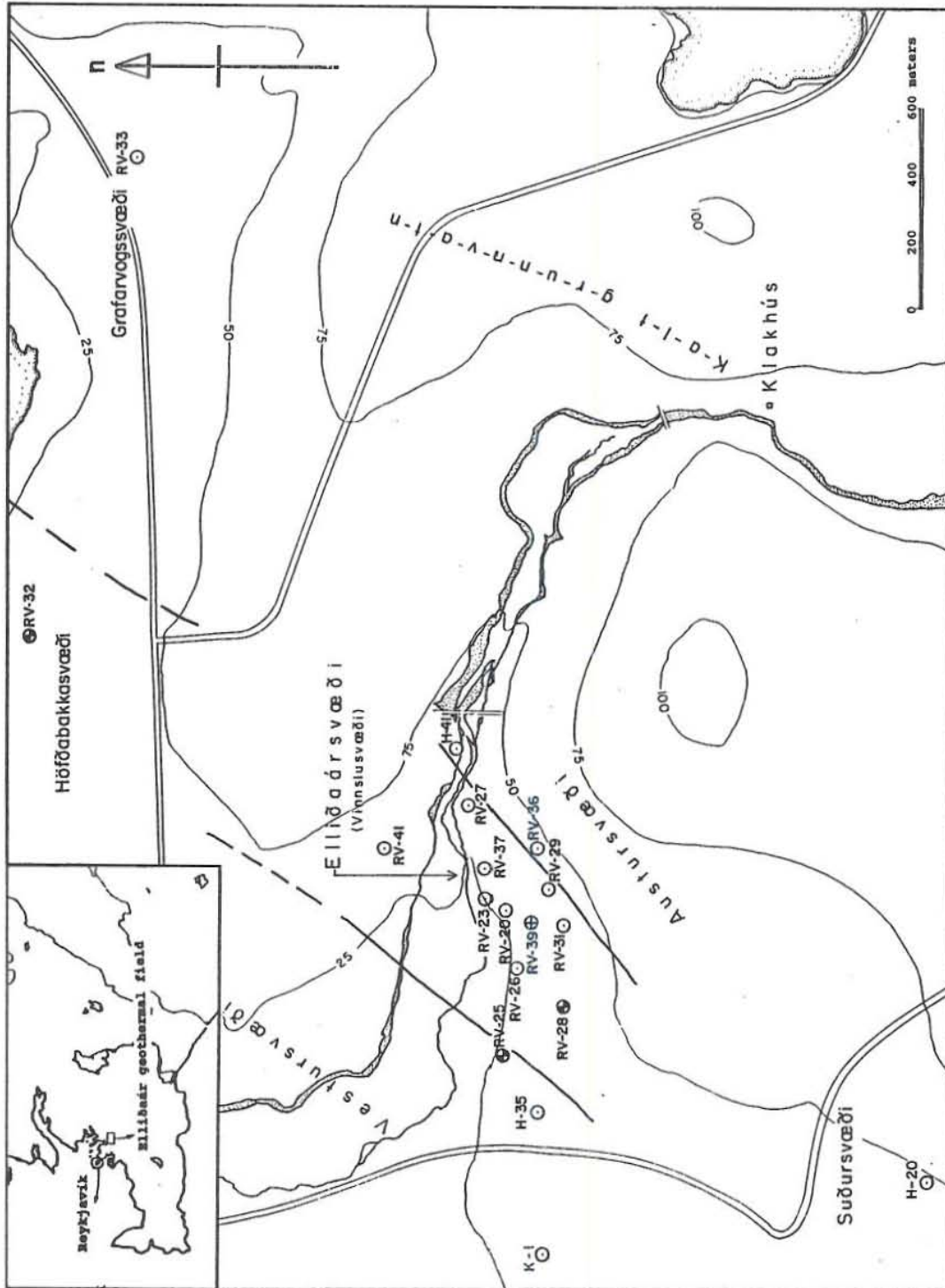


Figure 2 - Temperature profiles of wells RV-25, RV-28 and RV-32

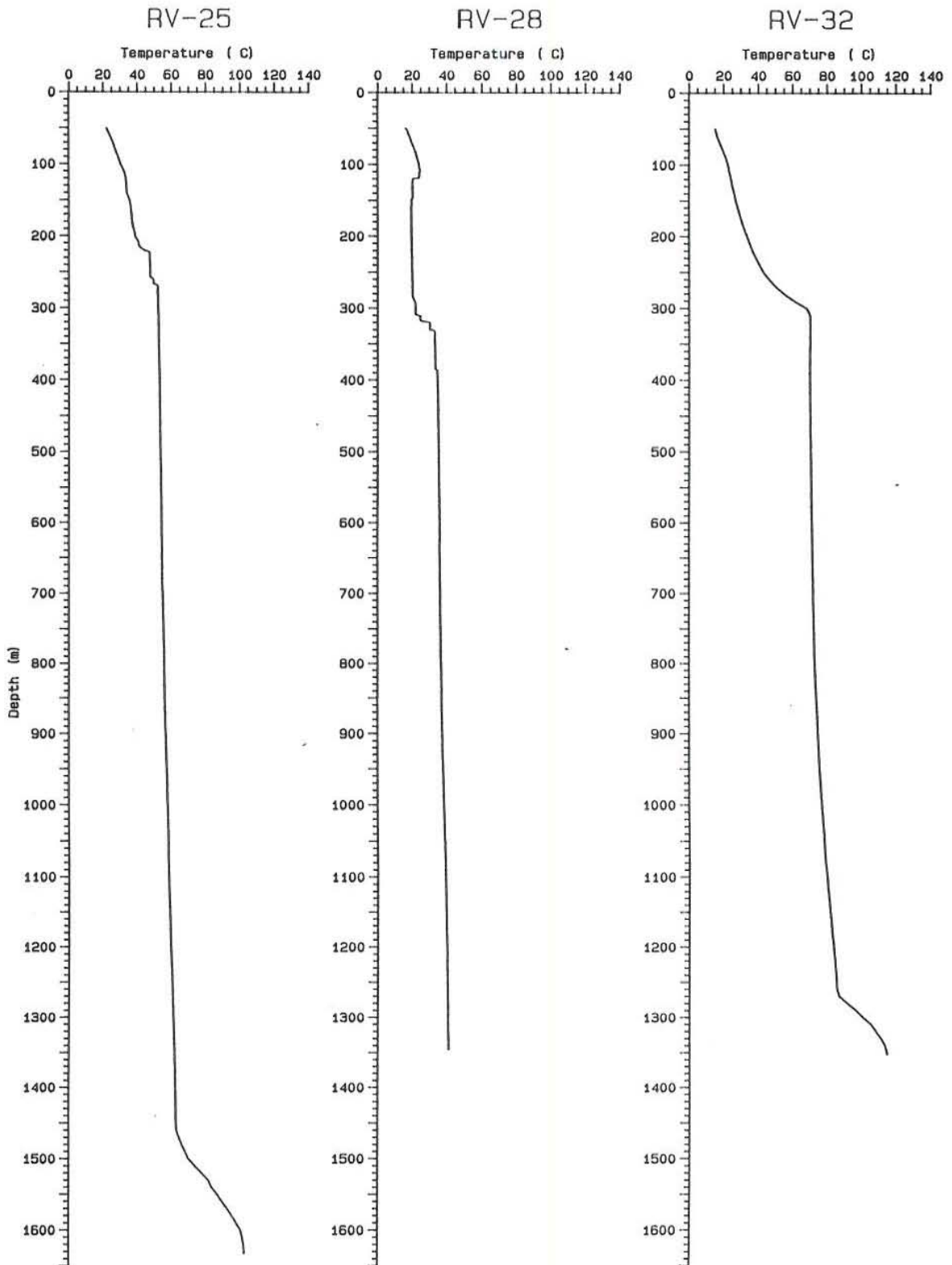


Figure 3 - Interpreted subsurface geology including wells RV-25 and RV-28

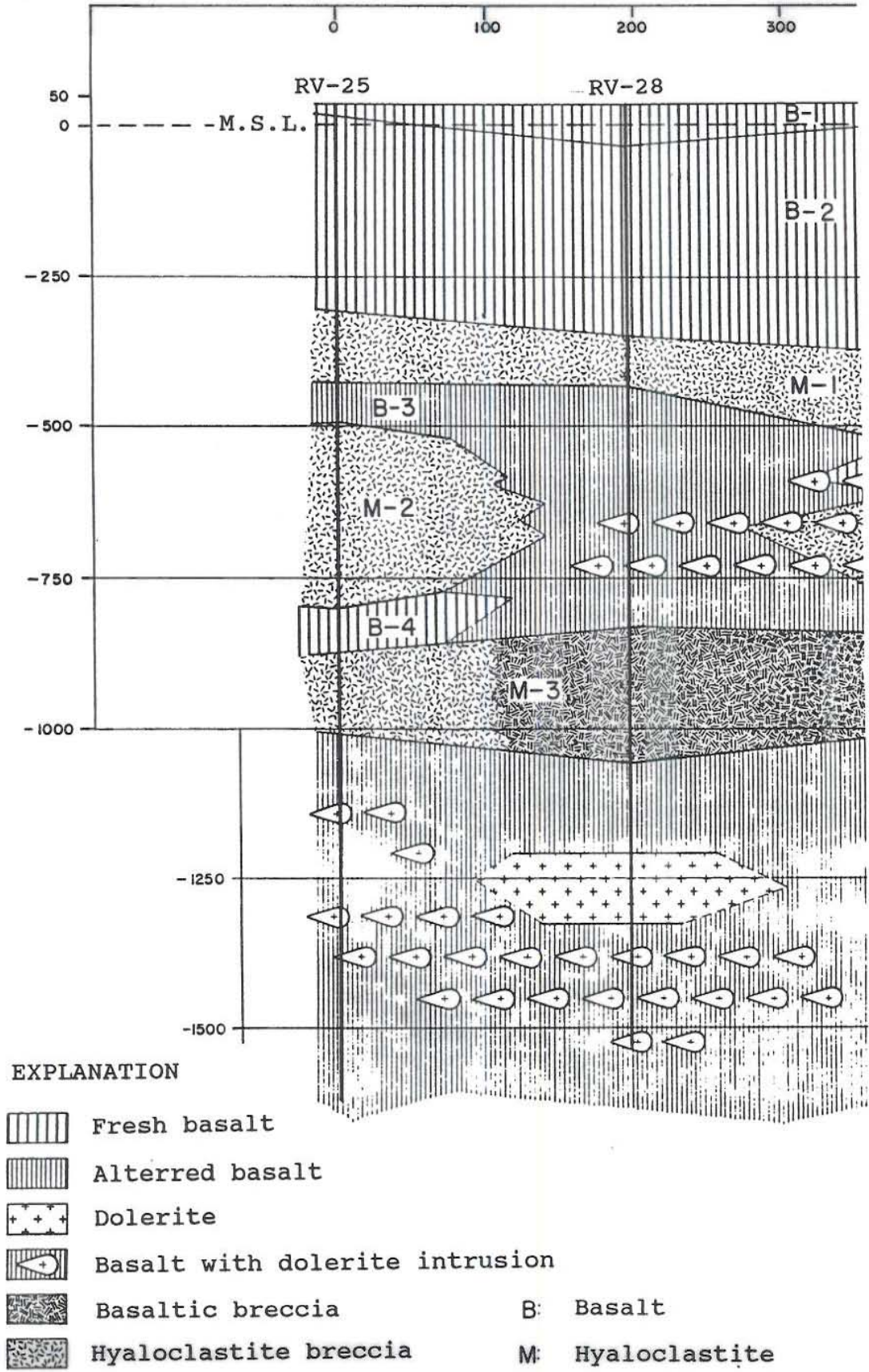
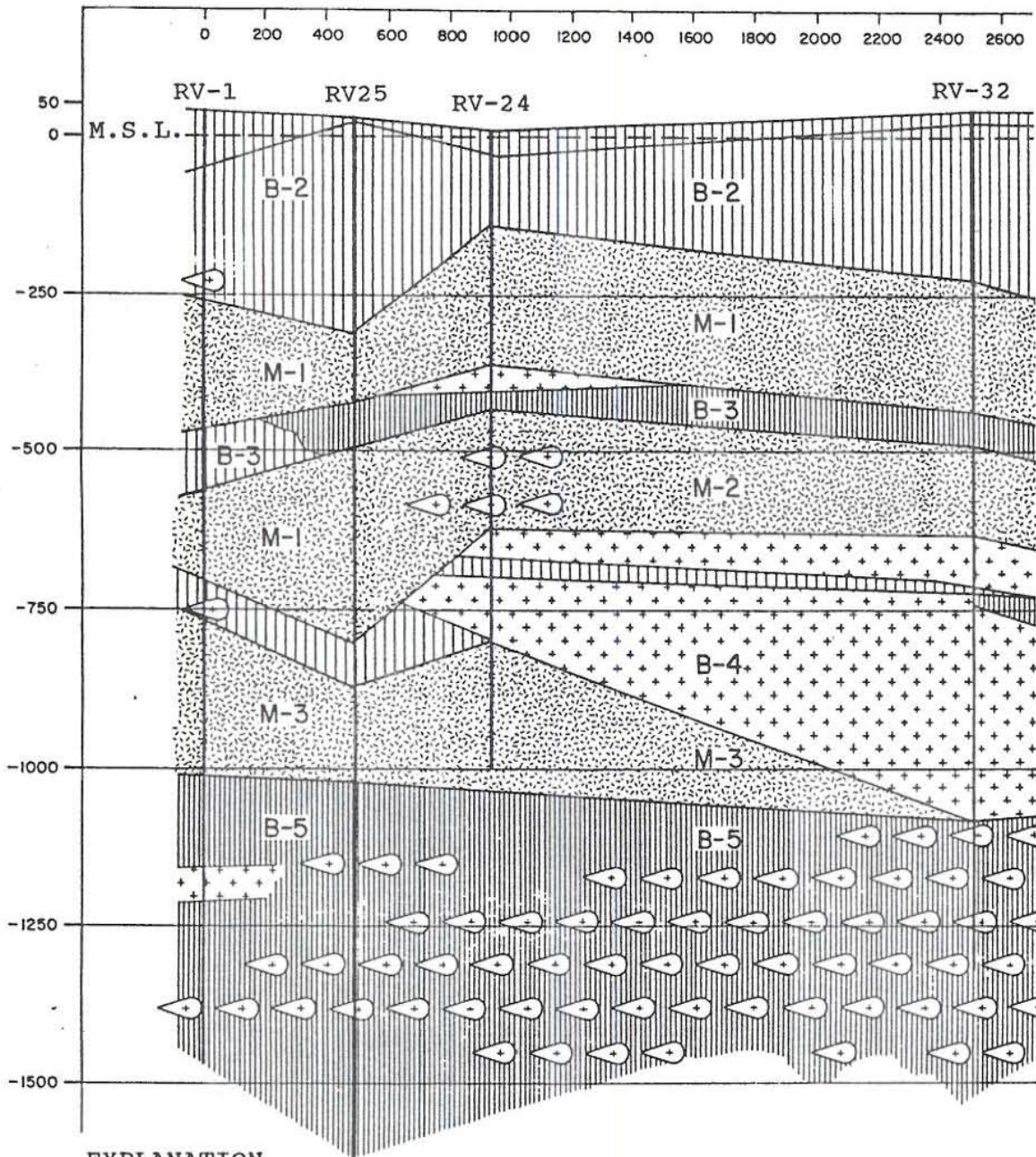


Figure 4 - Interpreted subsurface geology including wells RV-25 and RV-32



EXPLANATION




- | | | |
|-------------------------------------------------------------------------------------|--------------------------------|------------------|
|  | Fresh basalt | |
|  | Altered basalt | |
|  | Dolerite | |
|  | Basalt with dolerite intrusion | |
|  | Basaltic breccia | B: Basalt |
|  | Hyaloclastite breccia | M: Hyaloclastite |

Figure 5 - Normal configuration of resistivity log

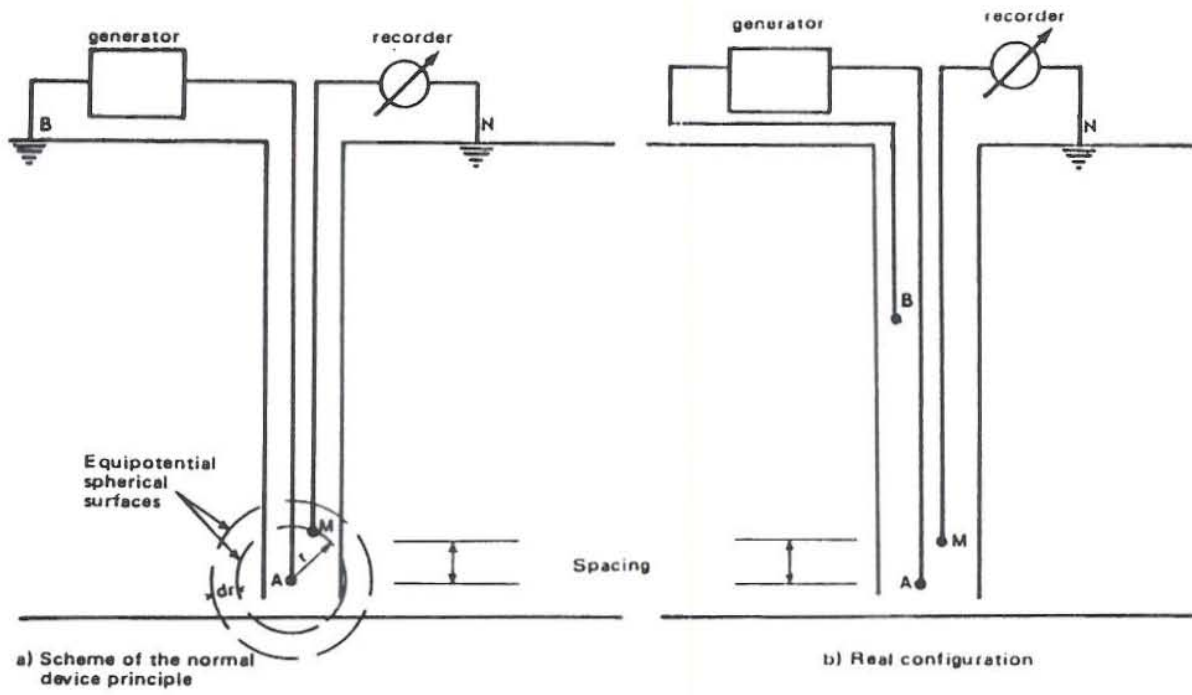


Figure 6 - Basic principle of resistivity measurement

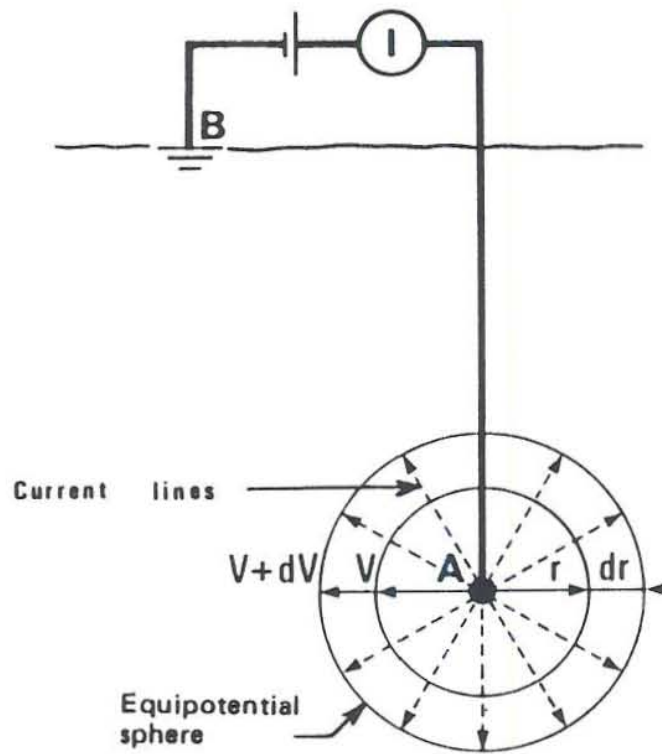


Figure 7 - Gamma ray emission spectra of radioactive elements

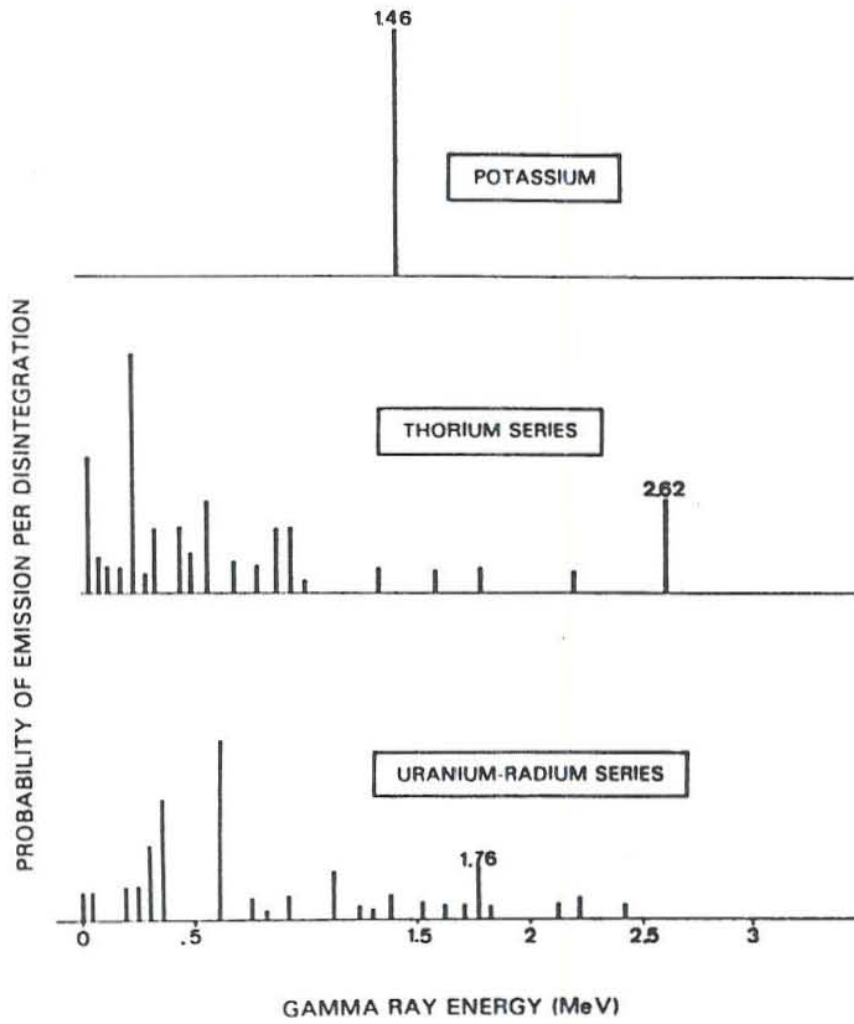


Figure 8 - Real spectrograms of K, Th and U obtained from NaI(Tl) crystal detector

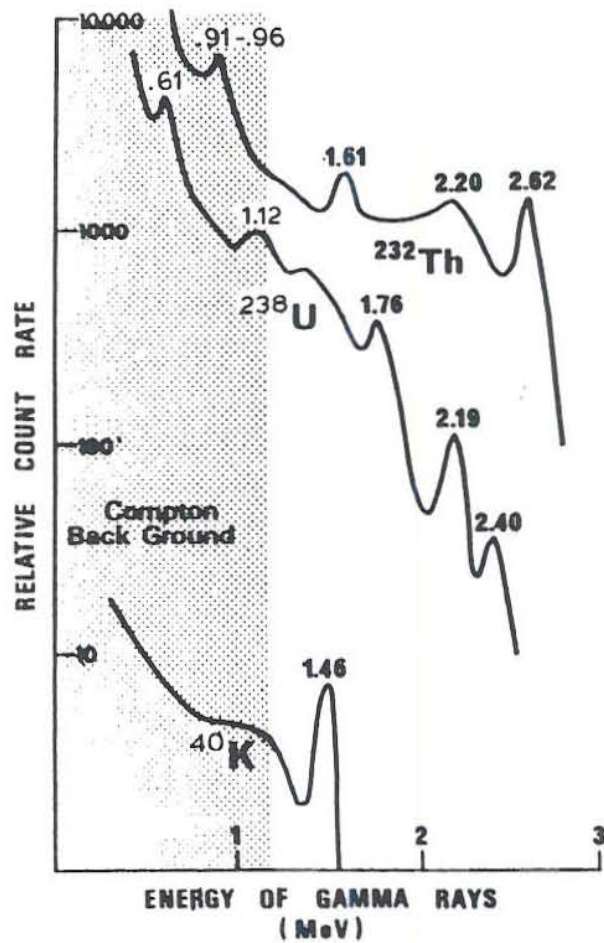


Figure 9 - Efficiency curves of gamma ray detectors

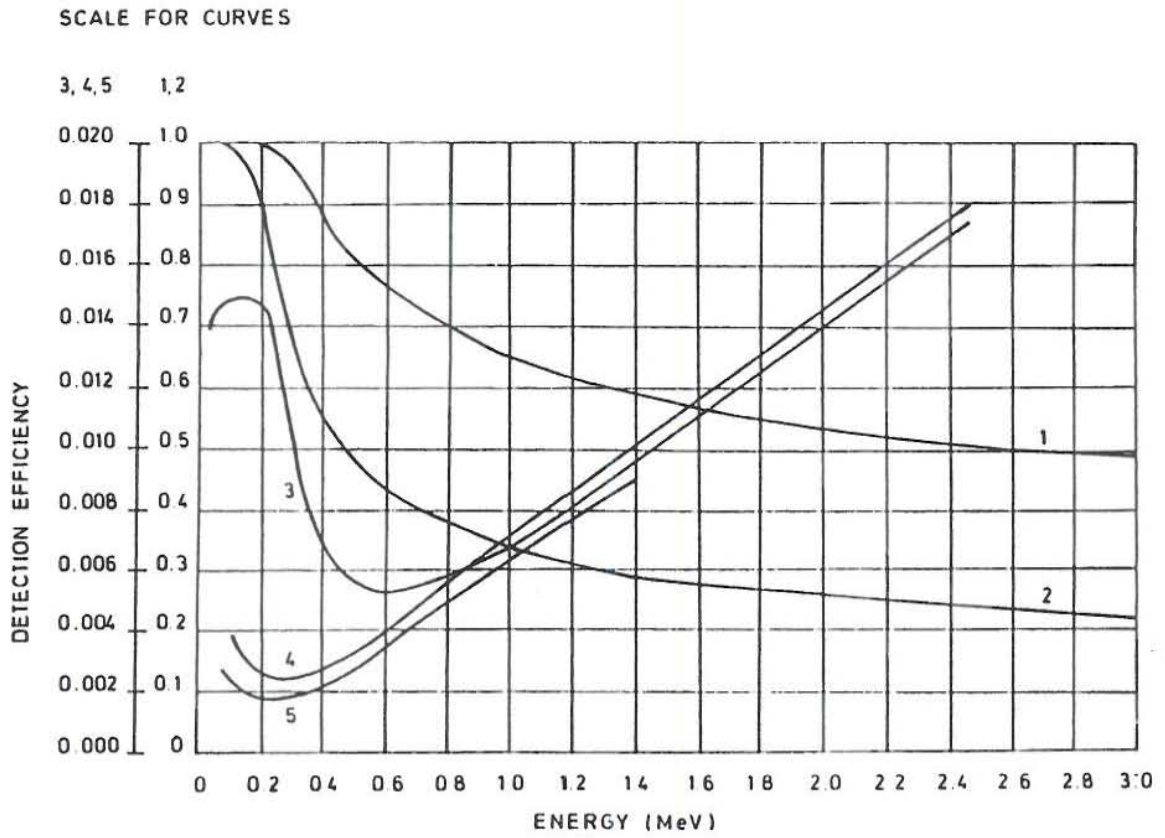


Figure 10 - Slowing down power of H, O and Si for different incident neutron energies

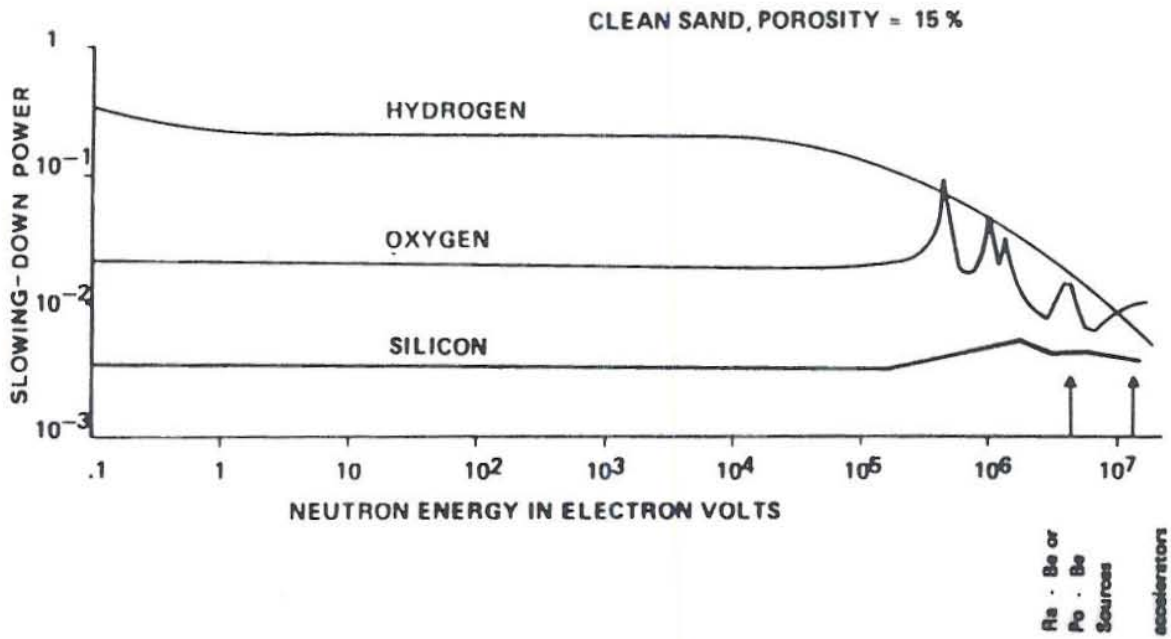


Figure 11 - Distribution of the measurements about the mean value

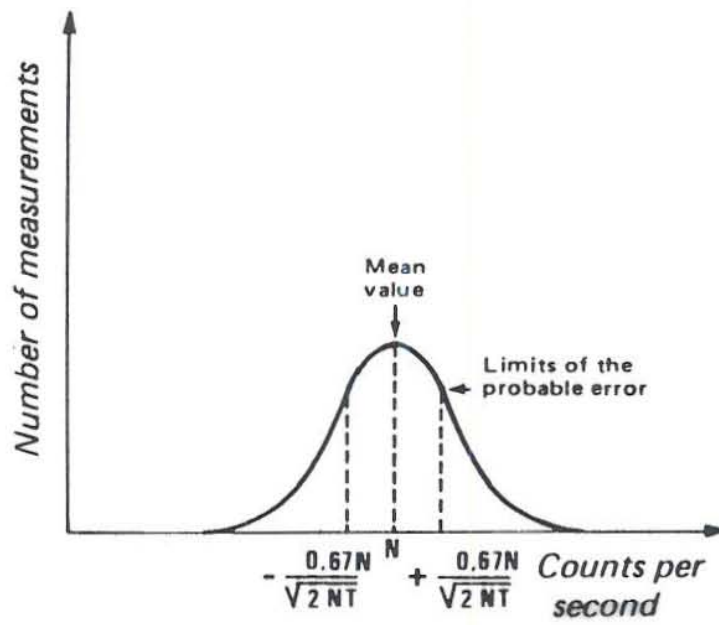


Figure 12 - Probable error as a function of counting rate

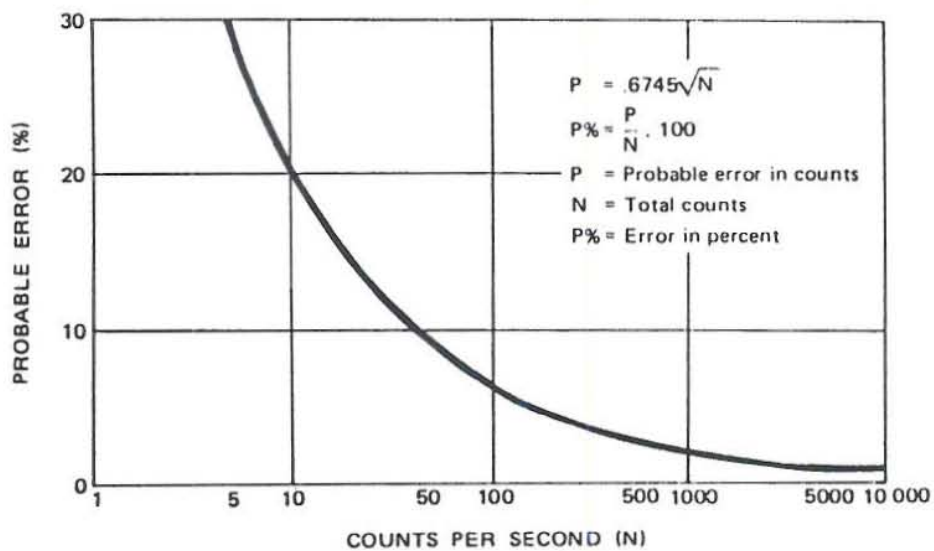


Figure 13 - Hydrothermal minerals in well RV-39

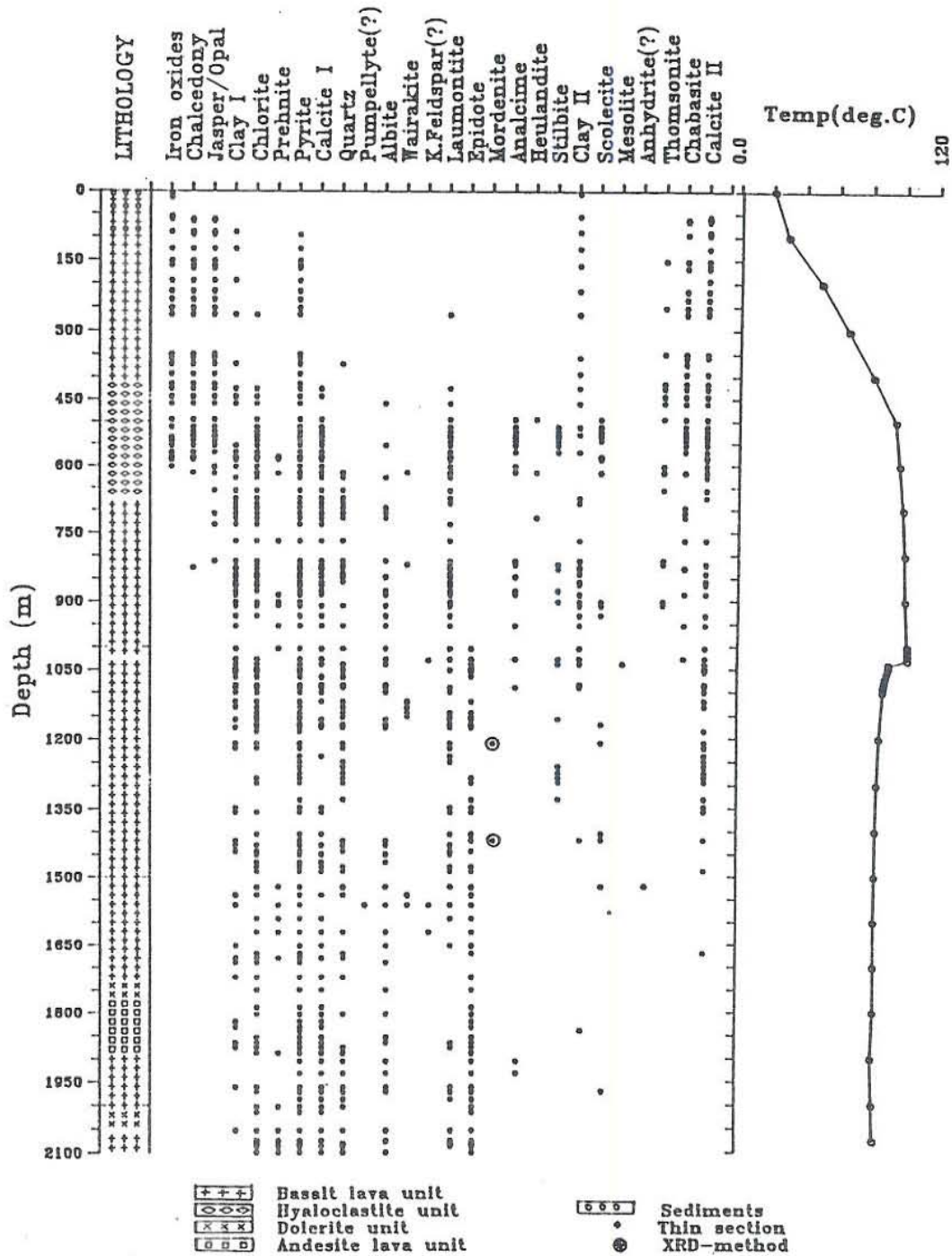


Figure 14 - Calibration curves for neutron-neutron log

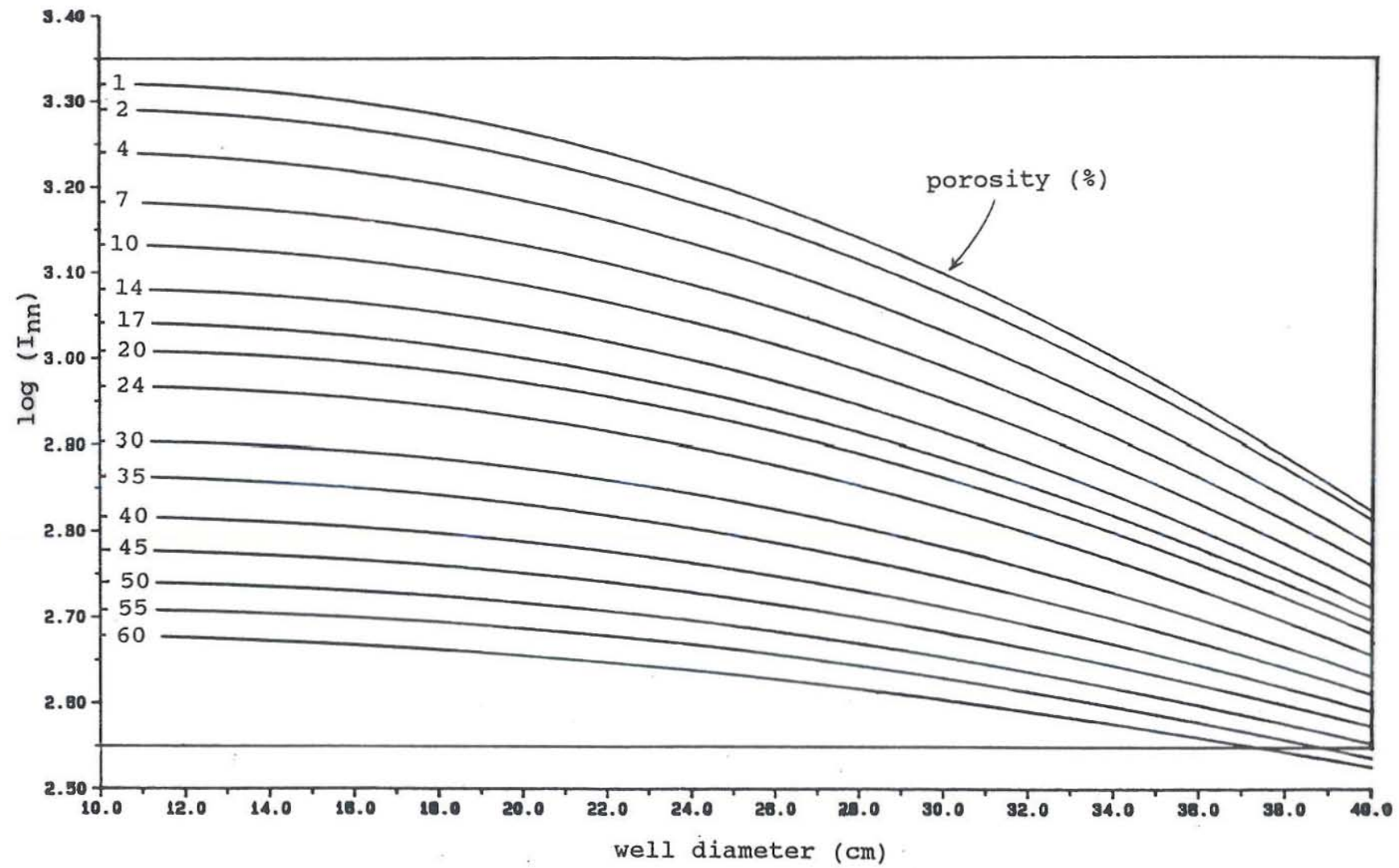


Figure 15 - Well size correction for 16" normal resistivity log

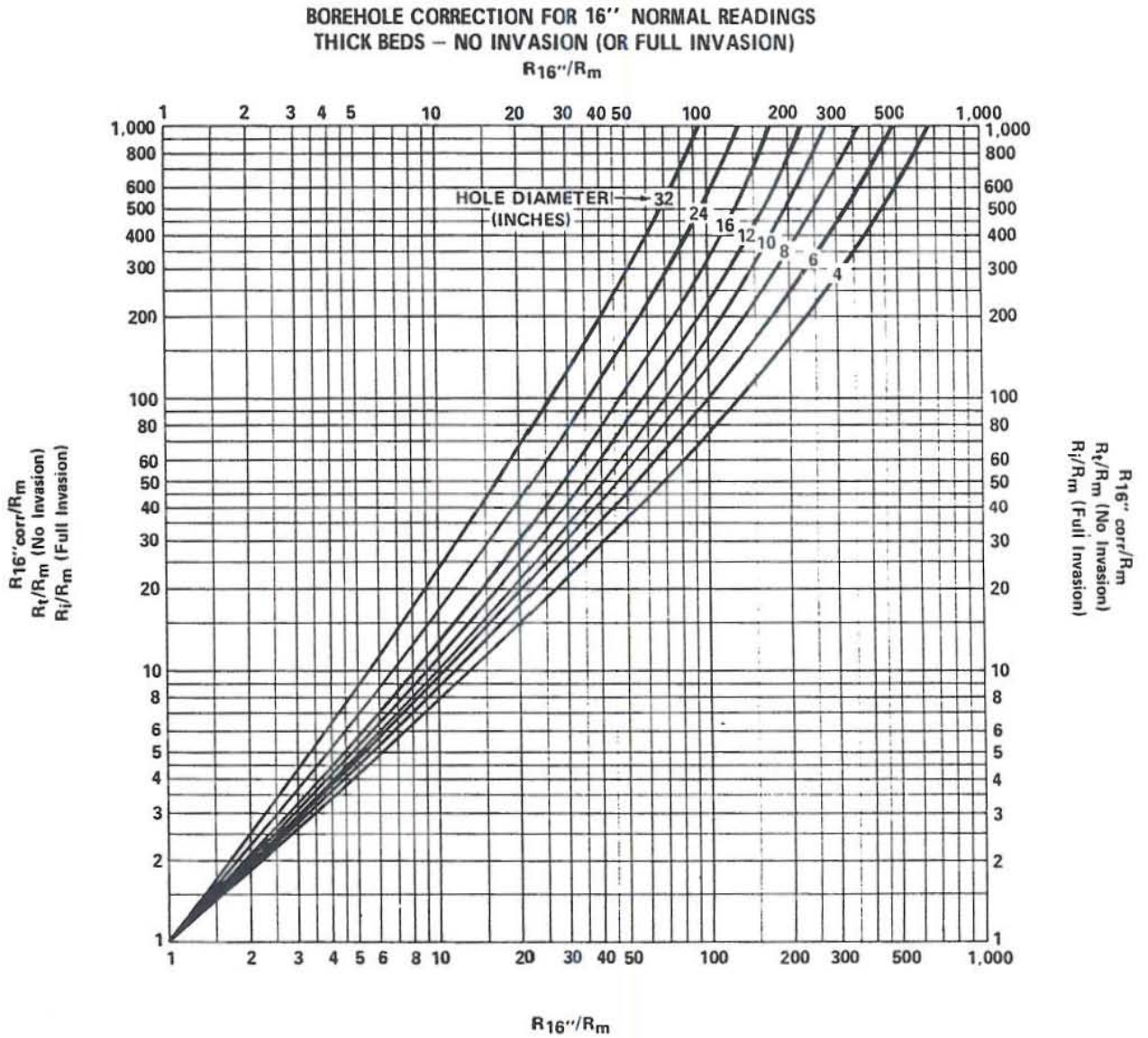


Figure 16 - Well size correction for 64" normal resistivity log

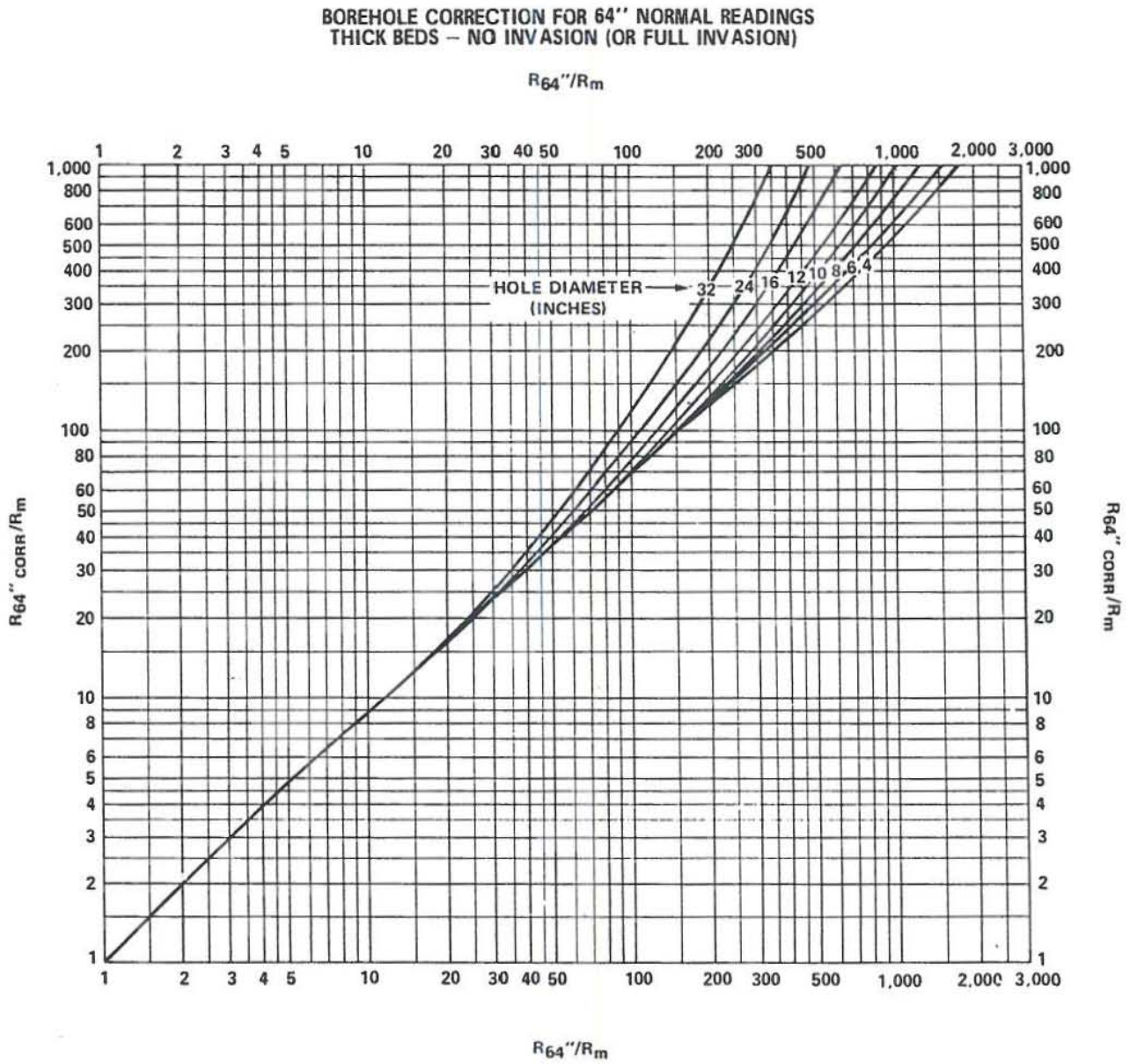
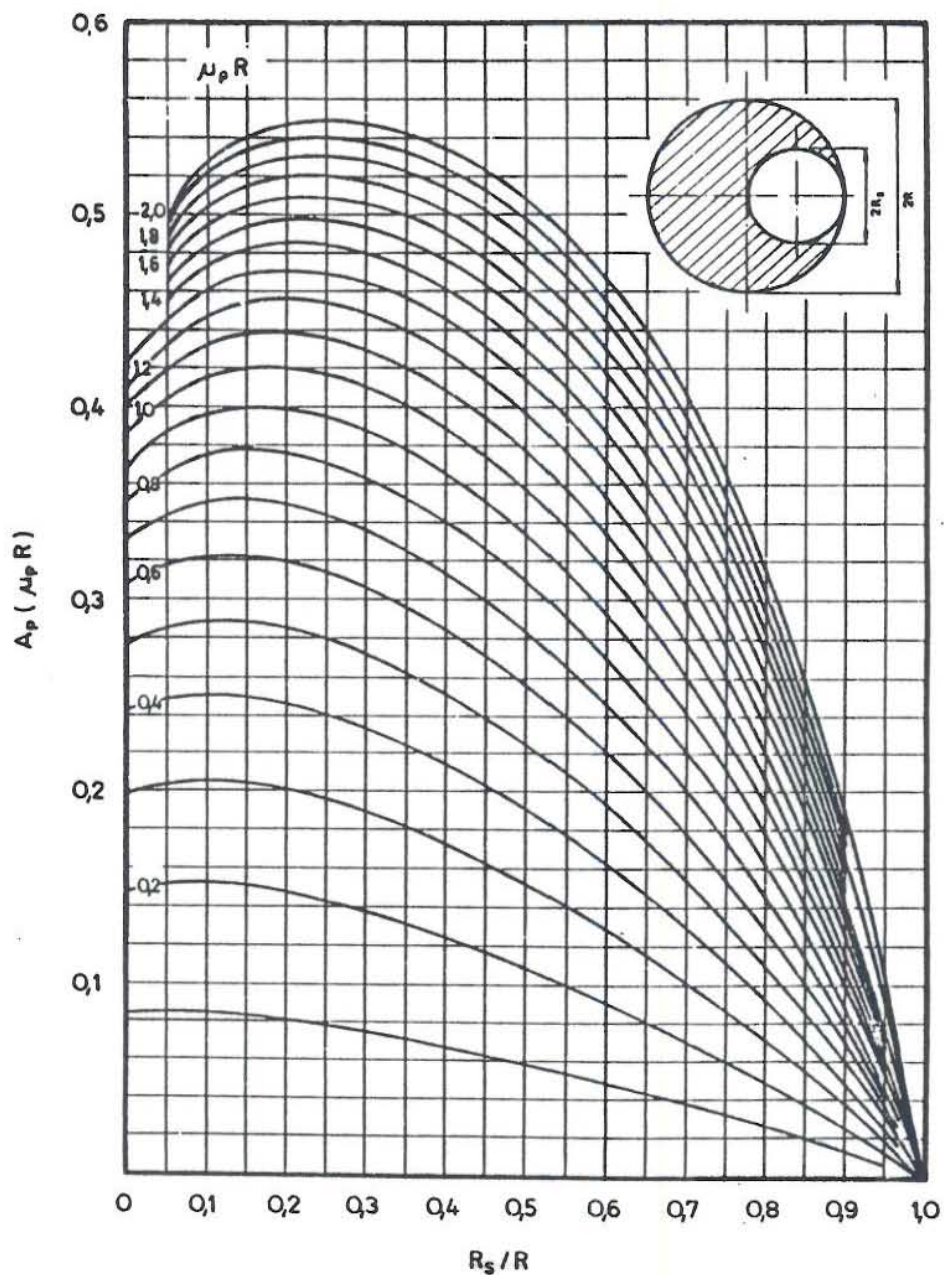


Figure 17 - Borehole absorption function used for well size correction of gamma ray log



R = borehole radius
 R_s = probe radius
 $\mu = 0.03 \times \rho$
 ρ = fluid density

Figure 18 - Distribution of resistivity in well RV-25

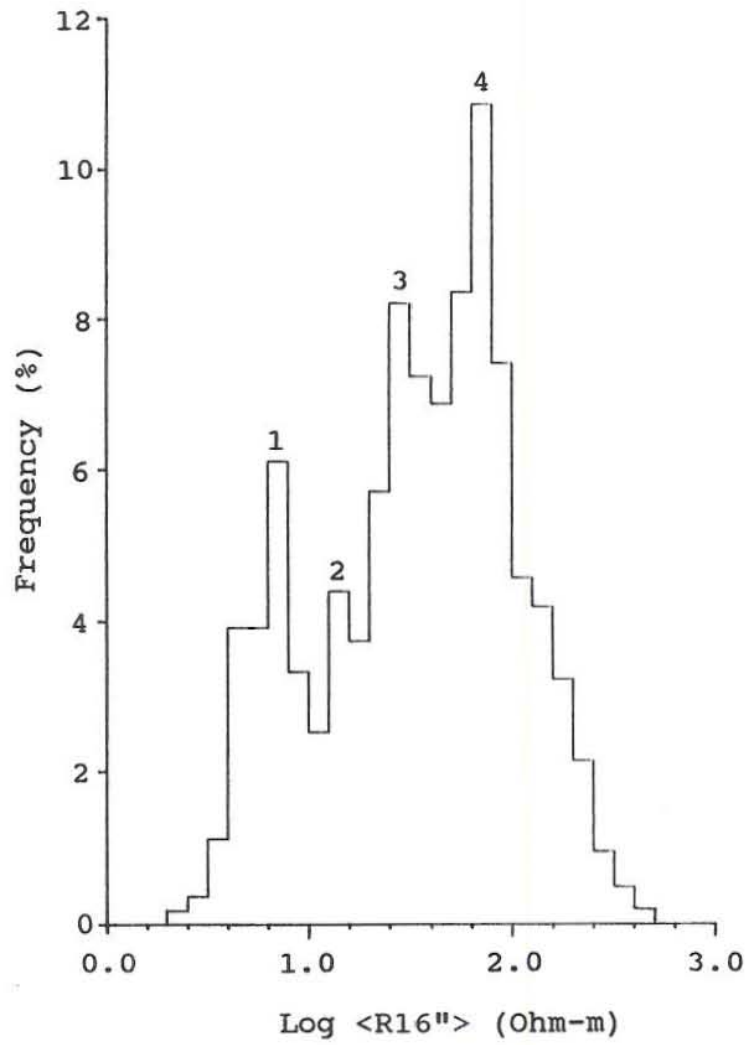


Figure 19 - Distribution of resistivity in well RV-28

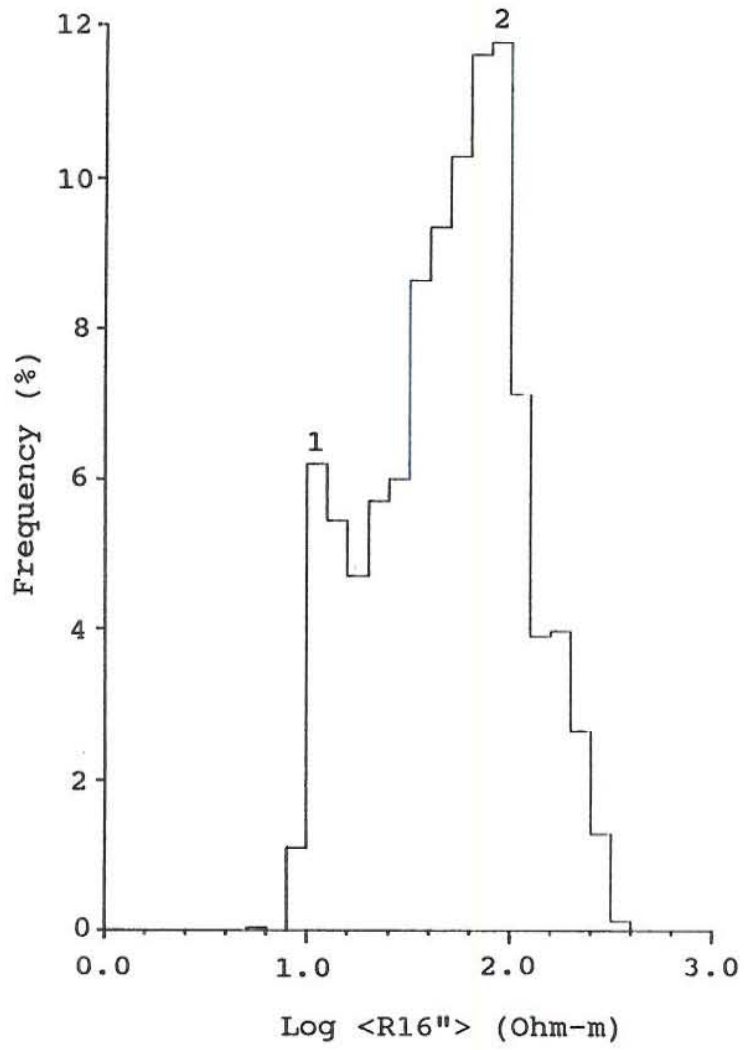


Figure 20 - Distribution of resistivity in well RV-32

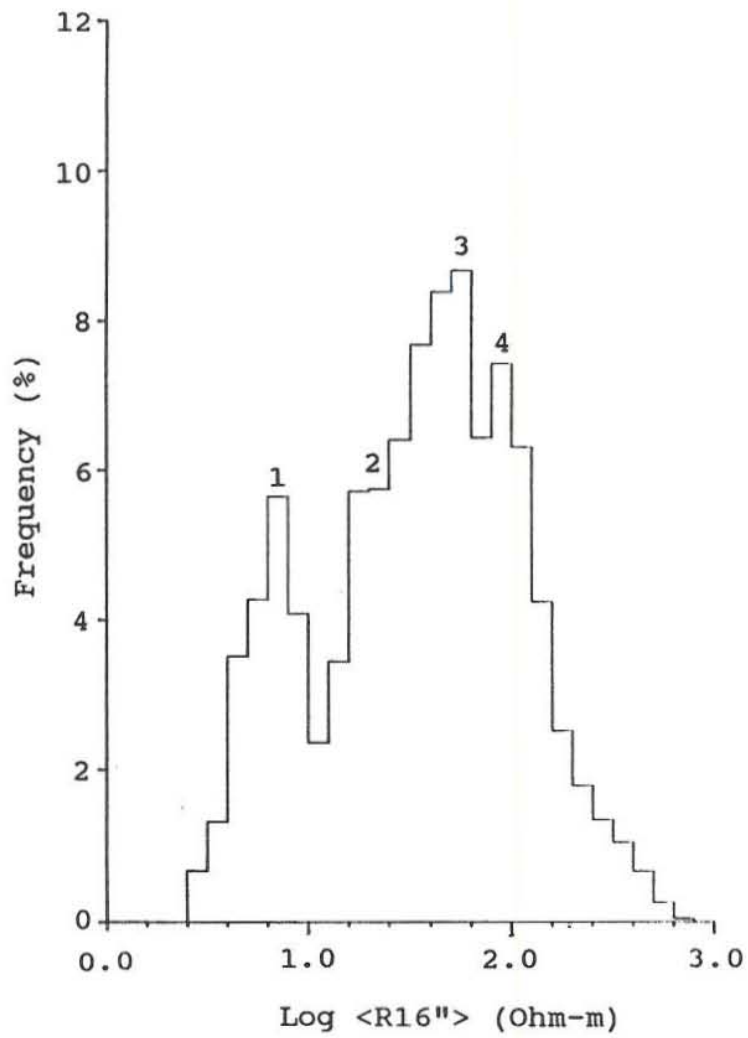


Figure 21 - Distribution of porosity in well RV-25

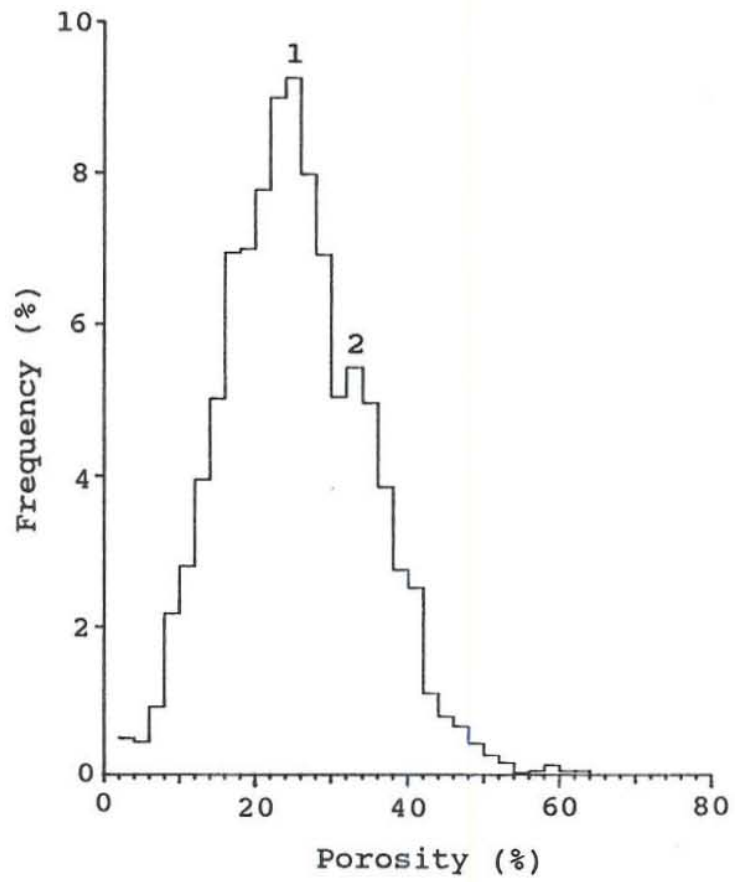


Figure 22 - Distribution of porosity in well RV-28

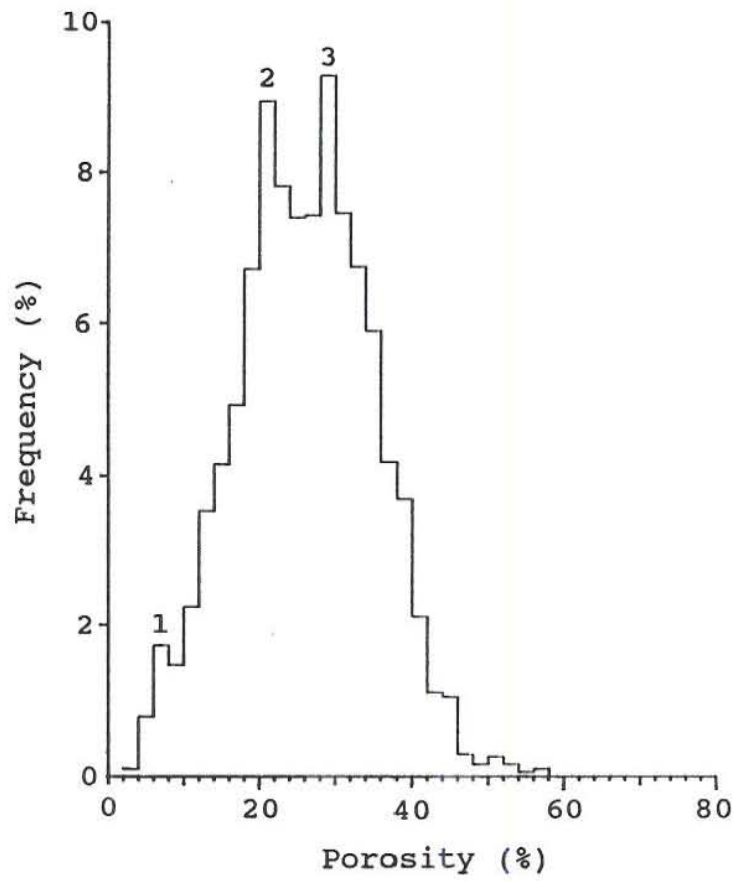


Figure 23 - Distribution of porosity in well RV-32

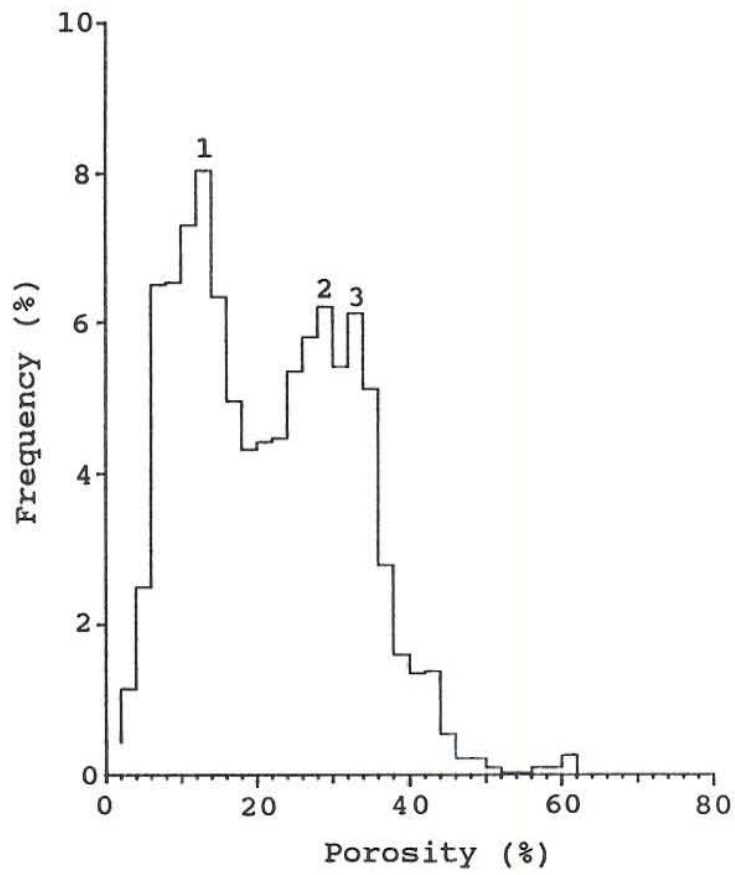


Figure 24 - Distribution of silica content in well RV-25

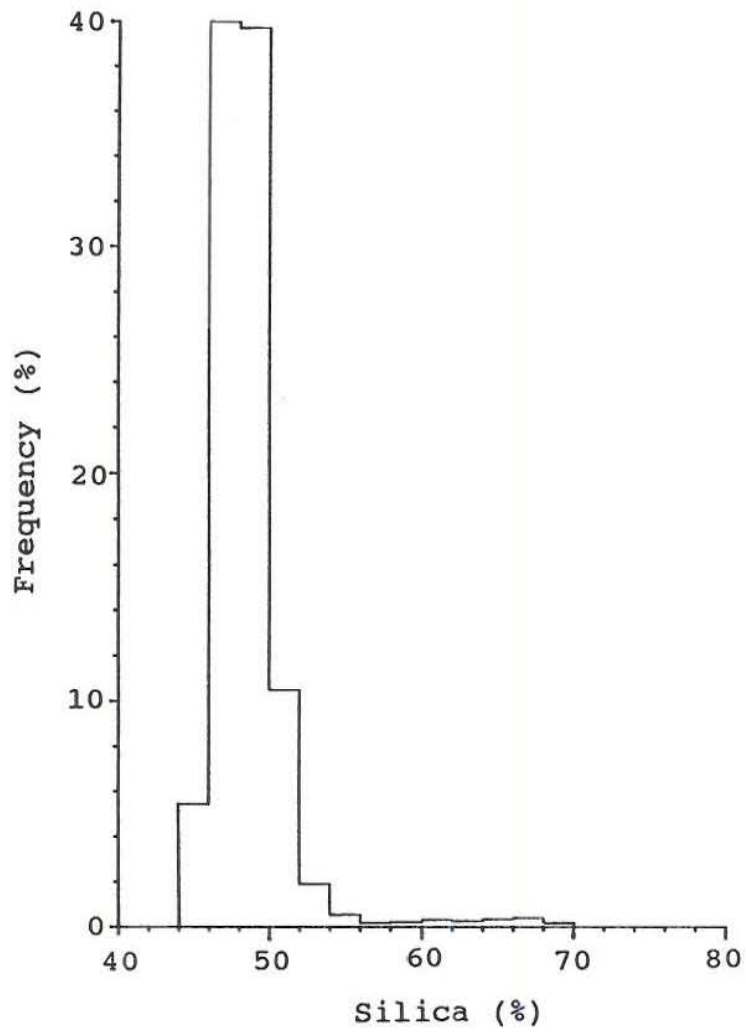


Figure 25 - Distribution of silica content in well RV-28

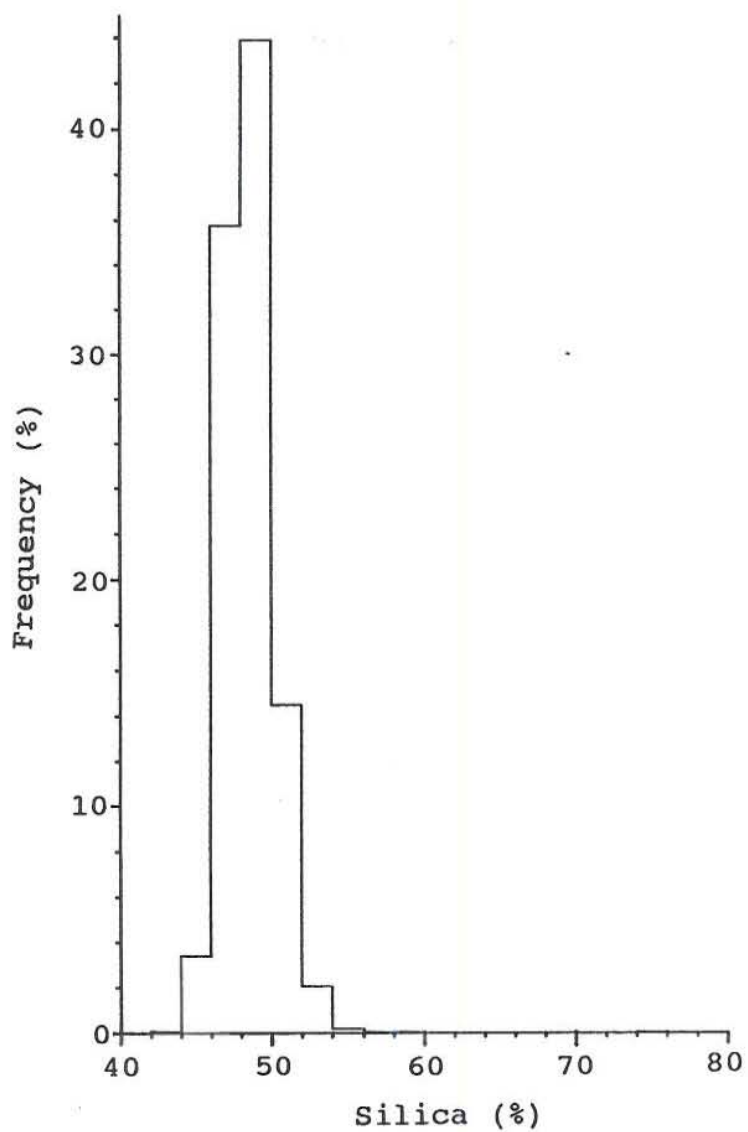


Figure 26 - Distribution of silica content in well RV-32

